Author/s:
Hay, MA;Boskovic, C

Title:
Lanthanoid Complexes as Molecular Materials: The Redox Approach

Date:
2021-02-19

Citation:
Hay, M. A. & Boskovic, C. (2021). Lanthanoid Complexes as Molecular Materials: The Redox Approach. Chemistry A European Journal, 27 (11), pp.3608-3637. https://doi.org/10.1002/chem.202003761.

Persistent Link:
https://hdl.handle.net/11343/298131

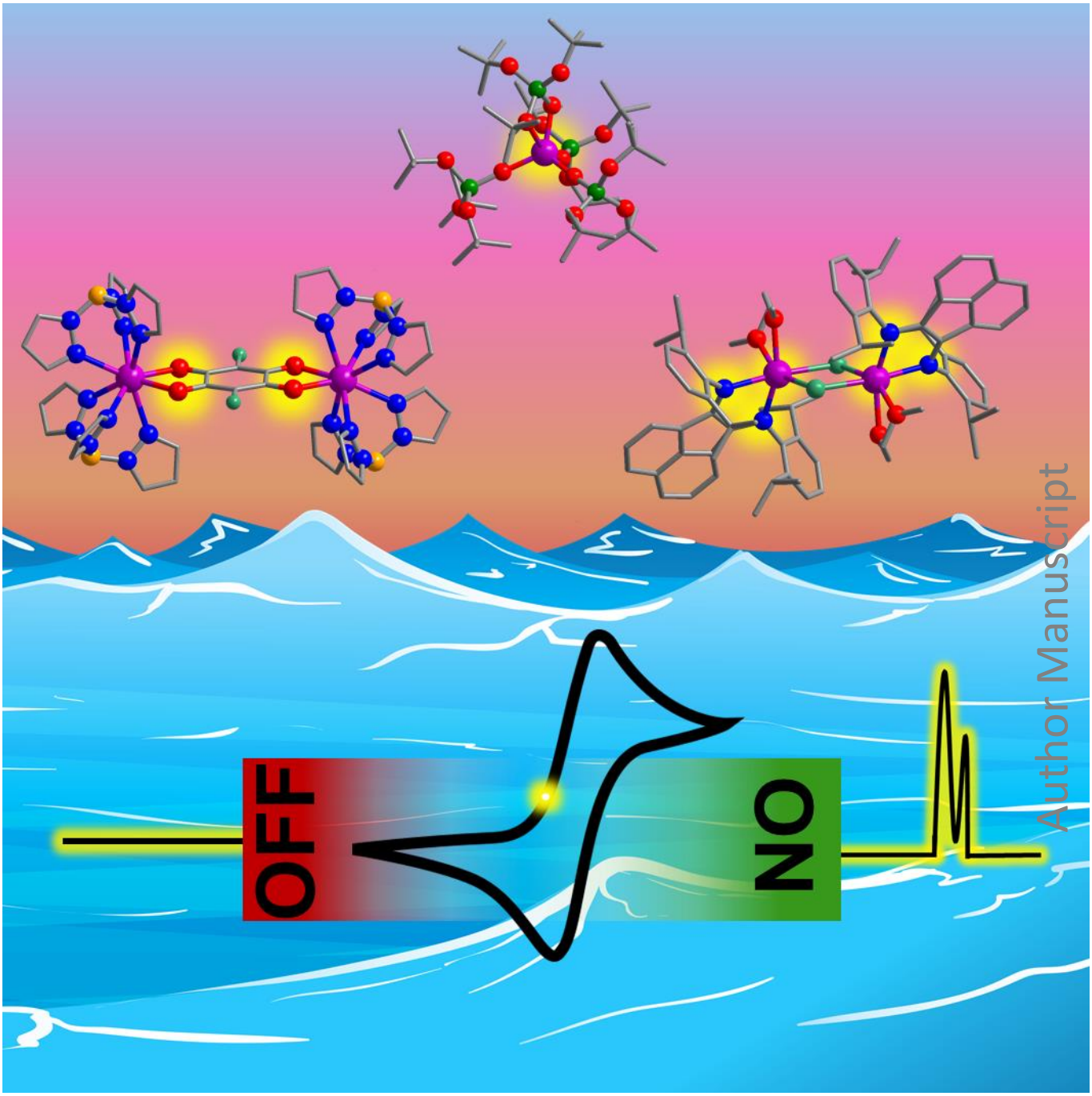

Exploring the redox approach to lanthanoid molecular materials: understanding fundamental electronic behavior, unlocking interesting and synergistic properties, and gaining control through redox switching.

Lanthanoid Complexes as Molecular Materials: The Redox Approach

Moya A. Hay,[a] Colette Boskovic*[a]

[a] *Dr. M. A Hay, Dr. C. Boskovic*
School of Chemistry, University of Melbourne, Victoria 3010 (Australia)
E-mail: c.boskovic@unimelb.edu.au

Abstract:

The development of molecular materials with novel functionality offers promise for technological innovation. Switchable molecules that incorporate redox-active components are enticing candidate compounds due to their potential for electronic manipulation. Lanthanoid metals are most prevalent in their trivalent state and usually redox-activity in lanthanoid complexes is restricted to the ligand. The unique electronic and physical properties of lanthanoid ions have been exploited for various applications, including in magnetic and luminescent materials as well as in catalysis. Lanthanoid complexes are also promising for applications reliant on switchability, where the physical properties can be modulated by varying the oxidation state of a coordinated ligand. Lanthanoid-based redox activity is also possible, encompassing both divalent and tetravalent metal oxidation states. Thus, utilization of redox-active lanthanoid metals offers an attractive opportunity to further expand the capabilities of molecular materials. This review surveys both ligand and lanthanoid centered redox-activity in pre-existing molecular systems, including tuning of lanthanoid magnetic and photophysical properties by modulating the redox states of coordinated ligands. Ultimately the combination of redox-activity at both ligands and metal centers in the same molecule can afford novel electronic structures and physical properties, including multiconfigurational electronic states and valence tautomerism. Further targeted exploration of these features is clearly warranted, both to enhance understanding of the underlying fundamental chemistry, and for the generation of a potentially important new class of molecular material.

1. Introduction

Understanding how the fundamental properties of individual molecules arise and can be manipulated is critical for the development of new functional molecular materials. Molecules that can switch between distinguishable stable states by application of an external stimulus have promise in such materials.[1] Within molecular inorganic chemistry there are several classes of compounds that fall into this category. Spin crossover (SCO) materials switch between high-spin and low-spin electronic configurations of metal ions on exposure to various physical stimuli, typically accompanied by a substantial change in physical properties that is amenable to chemical tuning.[2] Valence tautomeric (VT) compounds interconvert between states through stimulated intramolecular electron transfer between a redox-active ligand and metal, giving rise to redox isomers (valence tautomers).[3] This has been comparatively less well studied than SCO, but presents the opportunity to broaden the chromic-based applications.[4] Materials that exhibit charge transfer induced spin transitions (CTIST) are similar to VT materials in that both involve intramolecular electron transfer; however, in CTIST this occurs between two redox-active metals accompanied by a spin-transition at one of the metals.[5] Single-molecule magnets (SMMs) display slow relaxation of magnetization at low temperature, originating from an energy barrier to spin reversal between two magnetic states, evident as magnetic hysteresis.[6] Similarly to SCO, VT and CTIST materials, the magnetic response of SMMs can be controlled by various means to either enhance the properties, or switch the behavior on and off.[7] The characteristic electronic and physical properties of these classes of compounds gives rise to tremendous promise for new technological applications, for example molecular spintronics,[8] memory-based devices,[9] and quantum technologies.[10] Furthermore, SCO, VT and CTIST molecular materials exhibit distinct changes in color on moving from one electronic state to another, and so are excellent candidates for smart functional materials such as sensors,[11] actuators,[1a] and optical applications.[12]

Lanthanoid (Ln) ions are predominantly found in the trivalent state due to the poor stability of the Ln(II)/Ln(IV) states. They have been widely employed in chemical, magnetic, optical, and mechanical applications, including in petroleum refining, catalysis, optical fibers, lasers, superconductors, imaging contrast agents, and high-performance alloys.[13] Significant research is currently underway into the viability of lanthanoid compounds as new drug candidates for the treatment of neoplastic diseases,[14] quantum technologies,[15] and new catalytic processes.[16] The inherently large magnetic anisotropies of many lanthanoid ions has prompted much interest in their SMM behavior.[17] The luminescence properties of molecular lanthanoid compounds are also promising, as their emission covers a large spectroscopic range with narrow lines and sometimes

long associated lifetimes.[18] Lanthanoid compounds can be exploited in both homogeneous and heterogeneous Lewis acid catalysis, with their Lewis acidity tuned through the ligand environment.[19] Lanthanoid metals capable of accessing multiple oxidation states (Ce, Sm) have been widely used as oxidizing and reducing agents, with these same properties exploited in small molecule activation (*e.g.* CO_2, CS_2).[20] The development of multifunctional lanthanoid materials, where multiple properties of one molecule can be exploited in a concerted or complementary manner, is of considerable interest to expand their applicability (Figure 1). For example, luminescence can be used to probe the electronic structure of lanthanoid based SMMs deposited on a surface.[21] Photoredox catalysis, where light alters the redox properties of a compound to drive chemical reactions, can exploit the unparalleled reducing power of lanthanoid photoexcited states to activate substrates that would otherwise be inaccessible with more conventional photosensitizers.[22]

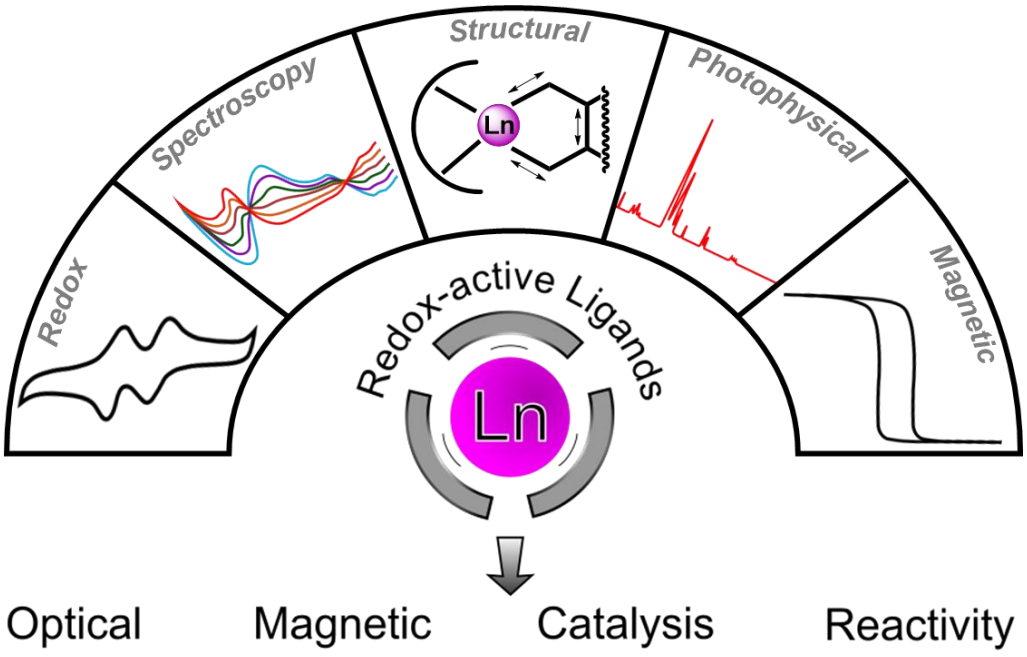

Figure 1. Areas of application and important physical properties of redox-active lanthanoid complexes.

Of the four types of molecular materials outlined above: SCO, VT, CTIST and SMMs, lanthanoids have only proved relevant for VT and SMM materials, and only VT compounds intrinsically involve redox-activity. The unique electronic, and resulting magnetic and

photophysical, properties of lanthanoid ions, as well as their catalytic and photocatalytic possibilities, imply that valence tautomerism in lanthanoid complexes would offer possibilities for applications that are not available with complexes of *d*-block metals. Stimulated intramolecular electron transfer necessarily requires a lanthanoid metal that can access a less common oxidation state coordinated to a suitable redox-active ligand. To date, only two, closely-related, ytterbium complexes have been reported to exhibit thermally-induced VT.[23] The deliberate extension of this property to other compounds requires consideration of several factors. The lanthanoid ion and ligands must be suitably 'redox matched' to allow for intramolecular electron transfer, which is associated with similar energies of the relevant frontier orbitals. It is thus important to understand how to stabilize lanthanoid ions in different redox states, as well as how redox-active ligands can be used to manipulate the properties of lanthanoid complexes. Other factors such as lattice stabilization and solvation effects must also be considered.

This review will focus on molecular lanthanoid complexes with accessible redox features in a broad sense, covering redox-activity involving both lanthanoid metal ions and coordinated ligands. Specifically, we will address molecular lanthanoid complexes of non-typical (Ln(II) and Ln(IV)) oxidation states and the coordination environments in which these have been stabilized. We will review how the properties of some lanthanoid complexes can be controlled using redox-active ligands, focussing on magnetic and photophysical properties and the associated possible applications. Finally, the combination of redox-active ligands and potentially redox-active lanthanoid metals within the same molecule will be considered, given the promise of such systems as basis for design of new molecular switches.

2. Fundamentals

2.1. Electronic Structure of Lanthanoid Ions

The lanthanoid metals' preference for the Ln(III) oxidation state, arises from the stability of the resulting [Xe]$4f^{n-1}$ configuration. Consequently, they are very susceptible to oxidation (or reduction) if isolated in the Ln(II) (or Ln(IV)) state. The ability of a lanthanoid ion to reach these unusual oxidation states is related to the possibility of achieving an electronic configuration involving an empty, half-filled, or completely full *f*-shell upon oxidation or reduction.

The interesting magnetic and photophysical properties for which lanthanoid metals are often exploited, arise because the deeply buried valence 4*f* orbitals are relatively close to the

nucleus, and are well-shielded by the 5*s* and 5*p* electrons. Correspondingly, the effect of the crystal field (CF) on the 4*f* orbitals is minimal and ligands bind predominantly through ionic interactions with steric effects typically determining the coordination geometry of their molecular complexes. However, in recent years it has become apparent that the role of covalency from the 5*d* orbitals can play a role in lanthanoid-ligand bonding.[24] Several interactions determine the electronic structure of lanthanoid ions (Figure 2). The interelectronic repulsion, spin-orbit coupling and CF interactions, through the electrostatic field of the ligand, result in splitting of the $2J + 1$ degeneracy of the free ion states, to give the M_J states.[25] The M_J states are then further separated in the presence of a magnetic field in accordance with the Zeeman interaction. Most lanthanoid ions possess innately large spin-orbit coupling (SOC) through unquenched orbital angular momentum. In fact, for lanthanoid ions SOC is a much stronger perturbation on the electronic structure than CF splitting. It is the CF splitting that determines the magnitude of the magnetic anisotropy, a prerequisite for SMM behavior. The highly paramagnetic nature of many lanthanoid ions also contributes to their magnetic applications, even for isotropic Gd(III) ($4f^7$), which has been widely used in applications such as MRI contrast agents and magnetic coolers.[26] In terms of the photophysical properties, the very weak interaction of the 4*f* orbitals with the coordination environment results in narrow luminescence emission lines, which serve as 'fingerprints' for the Ln(III) series.[27]

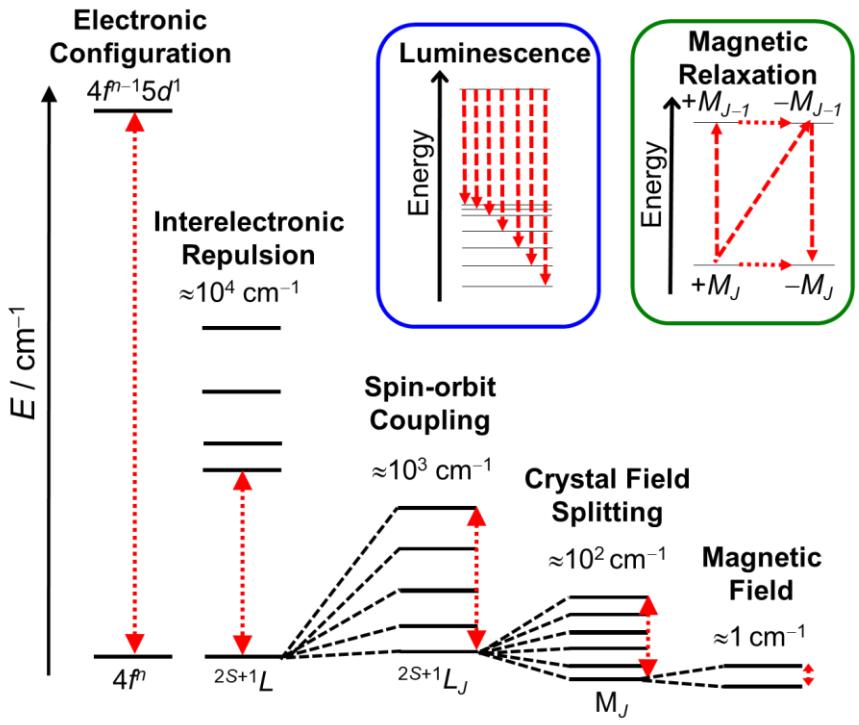

Figure 2. Perturbations that act on the electronic structure of lanthanoid ions showing approximate magnitudes. The inset in blue depicts typical luminescence emission lines from an excited state to the CF split ground multiplet. The inset in green depicts typical pathways of magnetic relaxation (Orbach and quantum-tunneling; dashed red arrows).

2.2. Photophysical Properties

The photophysical properties of lanthanoid ions result from transitions between the ground state and thermally-inaccessible excited states.[27] The most commonly studied ions are Eu(III) and Tb(III), which exhibit intense visible line-like emission.[18a, 28-29] However near infrared (NIR) lanthanoid emitters such as Nd(III), Er(III) and Yb(III) have gained recent interest with the longer wavelengths presenting some benefits for certain biomedical and telecommunications applications.[28] Due to their relative instability, divalent lanthanoid compounds have not been as well investigated for their emissive properties, with the exception of Eu(II) and some of the more stable divalent lanthanoids (Sm, Yb, Tm) within solid-state materials.[30] This poor stability has inhibited their application despite showing emission in similar spectral ranges to their trivalent counterparts, but there is merit in the insight they can provide with regards to electronic

structure.[30b] The isolated Ln(IV) molecular species consist almost exclusively of Ce(IV), which is an f^0 ion and therefore there are no $4f \leftrightarrow 4f$ transitions that afford emission.[31]

Lanthanoid(III) ions show very specific narrow line emission, which is associated with the metal-centered intra-configurational $4f \leftrightarrow 4f$ transitions, with the exceptions of the f^0 (La, Lu), f^1 (Ce) and f^{13} (Yb) ions.[27, 32] Inter-configurational $4f^n \leftrightarrow 4f^{n-1}5d^1$ transitions can also occur, but for most Ln(III) ions the emissions are in the vacuum UV range, and so are not of interest for materials applications. The notable exception is Ce(III), for which the $f^{n-1}5d^1$ states lie lower in energy due to the stability of the Ce(IV) state, and so is emissive in the UV range.[29] For the divalent lanthanoid ions, although the $4f^n$ levels will resemble that of its right-hand neighbor in the Ln(III) state (*e.g.* Eu(III) and Sm(II)), the $4f^{n-1}5d^1$ states in the divalent case lie lower in energy.[30b] Consequently, the metal centered $4f^n \leftrightarrow 4f^{n-1}5d^1$ transitions of Ln(II) ions are typically found within the UV-Vis-NIR range.[30b] The associated transitions are much broader in appearance due to the increased orbital overlap of the 5*d* orbitals with the ligand field.

The metal-centered emissions arising from $4f \leftrightarrow 4f$ and $4f^n \leftrightarrow 4f^{n-1}5d^1$ transitions are very different. Despite the well-defined character of the $4f \leftrightarrow 4f$ transitions due to well-shielded 4*f* orbitals, the absorptivity of the $4f \leftrightarrow 4f$ transitions is small due to their Laporte (parity) forbidden nature. Although these rules can be somewhat relaxed through molecular distortions or low-symmetry ligand environments that allow mixing of the wave-functions of the 4*f* and 5*d* orbitals, sensitization of the emission with ligands with large photon absorption is necessary (Figure 3).[28, 32] This sensitization occurs in a three-step process known as the antenna effect.[32] Firstly, the lowest-lying singlet excited state (S) of the sensitizer is populated. Intersystem crossing (ISC) can then occur to its triplet state (T), followed by energy transfer to the lanthanoid center. Therefore, the ligand must have excited states of the appropriate energy to allow for transfer to the lanthanoid. If the energy gap is too low (< 1850 cm^{-1}) back energy transfer can occur, limiting the overall quantum yield.[27-28] Another issue is population of various non-radiative charge transfer excited states, such as ligand to metal (LMCT) or ligand to ligand (LLCT) charge transfer states.[27] Therefore, overall efficiency of the sensitized emissions because of the absorption is dependent on intersystem crossing and energy transfer efficiency, as well as the intrinsic metal-centered quantum yield.[28] The divalent lanthanoids exhibit both Laporte allowed $4f^n \leftrightarrow 4f^{n-1}5d^1$ transitions and $4f^n \leftrightarrow 4f^n$ transitions, the former of which are more intense due to their increased probability.[30b] Unlike the 4*f* orbitals, the 5*d* orbitals strongly interact with the local ligand field,

hence changes in the ligand scaffold can influence the energy of the $4f^{n-1}5d^1$ states and accordingly the energetic positions of the $4f^n \leftrightarrow 4f^{n-1}5d^1$ transitions.[30a, b]

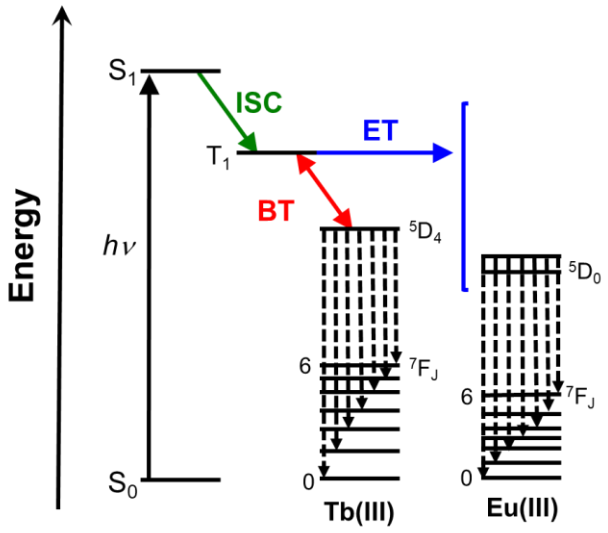

Figure 3. The antenna effect for sensitizing the luminescence of Ln(III) (Ln = Tb, Eu). The lowest-lying singlet excited state (S) of the sensitizer is populated (black arrow), intersystem crossing (ISC) can then occur to the triplet state (T) (green arrow). Where the energy gap between the sensitizer T state and the closest (lower lying) state of the Ln is small, back transfer (BT) can occur (red arrow) and where the energy gap is larger the energy transfer (ET) is complete (blue arrow).

2.3. Magnetic Properties

The magnetic properties of lanthanoid(III) complexes have been well studied in the field of molecular magnetism, but much less so those of the less common lanthanoid(II) ions. Tetravalent lanthanoid complexes predominantly consist of Ce(IV) with an f^0 configuration, which is diamagnetic and of limited magnetic interest. The substantial single-ion anisotropy associated with many lanthanoid ions, in combination with the large magnetic moments associated with the stabilization of high ± M_J states, are key factors that make Ln-SMMs preeminent in the field.[33] A requirement for SMM behavior is the existence of a magnetic doublet ground state, which must be well separated from relevant higher lying states such that a thermal energy barrier needs to be overcome for the spins to relax.[17a] As breaking of the degeneracy of the ± M_J states is

forbidden for Kramers ions such as Dy(III) in zero applied field, these are widely employed in the design of new SMMs.[34] However, for non-Kramers ions such as Tb(III), imposition of a specific CF symmetry is necessary to give rise to a ground doublet. The type of CF required is dependent on the shape of the *f*-electron charge cloud (electron density) of the free ion, which arises from the strong angular dependence of the *f*-orbitals.[17b] The divalent lanthanoid ions also exhibit significant magnetic anisotropy, however these have not been not very well explored as SMMs because of their relative instability.[35] A recent *ab initio* study by Ungur and Chibotaru assessed the potential for divalent lanthanoids to show SMM behavior, remarking that lanthanoid(II) compounds possess the potential for blocking the magnetization at equally high temperatures, or even exceeding those of top performing lanthanoid(III) SMMs.[36] Research into Ln-SMMs based on divalent lanthanoid ions therefore presents a new avenue for exploration.

Although the ideal pathway for magnetic relaxation is thermally activated excitation followed by relaxation to either of the ground state spin orientations, there are additional pathways which often contribute to the relaxation of SMMs, particularly in the ultra-low temperature regime. These pathways include three types of phonon assisted (spin-lattice) pathways — single phonon direct, two phonon Orbach and Raman processes — as well as quantum tunneling of magnetization (QTM) (Figure 4). As the different processes have different dependencies, within different applied field and temperature ranges, their relative contributions vary fro different SMMs.[6b, 37]

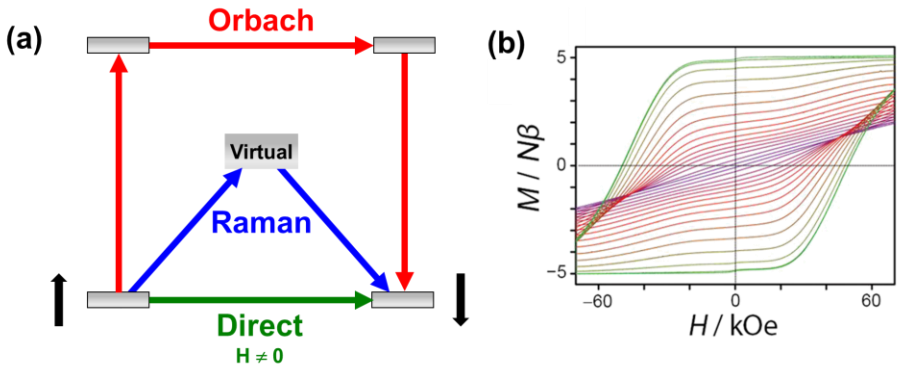

Figure 4. a) Simple schematic of phonon relaxation mechanisms that can contribute to the relaxation of magnetization in Ln-SMMs; b) Magnetization hysteresis of a high-performance Ln SMM $[(Cp^{iPr5})Dy(Cp^*)]^+$ (Cp^{iPr5} = penta-iso-propylcyclopentadienyl; Cp* = pentamethylcyclopentadienyl) with hysteresis observed up to 80 K. Figure 4b adapted with permission.[34a] Copyright (2018) Science.

2.4. Redox Properties

The ionization energies are correlated to the stability of the available lanthanoid redox states (II, III, IV).[38] For example, the third ionization energy (I_3) is high for Eu and Yb as this corresponds to loss of an electron from a half-shell and full-shell configuration, respectively. Similarly, the fourth ionization energy (I_4) is low for Ce. The cumulative ionization energies I_j ($I_1 + I_2 + I_3 + I_4$) reflect these trends (Figure 5).[38a] However, this does not account for the breadth of redox behavior observed across the series, for example molecular compounds of all divalent lanthanoids have now been reported despite lower I_3 values.[39] Appreciation of the thermodynamic considerations is required to better understand the redox properties.

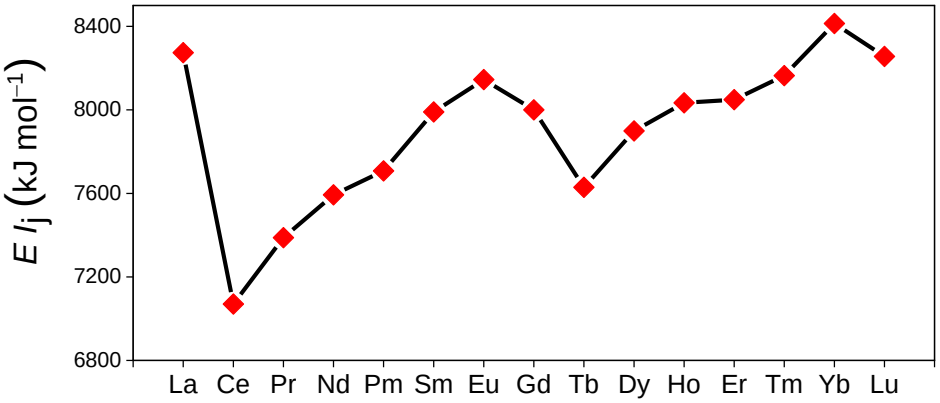

Figure 5. Sum of first four ionization potentials in kJ mol^{-1} where lower values suggest stabilization of the Ln(IV) state and higher values the stabilization of the Ln(II) state.[38a]

The characterization of thermodynamically stabilized divalent and tetravalent lanthanoid ions in solid-state materials has assisted with progress in overcoming the synthetic challenges associated with isolating these ions in molecular complexes, providing initial experimental data on these ions as well as information on stabilization in the solid-state. Thermodynamic stabilization in the solid-state has been particularly well reviewed in the context of the lanthanoid halides LnX_y (X = halide; y = 2, 3, or 4).[40] For simplicity, free energies will be approximated to enthalpies within this discussion, as is often encountered in relevant texts. The enthalpies of formation of LnX_y are largely accounted for by the lattice energy (exothermic contribution) and the sum of the first four ionization energies I_j (endothermic contribution).[38a] Smaller effects such as

the enthalpy of sublimation also contribute and can have substantial influence over the stabilization of 'non-traditional' LnX_2 or LnX_4 solids, particularly for Dy.[32, 41] If only the enthalpies of formation are considered, formation of LnX_n solids is unanimously favorable (exothermic).[40a, b] However, di- and tetravalent lanthanoid ions are susceptible to decomposition reactions (LnX_4) and disproportionation (LnX_2) leading to LnX_3.[40b] For example, despite being next to one another in the periodic table, Ce forms both CeF_3 and CeF_4, however La only forms LaF_3. Based on the enthalpy of formation, it should also be possible to obtain LaF_4.[40b] However, the decomposition of LaF_4 to LaF_3 is thermodynamically favorable as the sum of the enthalpies of formation of the products is much smaller than that of the reactants on both enthalpy and entropy grounds (with the production of fluorine gas). The enthalpies of formation for CeF_3 and CeF_4 are much more similar $\Sigma\Delta H_f$ *(products)* ~ $\Sigma\Delta H_f$ (reactants)), and the decomposition of CeF_4 is unfavorable at ambient temperatures.[38b, 40a] Stability of the dihalides are governed in a similar way with decomposition via disproportionation, which is exothermic unless the ratio of the enthalpies of formation for LnX_3 versus LnX_2 is small (< 1.5).[32, 40b] The disproportionation pathway is more likely to be endothermic and therefore stabilize the Ln(II) state when I_3 is high (Figure 5), which is most likely for Eu, Sm and Yb.[40b] Based on this criterion the halide most likely to stabilize many Ln(II) ions (Ln = Pr, Nd, Pm, Sm, Eu, Dy, Ho, Er, Tm, Yb) is the iodide ion, which will reduce the lattice energy of both tri- and divalent species and so the difference between these will become less significant, favoring the divalent ion, which is indeed reflected in the reported solid state structures.[40c, 42] This trend is also evident in the stabilization of the divalent state in molecular compounds, with the isolation of the first Ln(II) (Nd, Dy, and Tm) all involving iodide ligands.[43]

The aqueous chemistry of the lanthanoid metals is dominated by the Ln(III) state, with the Ln(III) $\rightarrow$ Ln(0) (aq) reduction potentials negative and Ln(II) and Ln(IV) ions readily oxidized and reduced, respectively, with processes 1 and 2 shown in Figure 6 thermodynamically favored.[38a, 44] There are some exceptions where kinetic stability is sufficient that decomposition or disproportionation to Ln(III) is slow enough to observe more unusual oxidation states, in particular for Ce(IV) and Eu(II).[45] The redox stabilities can be considered based on the enthalpies of oxidation (for Ln(II)) and reduction (Ln(III)), which are related to the enthalpies of hydration and I_3. The enthalpies of hydration are impacted most significantly by the size of the ions, so show a smooth increase as the ions become smaller with increasing atomic number, and their attraction for water molecules increases, with difference between hydration enthalpies of different oxidation states less as the size of the ion increases.[32, 40b] The most significant contribution is the I_3, with a high value associated with a more positive enthalpy.

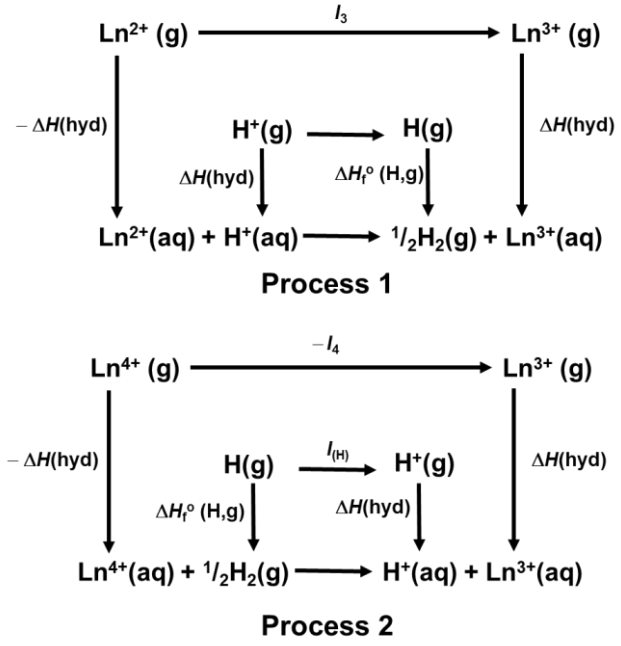

Figure 6. Thermochemical cycles for the stability of divalent process 1 (top) and tetravalent process 2 (bottom) aqua ions $E°(Ln^{II} \rightarrow Ln^{III})$ and $E°(Ln^{IV} \rightarrow Ln^{III})$.[74]

The trends in the redox potentials for the Ln(III) + $e^- \rightarrow$ Ln(II) reduction process and the Ln(IV) + $e^- \rightarrow$ Ln(III) oxidation process reflect the general stability of the ions (Figure 7).[32, 38a] As I_3 relates to the change in enthalpy for the process a relationship with ΔG (= $-nFE$ where ΔG = Gibbs free energy, n = number of moles of electrons, F = Faraday constant, E = redox potential) is expected.[32] Experimental data for the Ln(IV)/Ln(III) and Ln(III)/Ln(II) reduction potentials is limited, and so is often estimated based on Gibbs free energies of formation for the aqua ions, and spectroscopic measurements.[38a] However, for the most part Ln(III) ions are essentially redox-inactive under most conditions.

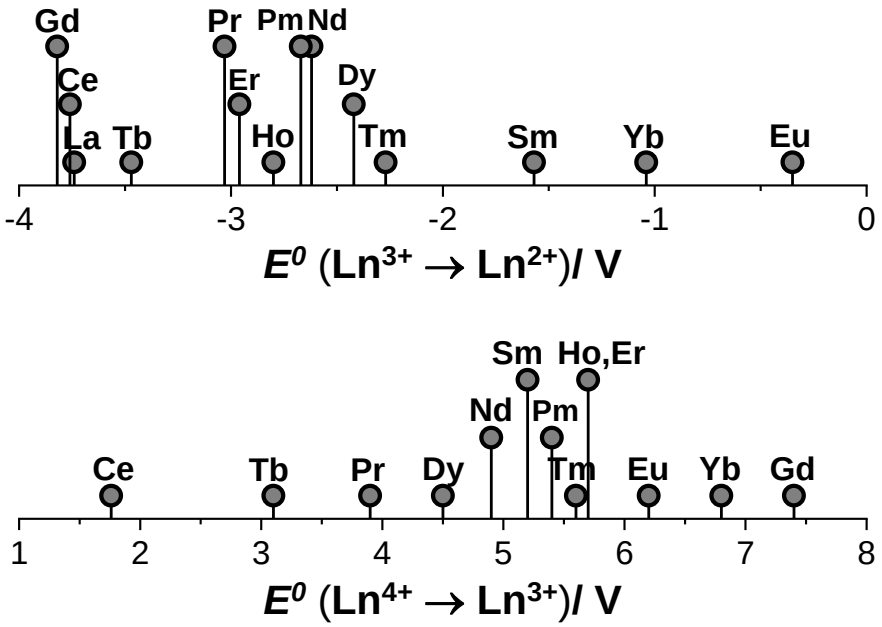

Figure 7. Standard reduction potentials for redox couples $Ln^{3+} \rightarrow Ln^{2+}$ and $Ln^{4+} \rightarrow Ln^{3+}$ (*E* vs. NHE) as calculated based on free energies of formation ΔG_f^0 (Ln^{2+}, Ln^{3+}, Ln^{4+}; aq).[38a]

In non-aqueous solvents, the range of accessible redox states of lanthanoid metals is much wider although observation is still often restricted to the metals which are most stable in the di- and tetravalent oxidation states.[45a, b, 46] Polar aprotic solvents can allow for the observation of metal-ligand interactions which would normally be hindered in aqueous conditions due to several factors (ligand protonation equilibria, Ln(III) hydrolysis, hydration of the cations). As the coordination of a ligand and a metal ion in solution occurs in competition with the solvation of the individual components (with highest competition for the cation), solvent binding strength of the lanthanoid plays an obvious role in the thermodynamics of ligand coordination in non-aqueous solvents, and thus the stabilities of the complexes.[45a] Kimura *et al.* found that the size of the free energy of transfer of the ions from water to a non-aqueous solvent followed the solvent donor number (DMSO > DMF ≈ H_2O > methanol > ethanol ≈ acetone > acetonitrile ≈ THF).[45a, 47] The solvation of the metal ion also depends on both electrostatic and steric factors including the ionic radius, the nature of the solvent, and molecular volume.[45a] The ligand environment influences the energy differences between the highest occupied and lowest unoccupied molecular orbitals (HOMO and LUMO, respectively), with the associated energy gap concurrently affecting the redox potentials. Factors that are considered with regards to ligand stabilization include the saturation

of the coordination sphere, type of donor atoms, and steric influence of the scaffold.[45a] Albrecht-Schmitt *et al.* compared the electrochemical behavior of a series of 222-cryptand complexes of Sm, Eu, and Yb under non-aqueous conditions (0.1 M $NPr_4BAr^F_4$, THF).[48] The ease of Ln(III)/Ln(II) reduction follows the expected stabilities based on the standard redox potentials (Eu > Yb > Sm), with all showing quasi-reversible behavior. The Sm analogue exhibited the least reversibility, suggesting that despite the stabilization of Sm(II) by the ligand, the divalent state in this case is still relatively unstable. The cyclic voltammogram for the Yb analogue showed greater reversibility, which was attributed to solvent dynamics. The Yb analogue has a higher charge density and so is more likely to be stabilized by the cryptand in relatively non-polar solvent such as THF, compared to Eu and Sm. Modulation of the ligand field in a series of Eu and Yb cryptand complexes was also recently reported, investigating whether the ligand effects observed originally for the Eu series were translatable to other divalent lanthanoid ions.[49] Coordination induced differences in the electrochemical properties between the small Yb(II) and mid-sized Eu(II) ions were observed when a series of four cryptand scaffolds were altered to induce variations in electronic and steric character.[49] Similar trends in the redox potentials (0.1 M $Et_4N(ClO_4)$ in N,N-dimethylformamide (DMF)) were observed for both ions across the ligand series (nitrogenous donors stabilizing the Ln(II) state) with Yb(II) cryptates having more negative potentials for the Ln(III)/Ln(II) couple in-line with the standard reduction potentials. Schelter *et al.* investigated the modulation of the coordination environment in a series of cerium(IV) tetrakis(pyridyl-nitroxide) compounds along with their Ce(II) counterparts with varying ligand field strengths used to assess the tuning of the reduction potentials in non-aqueous conditions (0.1 M $[^nPr_4N][BAr^F_4]$ in THF/MeCN (1:4) solution).[50] The complexes of general formula $[Ce^{III}(\mu\text{-(R-2-ON}^t\text{Bu)py))(R-2-(ON}^t\text{Bu)py)}_2]_2$ (**1**) and $[Ce^{IV}\text{(R-2-(ON}^t\text{Bu)py)}_4]$ (**2**) where R = 5-CF_3, 5-Me, 3-OMe, 5-*para*-NMe_2, and 4-*meta*-NMe_2 were synthesized to investigate the effect of electron-withdrawing and electron-donating substituents, with solution electrochemistry experiments indicating a shift in the potential of the Ce(IV)/Ce(III) couple of ~ 500 mV with −1.46 V for CF_3 and −1.94 V for *m*-NMe_2 substituted ligands (Figure 8), and corroborated by extensive density functional theory (DFT) investigations.

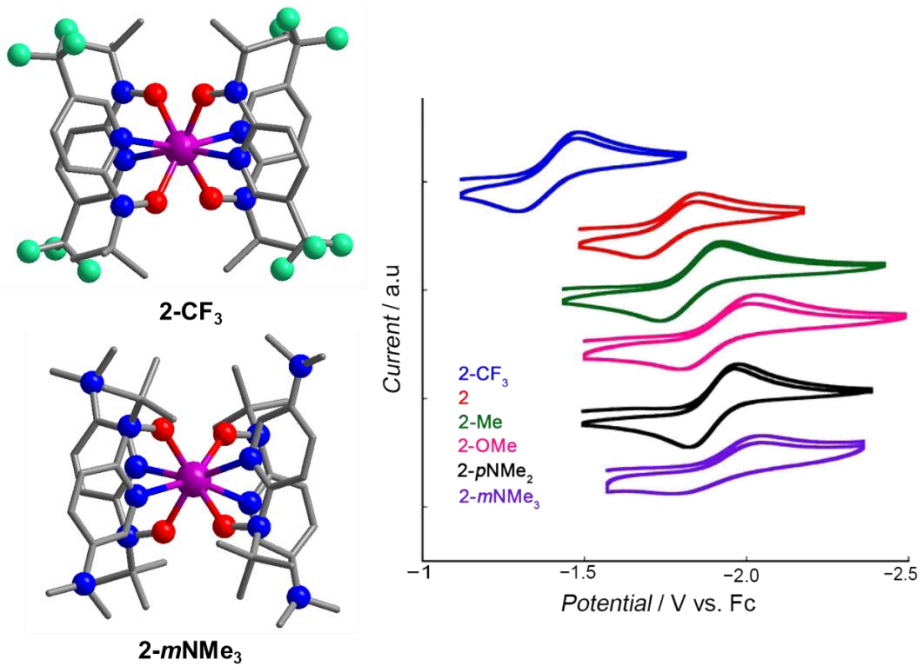

Figure 8. Structure of **2-CF$_3$** and **2-*m*NMe$_3$** (left) and cyclic voltammograms (0.1 M [nPr4N][BArF4] in THF/MeCN (1:4)) of the isolated Ce(IV)/(III) reduction features in the full series of **2-R** complexes (right).[50] Color scheme: lanthanoid (pink), carbon (dark gray), fluorine (mint green), nitrogen (blue), oxygen (red), cerium (purple). Hydrogen atoms have been omitted for clarity. Cyclic voltammograms adapted with permission.[50] Copyright (2015) American Chemical Society.

Table 1. Compounds discussed in this review with the lanthanoid oxidation state, innocent (redox-inactive) ligand and redox-active ligand provided where applicable.

	Formula [a,b]	Oxd. State	Innocent Ligand[c]	Redox-active ligand[d]	Ref.
1	[Ce(μ-(R-2-(^{t}BuNO)py))(R-2-(^{t}BuNO)py)$_2$]$_2$	III	R-2-(^{t}BuNO)py	-	50
2	[Ce(R-2-(^{t}BuNO)py)$_4$]	IV	R-2-(^{t}BuNO)py	-	50
3	[Eu^{II}(N(Si(CH$_3$)$_3$)$_2$)$_2$(DME)$_2$]	II	N(Si(CH$_3$)$_3$)$_2$	-	56a
4	[Eu^{II}(N(Si(CH$_3$)$_3$)$_2$)$_2$(bpy)]	II	N(Si(CH$_3$)$_3$)$_2$	-	56a
5	[Ln^{II}(N(Si(CH$_3$)$_3$)$_2$)$_2$(DMPE)$_{1.5}$]	II	N(Si(CH$_3$)$_3$)$_2$	-	54a
6	[LnI$_2$L^{Ph}(THF)]	II	L^{Ph}	-	57
7	[LnI$_2$L^{Cy}(THF)]	II	L^{Cy}	-	57
8	[Yb(N$_8$L$_{crypt}$)]	II	N$_8$L$_{crypt}$	-	49
9	[Yb(Me$_6$N$_8$L$_{crypt}$)]	II	Me$_6$N$_8$L$_{crypt}$	-	49
10	[Yb(O$_4$N$_2$L$_{crypt}$)]	II	O$_4$N$_2$L$_{crypt}$	-	49
11	[Yb(PhO$_4$N$_2$L$_{crypt}$)]	II	PhO$_4$N$_2$L$_{crypt}$	-	49

12	$[Ln(Me_2N_4L)(THF)_x]$	II	Me_2N_4L	-	60a
13	[Eu(DOTA-4AmC)]	II	DOTA-4AmC	-	60i
14	$[Ln(TPA)I_2]$	II	TPA	-	61
15	$[Ln(TPA)_2]I_2$	II	TPA	-	61
16	$[Eu(BPA)_2]$	II	BPA	-	61
17	$[Yb(BPA)I(CH_3CN)]_2$	II	BPA	-	61
18	$[Tm(\mu\text{-}OTf)_2(dme)_2]_n$	II	OTf	-	68a
19	$[TmI_2(18\text{-}c\text{-}6)]$	II	18-crown-6	-	35c
20	$[Nd(OTf)_2(crypt)]$	II	Aza-2.2.2-cryptand	-	68b
21	$[K(18\text{-}crown\text{-}6)(OEt_2)][LaCp''_3]$	II	Cp″	-	70b
22	$[K(2.2.2\text{-}cryptand)][LaCp''_3]$	II	Cp″	-	70b
23	$[K\ (18\text{-}crown\text{-}6)(OEt_2)][LnCp'_3]$	II	Cp′	-	74a, 75
24	$[K(2.2.2\text{-}cryptand)][LnCp'_3]$	II	Cp′	-	71a
25	[EuCl(aza-2.2.2-crypt)]	II	aza-2.2.2-cryptand	-	59a
26	$[Ce(salophen)_2]$	IV	salophen	-	86
27	$[Ce(5,5'\text{-}(OMe)_2\text{-}salen)_2]$	IV	$5,5'\text{-}(OMe)_2$-salen	-	86
28	$[Ce(5,5'\text{-}(Br)_2\text{-}salen)_2]$	IV	$5,5'\text{-}(Br)_2$-salen	-	86
29	$[Ce_2(O^tBu)_8]$	IV	O^tBu	-	88
30	$[Ce(O^tBu)_2\{N(SiMe_3)_2\}_2]$	III	O^tBu/ $N(SiMe_3)_2$	-	88
31	$[Ce(MBP)_2(THF)_2Li(THF)_2]$	III	MBP	-	89
32	$[Ce(MBP)_2(THF)_2]$	IV	MBP	-	89
33	$[Ce(MBP)_2(bpy)Li(THF)_2]$	III	MBP	-	89
34	$[Ce(MBP)_2(bpy)]]$	IV	MBP	-	89
35	$[Ce_2(p\text{TP}^R)_2(THF)_4]$	IV	$p\text{TP}^R$	-	90
36	$[K(THF)_n][\ Ce_2(p\text{TP}^R)_2(THF)_4K]$	III	$p\text{TP}^R$	-	90
37	$[Ce(NO_3)(O^tBu)_3(THF)_2]$	IV	O^tBu	-	90
38	$[\{O(OSiPh_2)_2\}]_2[Ce(O^tBu)_2]$	IV	$OSiPh_2$	-	91
39	$[\{KO^tBu(DME)\}\{O(OSiPh_2)_2\}_2][Ce\{KO(OSiPh_2)\}]_2$	IV	$OSiPh_2$	-	91
40	$[Ce(OSi(O^tBu)_3)_4]$	IV	$OSi(O^tBu)_3$	-	92
41	$Ce(OSi(O^tBu)_3)_4(THF)]$	IV	$OSi(O^tBu)_3$	-	92
42	$[M_3(THF)_n][Ce(BINOLate)_3]$	III	BINOLate	-	96a
43	$[Li_3(THF)_5][Ce(BINOLate)_3Cl]$	IV	BINOLate	-	96a
44	$[Ce(NP(pip)_3)_4]$	IV	$NP(pip)_3$	-	99
45	$[Ce(NP(pip)_3)_4(Et_2O)K]$	III	$NP(pip)_3$	-	99
46	[Tb(NP(1,2-bis-^{t}Bu-diamidoethane)$(NEt_2))_4$]	IV	NP(1,2-bis-^{t}Bu-diamidoethane)	-	97a
47	[Tb(NP(1,2-bis-^{t}Bu-diamidoethane)$(NEt_2))_4(Et_2O)K$]	III	NP(1,2-bis-^{t}Bu-diamidoethane)	-	97a
48	$[Tb(OSi(O^tBu)_3)_4K]$	III	$(OSi(O^tBu)_3)$	-	82b
49	$[Tb(OSi(O^tBu)_3)_4]$	IV	$(OSi(O^tBu)_3)$	-	82b
50	$[Tb(OSiPh_3)_4(MeCN)_2]$	IV	$OSiPh_3$	-	100
51	$[Tb(OSiPh_3)_4(THF)K]$	III	$OSiPh_3$	-	100
52	$[Pr(OSiPh_3)_4(MeCN)_2]$	IV	$OSiPh_3$	-	82a
53	$[Pr(OSiPh_3)_4(THF)K]$	III	$OSiPh_3$	-	82a
54	$[NdI_3(^{dipp}iq^o)_2]$	III	I	^{dipp}iq	105a

55	[Nd(^{dipp}isq$^{\bullet-}$)$_2$I(THF)]		I/THF	^{dipp}isq	105a
56	[K(18-crown-6)][Nd(^{dipp}ap)$_2$(THF)$_2$]	III	THF	^{dipp}ap	105a
57	[Eu(FOD)$_3$(L_{TERP})]	III	FOD	L_{TERP}	107
58	[Tb(NO_3)L_{phen}]	III	L_{phen}	L_{phen}	109a
59	[Yb(NO_3)L_{phen}]	III	L_{phen}	L_{phen}	109a
60	[Eu(tta)$_3$(L_1)]	III	tta	L_1 (TPA-bpy)	30d
61	[Sm(tta)$_3$(L_1)]	III	tta	L_1 (TPA-bpy)	30d
62	[Eu(tta)$_3$(L_2)]	III	tta	L_2 (TPA-xy-bpy)	30d
63	[Tb(Pc)$_2$]	III	-	Pc	110
64	[TBA][Tb(L_1)$_2$]	III	-	L_1	114
65	[TBA][Tb(L_2)$_2$]	III	-	L_2	114
66	[TBA][Tb(L_3)$_2$]	III	-	L_3	114
67	(R)/(S)-[Dy(Pc(OBNP)$_2$)(TClPP)H]	III	TClPP	Pc(OBNP)$_2$]	117
68	(R)/(S)- [Dy[(Pc(OBNP)$_2$)(TClPP)]	III	TClPP	Pc(OBNP)$_2$]	117
69	[K(18-crown-6)(THF)$_2$][(TbN(SiMe$_3$)$_2$)$_2$(THF))$_2$(μ-$N_2^{\bullet-}$)]	III	N(SiMe$_3$)$_2$	N_2	120
70	[(Ln(Cp*)$_2$)$_2$(μ-ind)]$^{n-}$	III	Cp*	μ-ind	122
71	[(Ln(Cp*)$_2$)$_2$(μ-ind)]$^{n-}$	III	Cp*	μ-ind	122
72	[Dy$_2$(tmhd)$_6$(bptz)]	III	tmhd	bptz	125
73	[CoCp$_2$]$^+$[Dy$_2$(tmhd)$_6$(bptz$^{\bullet-}$)]	III	tmhd	bptz	125
74	[(Ln(HB(pz)$_3$)$_2$)$_2$(μ-tetraoxolene)]	III	HB(pz)$_3$	μ-tetraoxolene	126
75	[CoCp$_2$][(Dy(HB(pz)$_3$)$_2$)$_2$(μ-CA$^{\bullet-}$)]	III	HB(pz)$_3$	μ-CA$^{\bullet-}$	126
76	[CoCp$_2$][(Tb(HB(pz)$_3$)$_2$)$_2$(μ-CA$^{\bullet-}$)]	III	HB(pz)$_3$	μ-CA$^{\bullet-}$	127
77	[CoCp$_2$][(Gd(HB(pz)$_3$)$_2$)$_2$(μ-CA$^{\bullet-}$)]	III	HB(pz)$_3$	μ-CA$^{\bullet-}$	127
78	[(Dy(HB(pz)$_3$)$_2$)$_2$(μ-CA)]	III	HB(pz)$_3$	μ-CA	127
79	[(Tb(HB(pz)$_3$)$_2$)$_2$(μ-CA)]	III	HB(pz)$_3$	μ-CA	127
80	[(Gd(HB(pz)$_3$)$_2$)$_2$(μ-CA)]	III	HB(pz)$_3$	μ-CA	127
81	[(Dy(HB(pz)$_3$)$_2$)$_2$(μ-CA)]	III	HB(pz)$_3$	μ-BA	128
82	[CoCp$_2$][(Dy(HB(pz)$_3$)$_2$)$_2$(μ-BA$^{\bullet-}$)]	III	HB(pz)$_3$	μ-BA$^{\bullet-}$	128
83	[Dy(hfac)$_3$(L)]$_2$	III	hfac	L_{TTF}	131
84	[Dy(tta)$_3$(L)]·1.41CH_2Cl_2	III	tta	L_{TTF}	131
85	[Yb(tta)$_3$(L)]·2CH_2Cl_2	III	tta	L_{TTF}	131
86	[Yb$_2$(hfac)$_6$(H_2L_{SQ})]·0.5CH_2Cl_2	III	hfac	H_2L_{SQ}	132
87	[Yb$_2$(hfac)$_6$(L_Q)]	III	hfac	L_Q	132
88	[Yb^{III}(Me_5C_5)$_2$(bpy$^{\bullet-}$)]	II/III	Cp*	bpy	135
89	[YbCp*$_2$(4-Me-bpy)]	II/III	Cp*	4-Me-bpy	133c
90	[YbCp*$_2$(5-Me-bpy)]	II/III	Cp*	5-Me-bpy	133c
91	[YbCp*$_2$(6-Me-bpy)]	II/III	Cp*	6-Me-bpy	133c
92	[YbCp*$_2$(4,4′-Me_2-bpy)]	II/III	Cp*	4,4′-Me_2-bpy	133c
93	[YbCp*$_2$(5,5′-Me_2-bpy)]	II/III	Cp*	5,5′-Me_2-bpy	133c
94	[YbCp*(6,6′-Me_2-bpy)]	II/III	Cp*	6,6′-Me_2-bpy	133c
95	[Yb(η^5-C_9H_7)$_2$(IPy^0)]	II	η^5-C_9H_{72}	IPy^0	139
96	[YbCp*$_2$(A-IPy)$^{\bullet-}$]	III	Cp*	H-IPy	138
97	[YbCp*$_2$(B-IPy)^0]	II	Cp*	C_4H_3O-IPy	138

98	[YbCp*$_2$(C-IPy)^0]	II	Cp*	C_4H_3S-IPy	138
99	[YbCp*$_2$(D-IPy)^0]	II/III	Cp*	C_6H_5-IPy	138
100	[Yb(dpp-BIAN)(μ-Br)(DME)]$_2$	III (278 K) II (368 K)	Cl/dme	dpp-BIAN	23a
101	[Yb(dpp-BIAN)(μ-Cl)(DME)]$_2$	III/III (< 150 K) III/II (> 150 K)	Cl/dme	dpp-BIAN	23b
102	[Eu(dpp-BIAN)(μ-Cl)(DME)]$_2$	II	Cl/dme	dpp-BIAN	140a
103	[Eu(dpp-BIAN)(μ-Br)(DME)]$_2$	II	Br/dme	dpp-BIAN	140a
104	[Eu(dpp-BIAN^{2-})(dme)$_2$]	II	dme	dpp-BIAN	140b
105	[Yb(dpp-BIAN^{2-})(dme)$_2$]	II	dme	dpp-BIAN	140b
106	[Eu(dpp-BIAN $^{2-}$)(bpy)$_2$]	II		dpp-BIAN/bpy	140b
107	[Yb^{III}(dpp-BIAN^{2-})(bpy$^{-\bullet}$)(bpy)]	III		dpp-BIAN/bpy	140b

[a] Ligand definitions can be found in main text. [b] Where Ln has been denoted, the associated lanthanoid metals are indicated in the main text. [c] Chemical drawings of the ancillary ligands can be found in Schemes 1 and 2. [d] Chemical drawings of the redox-active ligands can be found in Schemes 3 and 4.

3. Lanthanoid Complexes with Unusual Lanthanoid Oxidation States

3.1. Lanthanoid(II) Complexes

Isolated molecular complexes involving divalent lanthanoid ions are comparatively more accessible than those involving the tetravalent oxidation state, with all the divalent lanthanoids now reported in molecular compounds, except for radioactive promethium.[51] Although the existence of Ln(II) in solid state materials had been known for many years, it has taken much longer for molecular Ln(II) species to be isolated. The more accessible Ln(II) ions (Eu, Sm, and Yb) have been reasonably well explored in molecular species, and continue to gain attention for applications as reduction reagents, catalysts, and for small molecule activation.[20a, 52] Among the first Ln(II) complexes to be reported were those featuring the bulky cyclopentadienyl (Cp) and cyclooctatetraene (COT) ligands,[53] phosphane,[54] selenolate,[55] and silylamide ligands (

Scheme *1*).[56] For example, bis(trimethylsilyl)amine $((CH_3)_3Si)_2N)^-$ was used to prepare six-coordinate $[Eu^{II}(N(Si(CH_3)_3)_2)_2(DME)_2]$ (**3**) (DME = 1,2-dimethoxyethane) and four-coordinate $[Eu^{II}(N(Si(CH_3)_3)_2)_2(bpy)]$ (**4**) (bpy = 2,2'-bipyridine).[56a] Similar species were then used as precursors to obtain the phosphine complexes of Yb(II) and Eu(II) in which a silylamide ligand, and a coordinated diethyl ether in the case of Yb, was displaced by 1,2-bis(dimethylphophanyl)ethane (DMPE) giving $[Ln^{II}(N(Si(CH_3)_3)_2)_2(DMPE)]$ (**5**).[54a] More recently Nocton and co-workers have studied the coordination of Yb and Sm with iminophosphorane ligands.[160] Two related ligands were investigated: L^{Ph} and L^{Cy} (L = bis(methyliminophosphoranyl)pyridine, where Ph and Cy denote triphenyl and tricyclohexyl substitution at the phosphorus position, respectively) resulting in the formation of $[LnI_2L^{Ph}(THF)]$ (**6**) and $[LnI_2L^{Cy}(THF)]$ (**7**).[57] Reaction of the Yb analogues with benzophenone resulted in the displacement of the coordinated THF and one-electron reduction of the ketone, with the stability of the resulting ketyl radical found to be dependent on the steric demand of the ligand. Cryptand complexes of the traditional divalent lanthanoids were some of the first to be investigated, with the benefit of encapsulation aiding in the stabilization of Ln(II) state and facilitating studies of luminescent properties through prevention of quenching by deterring inner sphere solvent coordination.[58] A recent spectroscopic and electrochemical investigation of Eu(II) and Yb(II) complexes ($[Yb(N_8L_{crypt})]$ (**8**), $[Yb(Me_6N_8L_{crypt})]$ (**9**), $[Yb(O_4N_2L_{crypt})]$ (**10**), and $[Yb(PhO_4N_2L_{crypt})]$ (**11**) (Scheme 1)) probed the impact on the redox properties of systematic variation of the electronic and steric properties of cryptand ligands.[49] Although the Eu(II) analogues were previously reported,[58b, c, 59] these had not yet been investigated for Yb. Overall, similar trends in the order of redox potentials for the Yb series and the Eu series were observed, with the processes for the Yb(II) complexes exhibiting more negative potentials than the Eu(II). The study revealed that nitrogenous donors gave rise to bathochromic shifts resulting in visible light absorption.[49]

Scheme 1. Ligands and proligands for divalent lanthanoid ions discussed in this review.

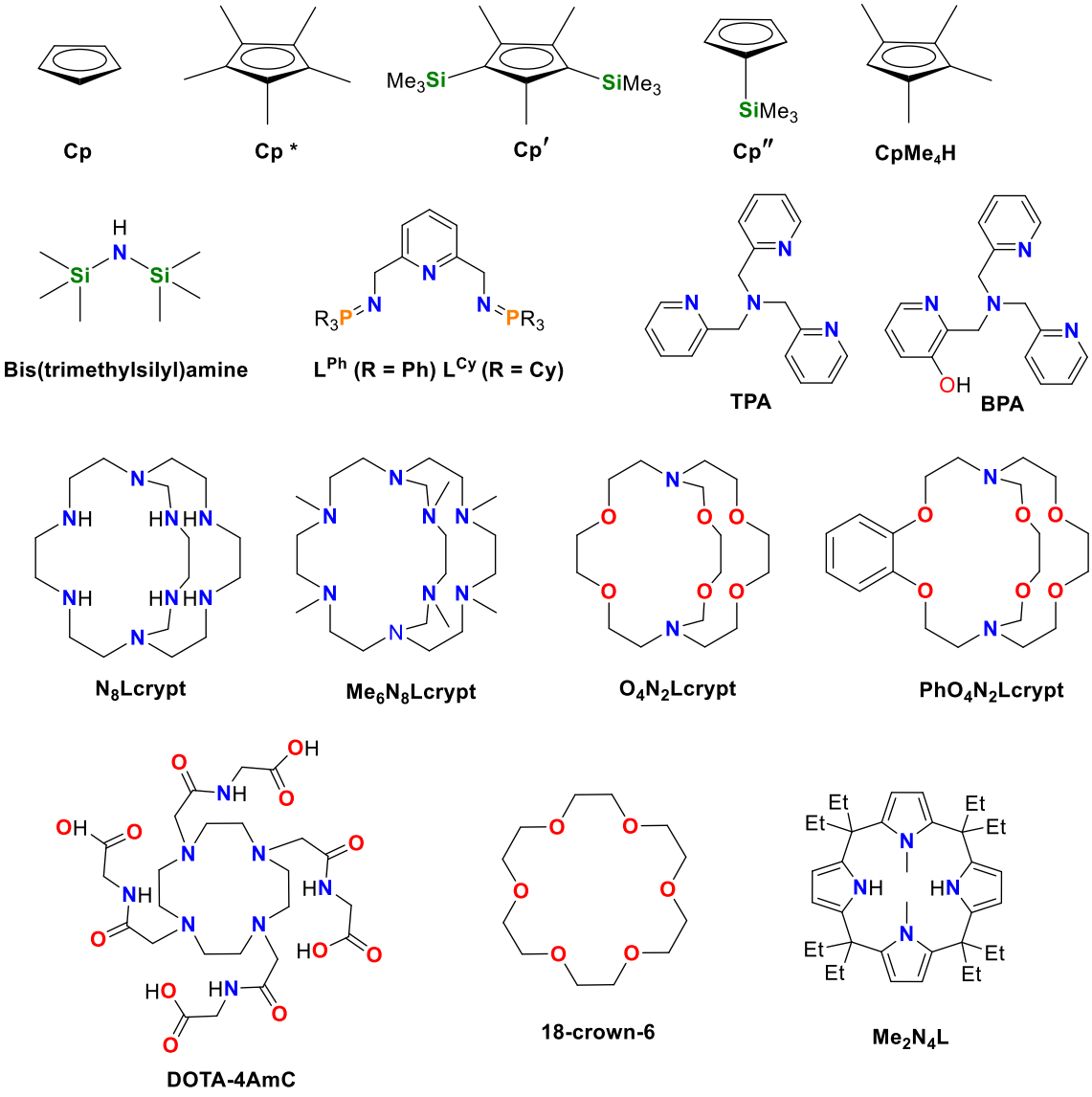

Other macrocycles such as the crown-ethers and polyethylene glycols have also been utilized.[60] For example, White and co-workers synthesized Sm(II), Eu(II), and Yb(II) complexes of doubly deprotonated trans-N,N′-dimethyl-meso-octaethylporphyrinogen (Me_2N_4L) as tetrahydrofuran adducts [Ln(Me_2N_4L)(THF)$_x$] (**12**) (x = 2 for Sm and Eu, x = 1 for Yb).[60a] In contrast to the Eu and Yb analogues, only the Sm adduct was found to oxidize when reacted with ^{t}Bu-DAB (= 4-di-t-butyl-1,4-diazabuta-1,3-diene), emphasizing the effects of the metal size and reduction potential on the reactivity. Allen and co-workers reported the facile conversion of a Eu(III) center

to Eu(II) in a tetraglycinate complex [Eu(DOTA-4AmC)] (**13**) (DOTA-4AmC = 1,4,7,10-tetraazacyclododecane1,4,7,10-tetrakis(acetamidoacetate)).[60i] Mazzanti and co-workers investigated several tripodal N-donor and mixed N,O-donor ligands to isolate Sm, Eu, and Yb complexes with the aim of investigating the stability of the di- and trivalent oxidation states on varying the electron richness of the ligand.[61] For the investigation three similar tetradentate ligands — N_4-donor (TPA), N_3O-donor (BPA) and N_2O_2 (MPA) – were selected with associated charges varying from neutral (TPA) to dianionic (MPA). The TPA ligand was found to be most successful in stabilizing the Ln(II) compounds forming isolated complexes [Ln(TPA)I_2] (**14**) (Ln = Eu, Yb) and [Ln$(TPA)_2$]I_2 (**15**) (Ln = Sm, Eu, Yb). The dianionic ligand MPA was only able to stabilize a Eu(II) intermediate, observed by NMR. The BPA ligand is intermediate in terms of stabilizing an isolated Ln(II) species, forming complexes [Eu$(BPA)_2$] (**16**) and [Yb(BPA)I$(CH_3CN)]_2$ (**17**), with the single phenol group reducing the stability of the Yb(II) complex. Cyclic voltammetry performed on the bis-ligand compounds of Eu and Yb showed that the metal centered reduction occurs at significantly lower potentials for the BPA compounds, with the added electron-richness yielding much more reductive Ln(II) species, hence preferring the trivalent state. This was also demonstrated through reduction of CS_2 using the intermediate BPA complexes.[61] Research into the stabilization of the more accessible divalent lanthanoids using various ligands has continued to grow over the years with systems such as formamidinates,[52c, 62] siloxides,[63] pyrazolates,[64] phenolates,[33c, 65] and various others.[66]

Before the isolation and crystallographic characterization of divalent Tm, Dy and Nd in their solvated diiodo form [LnI_2(solv)$_3$] (solv = DME, THF), it was believed that molecular complexes of these ions would result in the decomposition of any solvent due to their reactivity.[43, 67] Since then, harnessing the coordinative control necessary to isolate divalent ions of Tm, Dy, Nd has presented a synthetic challenge. Divalent ions of these three metals have now been reported, mainly as cyclopentadienyl derivatives, and the majority involving thulium.[35c, 56b, 68] A few notable recent examples include a divalent thulium complex [Tm(μ-OTf)$_2$(dme)$_2$]$_n$ (**18**) on which the first molecular Tm(II) luminescent measurements were reported.[68a] The luminescent measurements in corroboration with extensive EPR studies were used to unambiguously define the nature of the electronic ground state.[68a] Soon after, Tm(II) in the crown ether complex [TmI_2(18-crown-6)] (**19**) was found to display field induced slow relaxation of magnetization.[35c]

Very recently the isolation of a Nd(II) in a cryptand complex was reported [Nd(OTf)$_2$(crypt)] (**20**), isolated via the chemical reduction of the Nd(II) cryptand precursor.[68b]

All six divalent lanthanoid ions discussed so far — Nd, Sm, Eu, Dy, Tm, Yb — share a common [Xe]4f^{n+1}5$d^0$6s^0 configuration. With regards to the rest of the lanthanoids, four are known to form diiodide salts (La, Ce, Pr, Gd) which in the solid state show evidence of occupation of the 5*d* orbitals, such that their configuration is [Xe]4f^n5$d^1$6s^0.[40c, 42, 69] This 'configuration crossover' was found to persist in molecular species of La and Ce.[70] This prompted a race towards accessing the rest of the divalent lanthanoids (Tb, Ho, Er, Lu) in molecular compounds, which were later found to have a similar configuration crossover with occupation of the 5*d* orbital.[51, 71] Therefore, the stabilization of these harder to achieve divalent lanthanoid ions was attributed to lowering the energy of a *d*-orbital, allowing *d*-electron participation in metal to ligand bonding.[72]

Lappert and Evans were at the forefront of Ln(II) chemistry with their pioneering work on Ln cyclopentadienyl (Cp) ligand systems. With the aim of isolating the complexes in the divalent oxidation state, Lappert and co-workers investigated the Cp″$_3$Ln (Cp″ = $C_5Me_3(SiMe_3)_2$-1,3) system.[73] Ultimately, this resulted in a crystal structure of an isolated La(II) molecular complex [KR][LaCp″$_3$] where (**21** = R = (18-crown-6)(OEt$_2$); **22** = R = (2.2.2-cryptand)).[70b] Based on La(II)-Cp″ centroid distances in these complexes, which were slightly longer than for the La(III) analogue, and in contrast to the previous Ln(III) and 4f^{n+1} Ln(II) complexes, it was proposed that La(II) possesses a 5d^1 (rather than a 4f^1) configuration. This is in agreement with EPR, magnetic susceptibility and DFT studies.[70b] Evans and co-workers expanded on this by testing the dinitrogen reduction of multiple Cp$_3$La complexes with various substituents on the Cp rings, suggesting some ligands (those that don't reduce N$_2$) are better for isolating Ln(II) complexes.[74] This then led to the isolation of the related [K(18-crown-6)][LnCp′$_3$] (**23**) analogues where Ln = Y, Ho, Er and Cp′ = $(C_5H_4SiMe_3)^-$.[74a, 75] Similarly to [LaCp″$_3$], it was found through DFT studies that the LUMO of the LnCp′$_3$ precursor and HOMO of [LnCp′$_3$]$^-$ products (Ln = Y, Ho, Er) are d_{z^2} orbitals, with the UV-Visible spectra of Ho and Er analogues very similar to the 4d^1 Y(II) complex.[74a, 75] Hence the electronic structure was concluded to be the non-traditional 4f^n5d^1 configurations. This is rationalized on the basis of the crystal field created by the cyclopentadienyl ligands lowering the d_{z^2} orbital so that it can be populated competitively with the 4*f* orbitals.[76] The series was then expanded through use of a different counter cation [K(2.2.2-cryptand)] (**24**), to give complexes of Pr, Gd, Tb and Lu, all of which agreed with the 4f^n5d^1 configurations (Figure 9).[71a] Eventually complexes of this form were synthesized across the lanthanoid series to

compare the configurations and spectroscopic properties. All but Sm, Eu, Tm and Yb were found to have $4f^n5d^1$ configurations, which is evident from analysis of the promotion energies between the $4f^{n+1}$ to $4f^n5d^1$ configurations (Figure 9).[74b, 77] This is a particularly important observation, as given that previous reports had suggested $4f^n$ configurations, it appears that the electronic ground state of Dy(II) and Nd(II) could depend on the coordination environment.[77-78]

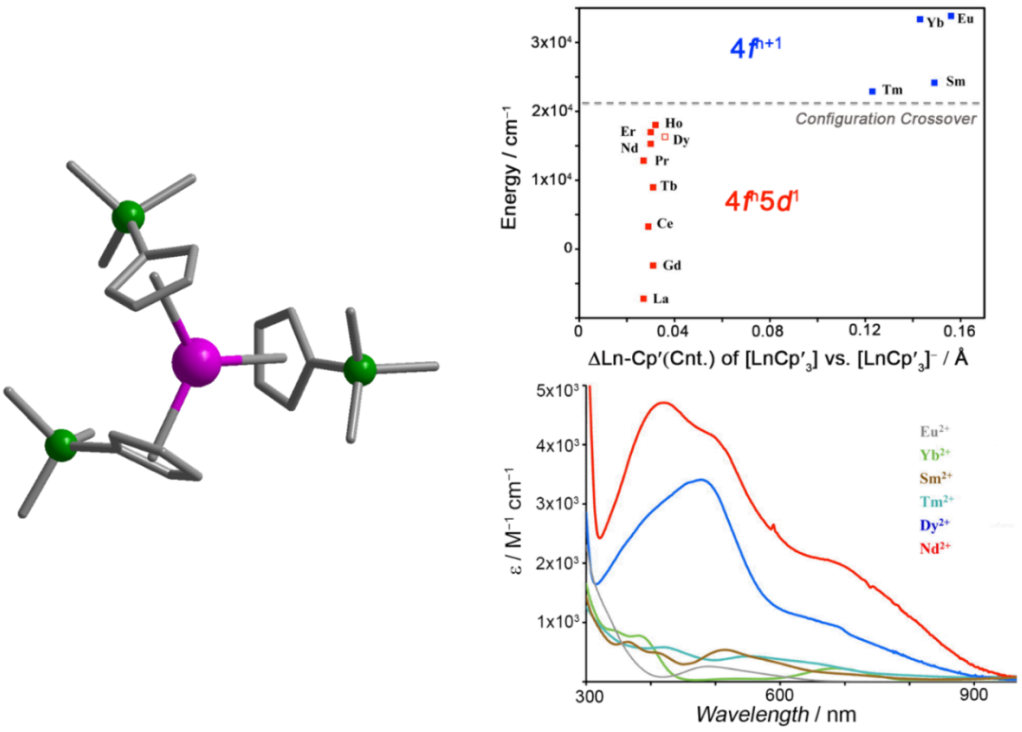

Figure 9. Left: Crystal structure of anionic complex **24** (color scheme as per Figure 8 and silicon (green)). Top right: Plot of the differences in Ln−Cp′ centroid distances of $[Ln^{III}(Cp')_3]$ and anionic $[Ln^{II}(Cp')_3]^-$ (**24**) vs the $4f^{n+1}$ to $4f^n5d^1$ promotion energies where the grey dashed line indicates the barrier in promotion energies to reduce the Ln(III) to a Ln(II) with a $4f^{n+1}$ (blue squares) or $4f^n5d^1$ (red squares) configuration. Bottom right: Experimental UV−vis spectra in THF of **24** (Ln = Nd, Sm, Eu, Dy, Tm, Yb). Adapted with permission.[77] Copyright (2015) American Chemical Society.

With a deeper understanding of stabilization of the divalent lanthanoid ions has come the investigation of potential applications of molecular lanthanoid(II) chemistry, for example, the recent use of Eu(II) as a photoredox catalyst by Allen and co-workers.[79] Metal-assisted

photoredox catalysis involves the use of light to alter the redox properties of compounds to drive chemical reactions, and has been demonstrated for the generation of a variety of reactive species.[44,215,216] Lanthanoid based photocatalysts have the potential to access challenging organic substrates due to their exceptional reducing power in their photoexcited states. The first instance of a lanthanoid(II) ion used in a catalytic capacity employed the complex [$Eu^{II}Cl$(aza-2.2.2-crypt)] (**25**) (aza-2.2.2-crypt = 1,4,7,10,13,16,21,24-octaazabicyclo[8.8.8]hexacosane), which had previously been investigated for its luminescent properties.[30a, 59a] On absorption of blue light, the Eu(II) cryptand complex luminesces via a 5*d*-4*f* transition in the visible region with a long associated lifetime and high quantum yield (0.98 μs and 37% in methanol respectively).[79] Using a sacrificial reducing agent (Zn^0) to ensure the Eu remains catalytic, Allen and co-workers reported the first example of catalytic C-C bond formation using a divalent lanthanoid and visible light.[58b] Through various experiments, they were able to propose the catalytic cycle shown in Figure 10, whereby two molecules of the photoexcited Eu(II)* complex reduce two molecules of benzyl chloride through electron transfer, followed by reductive coupling.[79] The demonstration of the negative electrochemical potential (comparable to SmI_2) [80] and the use of air-stable, and relatively inexpensive, starting materials suggests that there's significant potential to develop further Eu(II) photocatalysts for wider reaction scope.

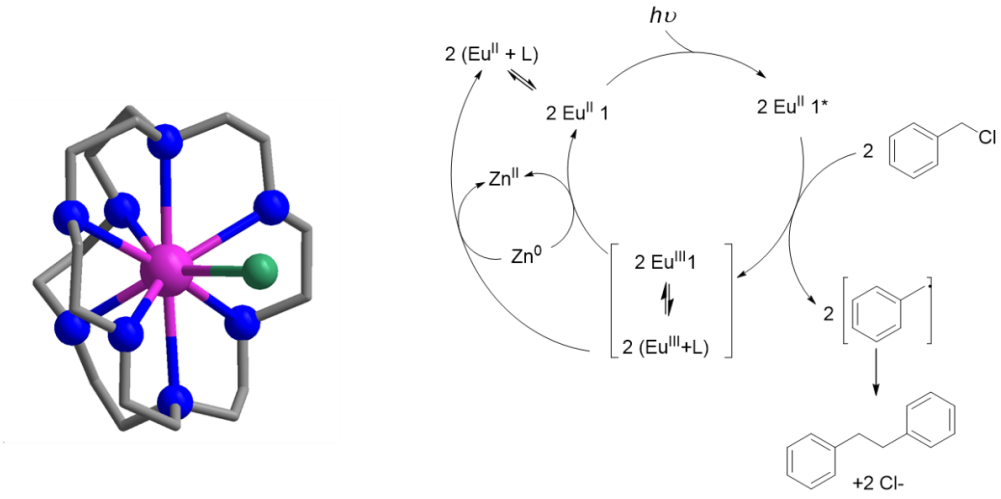

Figure 10. Structure of **25** (color code as per Figure 8 and chlorine (green)) (left) and proposed catalytic cycle for photoredox catalysis (right).[79]

3.2. Lanthanoid(IV) Complexes

With increasing demand for lanthanoid metals, and concerns over their availability, improving processes such as separation, purification, and recycling is crucial both for ensuring adequate supply and the development of new applications.[13, 81] Cerium is the only lanthanoid that can readily cycle between the Ce(III) and Ce(IV) oxidation states due to its low fourth ionization potential, with the next most accessible tetravalent lanthanoids, Tb(IV) and Pr(IV), only recently isolated in molecular compounds.[45c, 82] Cerium compounds are well known as one-electron oxidants, with ceric ammonium nitrate (CAN) widely used. However, its substantial oxidizing power has inhibited investigation of Ce(IV) reaction chemistry, which has been little explored.[83]

In the absence of other Ln(IV) molecular species, Ce(IV) has acted as a surrogate for understanding the rational design of molecular compounds containing tetravalent lanthanoid ions. As the 5d orbital is occupied in the Ce(III) state, the coordination sphere can be used to tune the Ce(III)/Ce(IV) redox couple.[83a, 84] Several early examples demonstrated the capability of electron-rich polyanionic ligands such as alkoxides, siloxides, aryloxides and β-diketonates to reduce the Ce(III)/(IV) potentials thus stabilizing the tetravalent state (Scheme 2).[85] For example, a series of Ce(IV) bis(salen) complexes have been reported, with the electron-donating ability of the ligand modulated through different substituents used to tune the redox potential.[86] The unsubstituted complex [Ce(salophen)$_2$] (**26**) has a reversible Ce(III)/(IV) potential of −0.521 V (MeCN), whereas the more electron rich methoxy substituted [Ce(5,5′-(OMe)$_2$-salen)$_2$] (**27**) shifts the potential to −0.776 V, and the less-donating [Ce(5,5′-(Br)$_2$-salen)$_2$] (**28**) to −0.529 V. Butoxides have been commonly employed to stabilize Ce(IV).[87] For example, a homoleptic octakis(tert-butoxo)dicerium(IV) complex [Ce$_2$(OtBu)$_8$] (**29**) was synthesized via the starting material [Ce(O^{t}Bu)$_2${N(SiMe$_3$)$_2$}$_2$] (**30**), which on heating above 150°C decomposes to form mixed-valence oxo clusters.[88] Stabilization of the tetravalent state was observed in a series of bis-phenolate complexes using 2,2′-methylenebis(6-tert-butyl-4-methylphenolate) (MBP^{2-}), accessed via [Ce^{III}(MBP)$_2$(THF)$_2$Li(THF)$_2$] (**31**) using common oxidants such as CuX$_2$ (X = Cl, Br).[89] The reversible metal based oxidation wave in the cyclic voltammogram of **31** at −0.93 V vs Fc/Fc$^+$ (THF) indicates the reducing power of Ce(III) in this case, with a significant shift relative to the standard oxidation potential of approximately 2.25 V. The isolated [Ce^{IV}(MBP)$_2$(THF)$_2$] (**32**) exhibits ligand π to vacant 4*f* transitions characteristic of Ce(IV), with electrochemical studies showing reversible reduction at the same potential as the oxidation of its Ce(III) counterpart. Also prepared were [Ce^{III}(MBP)$_2$(bpy)Li(THF)$_2$] (**33**) and [Ce^{IV}(MBP)$_2$(bpy)]] (**34**), however due to

displacement of the bpy in solution by THF, solution electrochemical studies were not possible. Solid-state investigation showed that despite the ability of bpy to act as a redox-active electron acceptor, electron transfer from the metal center was not induced. Recently, tetraphenolate (*p*TP = [{2-($OC_6H_2R_2$-2,4)$_2$CH}-C_6H_4-1,4]$^{4-}$) ligands were used to access the metallacyclic 2+2 [Ce^{IV}_2(*p*TP^R)$_2$(THF)$_4$] (**35**) (R = Me, *t*Bu) with an unusual "letterbox" topology. This was achieved via the oxidation of the Ce(III) analogue [K(THF)$_n$][Ce_2(*p*TP^R)$_2$(THF)$_4$K] (**36**) with a range of oxidants (CuX_2 (X = Cl, OTF), I_2, XeF_2, HgX_2 (X = Cl, I, OAc)), involving a rare concerted two-electron redox process within a single molecule.[90] Solution electrochemistry (THF with 0.1 M [^{n}Bu$_4$N][PF_6]) indicates significant stabilization of the Ce(IV) cation (−1.83 V vs. Fc/Fc^+). Edelmann and co-workers reported the use of [Ce^{IV}(NO_3)(^{t}BuO)$_3$(THF)$_2$] (**37**) as a precursor to prepare the first disiloxanediolate complexes of Ce(IV) to give [{K(THF)$_2$}{O($OSiPh_2$)$_2$}]$_2$[Ce(O^{t}Bu)$_2$] (**38**) and [{KO^{t}Bu(DME)}{O($OSiPh_2$)$_2$}$_2$][Ce{KO($OSiPh_2$)}]$_2$ (**39**).[91] The ability to stabilize tetravalent cerium using a tris(tert-butoxy)siloxy ligand was described by Anwander and co-workers in the synthesis of homoleptic [Ce(OSi(O^{t}Bu)$_3$)$_4$] (**40**) and [Ce(OSi(O^{t}Bu)$_3$)$_4$(THF)] (**41**).[92] An electrochemical investigation found a redox-modulated molecular rearrangement process, featuring oxidation-state dependent formation and release of Ce-O^{t}Bu coordination, which aids the overall stabilization of the Ce(IV) state. Catecholates are also well known to stabilize the Ce(IV) state, both in bidentate form and incorporated into larger polydentate ligands such as the octadentate terephthalamide macrocyclic (LH_8) ligand.[93] Schelter and co-workers have contributed significantly to the investigation of nitroxides which have been found to support tetravalent cerium ions with low reduction potentials achieved, for examples complexes **1** and **2** (as discussed in section 2.4) with potentials of −1.95 V vs Fc/Fc^+ *cf*. $CoCp_2$ −1.94 V.[50, 94] The stabilization of the tetravalent state was attributed to two factors: i) the strong ionic interactions between the Ce(IV) and the pyridine nitroxide ligand and ii) the mixing of the nitroxide π^* orbitals with the 4*f* orbitals of the cerium. Through variation of the electron-withdrawing and electron-donating substituents, solution electrochemistry experiments indicated a stabilization of the Ce(IV) when electron-donating substituents (e.g. *m*-NMe_2) were employed. In addition to O- and mixed O,N-donor ligands, other ligands such as amides, silyamides, amidinates, and various organometallic ligands (cyclooctatetraene, cyclopentadienyl, carbenes) have been reported, which rely on increased orbital overlap to stabilize the higher oxidation state.[95]

Scheme 2. Ligands and proligands used to access tetravalent lanthanoid ions.

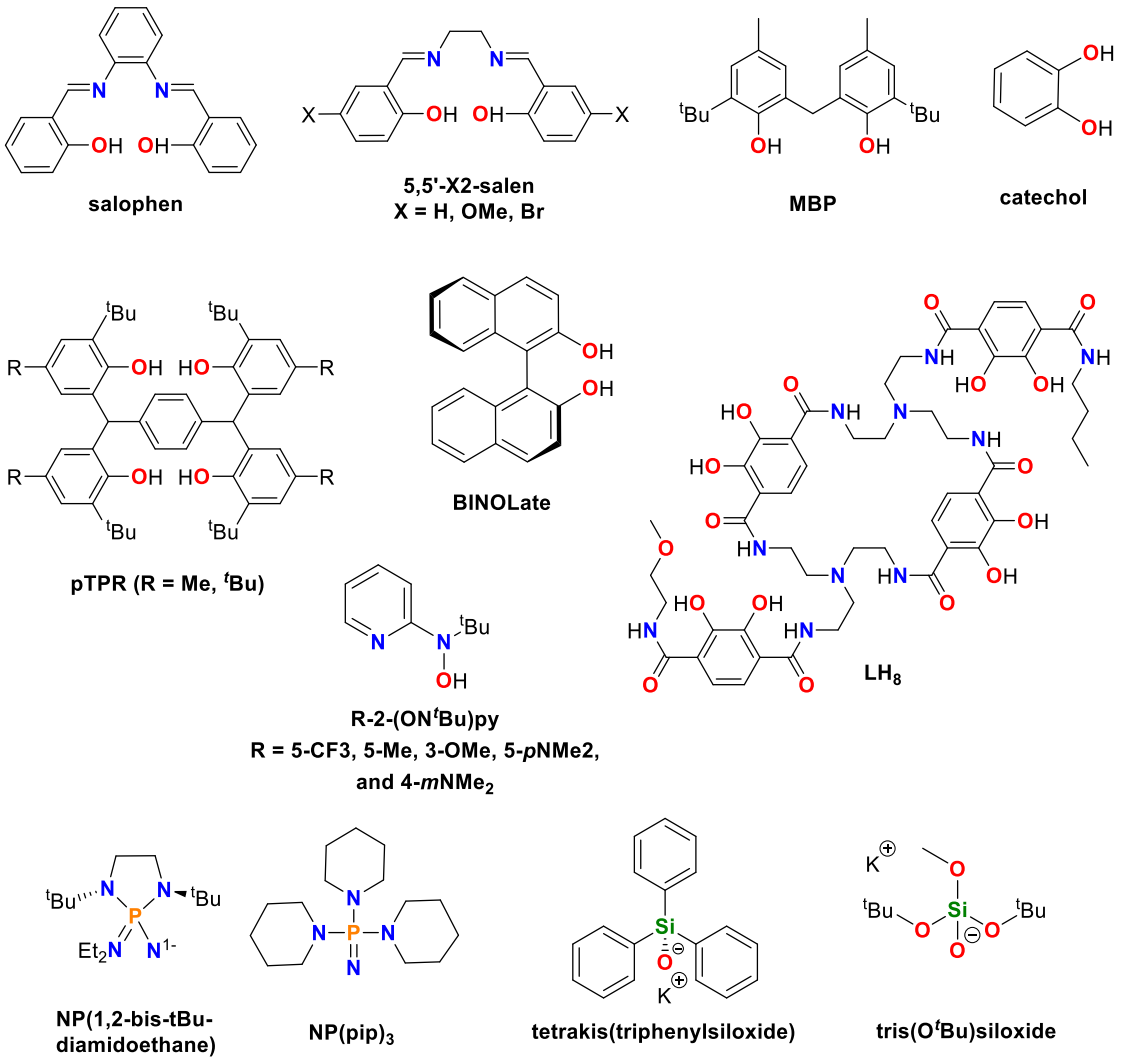

There are factors in addition to electron richness that are relevant to whether a ligand can stabilize a tetravalent lanthanoid ion. For example, flexibility of the coordination environment is necessary as the inner coordination sphere contracts with changes in the atomic radii moving between Ce(III) and Ce(IV).[94d, 96] Thus, the inner sphere reorganization energies must be considered. A series of trivalent cerium complexes of general formula $[M_3(THF)_n][Ce(BINOLate)_3]$ (**42**) (BINOLate = 1,10-di-2-naphthate; M = Li^+, K^+, Na^+ and Cs^+) were synthesized by Walsh, Schelter and co-workers using the silyamide precursors of both the Ce and alkali metal.[96a] The goal was to assess the impact of ligand reorganization on the oxidation of Ce(III) to Ce(IV) in each

case. Using thorough electrochemical and kinetics experiments, electron transfer rates were found to differ from their chemical oxidation rate, implying ligand reorganization plays a substantial role in determining the Ce(III)/Ce(IV) potential. In addition, the properties and reactivity are tunable by changing the alkali metal present in the secondary coordination sphere, with only the case where M = Li amenable to chemical oxidation to $[Li_3(THF)_5][Ce^{IV}(BINOLate)_3Cl]$ (**43**). Consequently it is clear that outer-sphere mechanisms play a role and thus thermodynamics and kinetic effects must be considered in the design of tetravalent lanthanoid complexes.[45c, 50, 97] The role of 4*f* covalency in targeting the isolation of new Ce(IV) compounds, as well as new tetravalent Ln compounds of Tb, has gained significant attentions in recent years, and has been at the core of the design strategy by La Pierre and co-workers.[24, 46, 98]

Using a dialkyamide-substituted imidophosphorane, La Pierre and co-workers investigated the role of covalent bonding in controlling the stability of Ce(III) and Ce(IV).[99] As imidophosphoranes are 1σ and 2π donors with respect to the metal-ligand bond in pseudo-tetrahedral (Td) geometries, the ligand orbitals have the correct symmetry and energy to effectively covalently bond with tetravalent lanthanoids.[24] The Ce(IV) complex $[Ce^{IV}(NP(pip)_3)_4]$ ($[NP(pip)_3]^-$ = tris(piperidinyl)imidophosphorane; **44-Ce(IV)**) was prepared via salt metathesis and *in-situ* oxidation of the potassium cluster $[K(NP(pip)_3)]$. This could then be reduced by KC_8 to produce $[Ce^{III}(NP(pip)_3)_4(Et_2O)K]$ (**45-Ce(III)**), which includes an inner-sphere potassium ion. The Ce(III)/(IV) redox couple, as determined via chemical bounding, appeared at much more negative values on oxidation of **45-Ce(III)** (between −2.64 and −3.10 V (*cf.* **44-Ce(IV)** between −2.30 and −2.47 V)). This asymmetry in the redox properties of the **44-Ce(IV)**/**45-Ce(III)** redox pair was attributed to the impact of the binding of the potassium in the inner coordination sphere, contributing thermodynamic driving force for the oxidation of Ce(III) to Ce(IV), upon which the potassium ion is eliminated. Confirmation of the Ce(IV) oxidation state in **44-Ce(IV)** was provided through an investigation of the electronic structure in comparison with **45-Ce(III)** via DFT computational methods and extensive spectroscopic studies (electronic absorption spectroscopy, X-band EPR, L_3-edge XANES) as well as magnetic measurements (Figure 11). The extremely negatively shifted redox couple established through reactivity and theoretical studies suggests remarkable stabilization of the Ce(IV) oxidation state.[99] Significant electron donation to the metal was supported by Mulliken charge analysis with **44-Ce(IV)** showing a smaller positive charge than related complexes as well as by the Ce L^3-edge XANES, where destabilization of the Ce(III) character is evidenced.

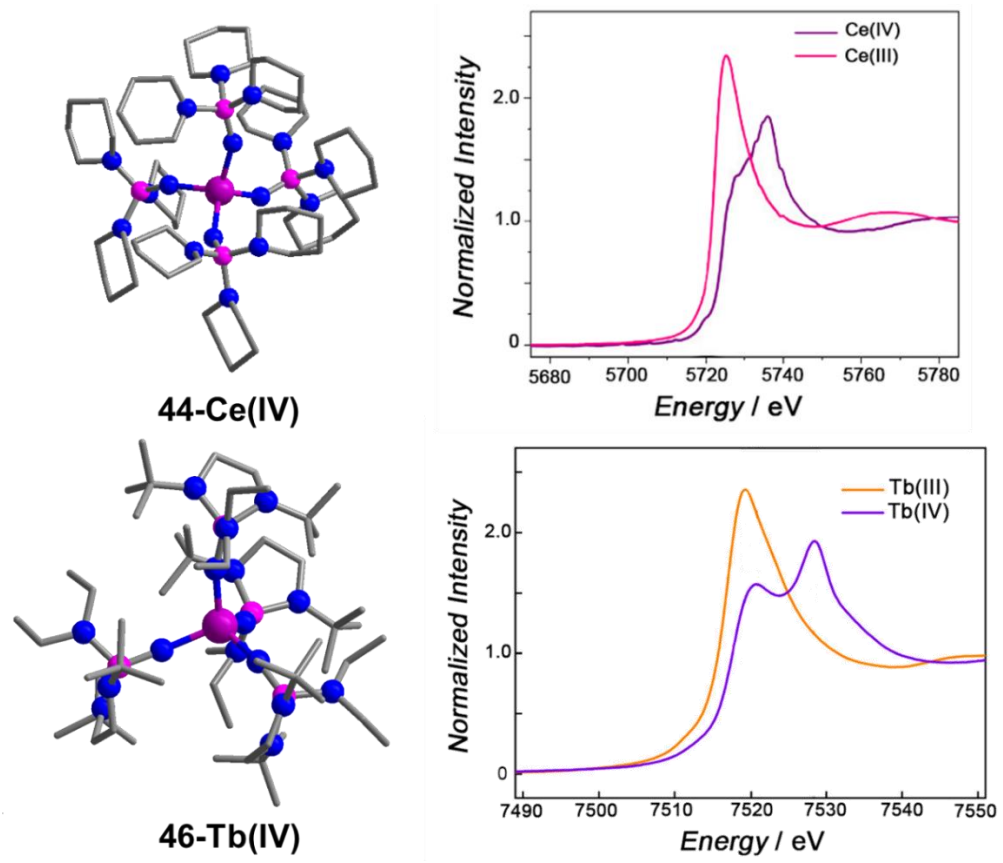

Figure 11. Structures of **44-Ce(IV)** (above) **46-Tb(IV)** (below, color scheme as per Figure 8), and L_3-edge XANES spectra for these complexes and their Ln(III) counterpart. L_3-edge XANES spectra adapted with permission.[97a, 99] Copyright (2019) American Chemical Society.

The same strategy was later used to isolate one of the first Tb(IV) molecular complexes [Tb(NP(1,2-bis-^{t}Bu-diamidoethane)(NEt_2))$_4$] (**46-Tb(IV)**) via a Tb(III) precursor [Tb(NP(1,2-bis-^{t}Bu-diamidoethane)(NEt_2))$_4$(Et_2O)K] (**47-Tb(III)**) (Figure 11).[97a] This made use of an adapted imidophosphorane ligand with increased steric bulk to impose the same pseudo-tetrahedral coordination environment on the smaller ion. Initial investigations using the same ligand system as **44-Ce(IV)** yielded a distorted coordination environment preventing good overlap between metal and ligand orbitals, resulting in reduced covalency and isolation of a Tb(III) species. The isolation of **46-Tb(IV)** was confirmed in both the solid state and solution through a similar method of investigation as its Ce counterpart.

However, it was Mazzanti and coworkers who isolated the first molecular Tb(IV) complex using the electron rich O-donor tris(tertbutoxy)siloxide ligand, a strategy previously used to stabilize the Ce(IV) analogue.[63b] The complex was prepared via oxidation of the Tb(III) precursor $[Tb^{III}(OSi(O^tBu)_3)_4K]$ (**48**) employing $[N(C_6H_4Br)_3][SbCl_6]$ to give $[Tb^{IV}(OSi(O^tBu)_3)_4]$ (**49**) shown in Figure 12, with the oxidation occurring at significantly less positive potentials compared to the standard Tb(IV)/Tb(III) redox couple.[82b] The isolation of the Tb(IV) compound was confirmed via X-band EPR spectroscopy, where no intense features for non-Kramers Tb(III) were evident, but instead those characteristic of Tb(IV) in solid-state materials were observed at 20 K. Not long after this report, Mazzanti *et al.* reported a related Tb(IV) complex $[Tb^{IV}(OSiPh_3)_4(MeCN)_2]$ (**50**) which showed increased stability, despite the bulky siloxide ligand preventing a saturated coordination sphere.[100] This increased stability was found to originate from a large covalent contribution to the Tb-O bond which was not observed for the Tb(III) precursor complex $[Tb(OSiPh_3)_4(THF)K]$ (**51**). This extra stabilization was exploited to achieve the isolation of the first molecular complex of Pr(IV) for the analogue $[Pr^{IV}(OSiPh_3)_4(MeCN)_2]$ (**52**) reported earlier this year, again accessed via the Ln(III) precursor $[Pr^{III}(OSiPh_3)_4(THF)K]$ (**53**).[82a] The electrochemical behavior of **52** and **53** were compared to their Tb analogues, as well as the Ce(IV) analogue of complex **52** (Figure 12). The oxidation event for Pr(IV) (**52**) occurs at a slightly more positive potential than for the Tb(IV) complex **50** (0.67 V for **52-Pr** vs 0.49 V for **50-Tb**), which agrees with the trends in their standard redox potentials.[32] The metal-based reduction feature of **52-Pr** occurs at a more positive potential than for the Tb analogue (–0.38 V for **52-Pr** vs –0.96 V for **50-Tb**), suggesting it is easier to reduce Pr(IV) to Pr(III) than the analogous Tb process, and that therefore Pr(IV) has a lower kinetic stability.

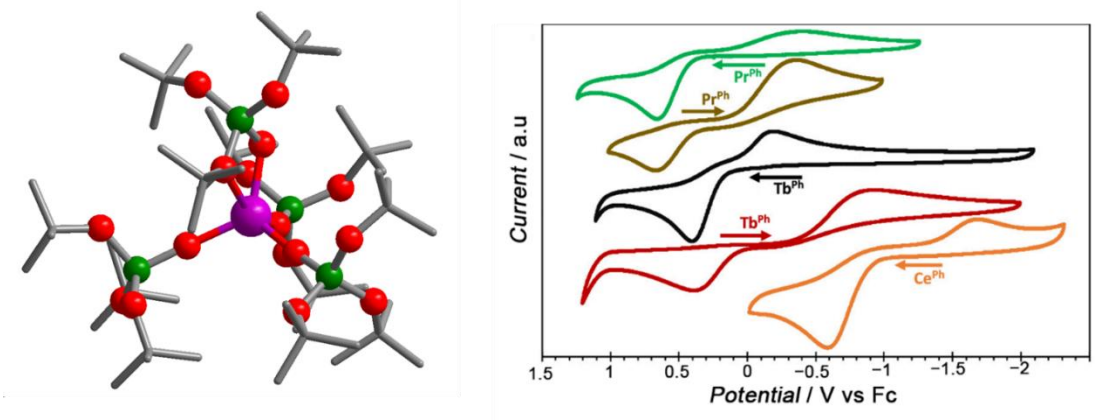

Figure 12. Left: Structure of **49-Tb(IV)** (color scheme as per Figure 8).[82b] Right: cyclic voltammograms at ambient temperature of 2 mM solutions of **53-Pr(III)** (green), **52-Pr(IV)** (brown), **51-Tb(III)** (black), **50-Tb(IV)** (red), and the Ce(IV) analogue (orange) measured in 0.1 M $[NBu_4][B(C_6F_5)_4]$ in THF. Cyclic voltammograms adapted with permission.[82a] Copyright (2020) American Chemical Society.

4. Lanthanoid(III) Complexes with Redox-Active Ligands

Combining a lanthanoid(III) ion with a redox-active ligand can provide a route for manipulation of the detectable properties of a compound,[101] as well as expanding its reactivity.[102] Redox-active ligands are those with energetically accessible levels for oxidation or reduction, with redox-activity consequently centered on the ligand, or in some cases the ligand and metal oxidation states simultaneously (*e.g.* VT).[3, 102a] Redox-active ligands such as catecholates, amidophenolates and diimines have been widely utilized in coordination chemistry due to their ability to form solution stable radical species when coordinated. The elucidation of the true electronic structure of such complexes sometimes requiring significant investigation.[102e, 103] Pairing lanthanoid metals with redox-active ligands typically affords solely ligand-based redox events with the metal remaining in the trivalent state.[104] The consequent prospects for catalysis and reaction chemistry are enticing. For example Bart and co-workers exploited the multi-electron redox chemistry of 4,6-di-tert-butyl-2-[(2,6-diisopropylphenyl)imino]quinone ($^{dipp}iq^0$), with access to the iminosemiquinone ($^{dipp}isq^{\bullet-}$) and amidophenolate ($^{dipp}ap^{2-}$) states, to isolate a family of Nd(III) complexes, all exhibiting distinctly different colors: $[NdI_3(^{dipp}iq^0)_2]$ (**54**), $[Nd(^{dipp}isq^{\bullet-})_2I(THF)]$ (**55**), and [K(18-crown-6)][Nd($^{dipp}ap)_2(THF)_2$] (**56**) (Figure 13).[105] The reverse multi-electron oxidation of **56**,

containing the amidophenolate (^{dipp}ap) ligand, was tested for its capacity to act as an electron store for future reductants using elemental chalcogens (S_8 and Se), with formation of the isoquinone state (via two one-electron oxidations) accompanied by isolation of the S_5 and Se_5 complexes.[105a] As well as for the implications for catalysis and reaction chemistry, understanding how ligand-centered redox events can modulate the photophysical and magnetic properties of lanthanoid complexes is of interest for extending the capabilities of optically or magnetically functional lanthanoid materials.

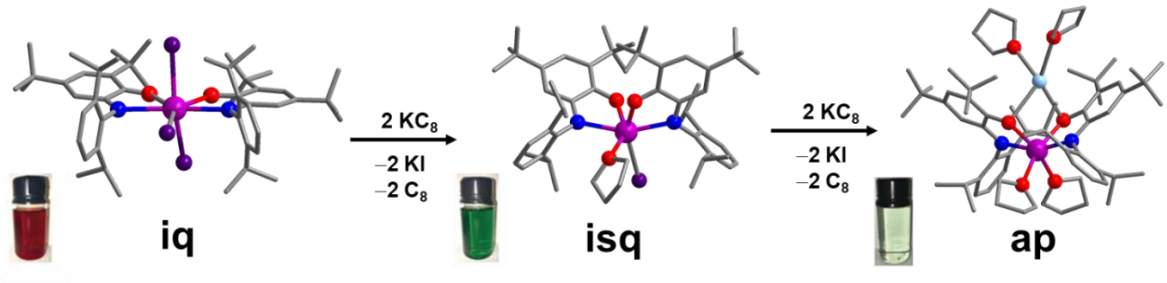

Figure 13. Structures of Nd(III) complexes (color scheme as per Figure 8; iodine (dark purple)) reported by Bart *et al*. with ligands in iq (**54**), isq (**55**) and ap (**56**) forms. Images of coloured solutions (THF) reprinted with permission.[105a] Copyright (2017) Wiley-VCH Verlag GmbH & Co. KGaA, Weinheim.

4.1. Switching Lanthanoid(III) Luminescence with Redox-Active Ligands

Initial investigations of lanthanoid complexes exhibiting luminescence switching were focused on combining redox-active metal centered units (*e.g*. ferrocene)[104h, 106] to control the switching process. However, more recent strategies have involved the use of redox-active organic ligands, presenting advantages in their comparative flexibility and potential to be fine-tuned to deliver the desired properties. This can be achieved either through use of distinct emission sensitizing and redox-active ligands within the same molecule, or instead incorporating a ligand that fulfils both roles simultaneously.

In 2012, the first example of an organic redox-active ligand used to induce luminescence switching, a triarylamine terpyridine, was reported by Yano *et al*.[107] The compound $[Eu^{III}(FOD)_3(L_{TERP})]$ (**57**) (FOD = 6,6,7,7,8,8,8-heptafluoro-2,2-dimethyl3,5-octanedionate, L_{TERP} = 4, 4'-dimethoxytriphenylamine) incorporates a distinct sensitizer (FOD) and redox-active ligand (L_{TERP}). The terpyridine ligand had previously been shown to form a stable radical cation upon both chemical and electrochemical oxidation with associated intense absorptions in the visible

region.[108][Although single crystals of **57** could not be isolated, complexation was confirmed through UV-Vis spectral titration and mass spectrometry. Photoexcitation of **57** at 290 nm resulted in Eu emission at 615 nm, which could then be quenched by addition of the oxidizing agent CAN, upon which $L_{TERP}^{\bullet+}$ is formed, as evidenced by a new broad adsorption band at 754 nm. Spectroelectrochemistry was used to investigate the reversibility of the process, which was found to be robust over multiple cycles (100 s to switch to ~ 1/10th emission) with emission intensity recovered on reduction (Figure 14). The importance of the redox-activity of the ligand on the Eu(III) luminescence was confirmed through a control study with an analogue using a related non-redox-active ligand, for which the luminescence spectral change was absent. The quenching process is facilitated by $L_{TERP}^{\bullet+}$, which allows energy transfer from the excited $Eu(FOD)_3$ moiety, forming a non-emissive short-lived excited state. Thus, **57** provides a unique example of how Eu(III) luminescence can be switched through intramolecular energy transfer.

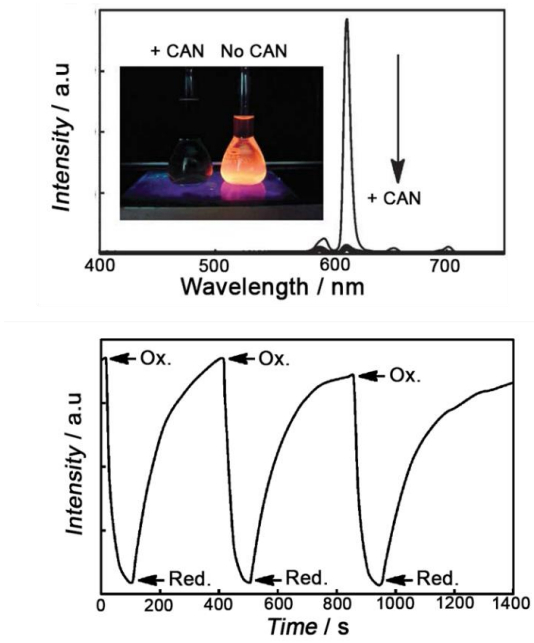

Figure 14. Top: emission spectra of **57** before and after oxidation with 1 equiv. of CAN with images of the solution with and without CAN on a UV-Lamp illuminator shown inset. Bottom: electrochemical switching of luminescence of **57** at 615 nm (1 mM, dry MeCN, 0.1 M NBu_4PF_6) with alternate oxidation at 0.50 V vs. Fc/Fc+ and reduction at –0.50 V. Adapted with permission.[107] Copyright (2012) Royal Society of Chemistry.

The incorporation of both sensitization and redox-activity within a single ligand was demonstrated by Thomas and co-workers through use of a phenolate ligand (L_{phen};

Scheme **3**). This investigation stemmed from their interest in assessing lanthanoid compounds paired with redox-active ligands as *in vivo* redox probes, where the redox status of the ligands provides information on a biological process.[109] Two analogous compounds were investigated: [Tb(NO_3)L_{phen}] (**58**) and [Yb(NO_3)L_{phen}] (**59**) (L_{phen} = N,N',N,N'-bis[(2-hydroxy-3,5-di-tert-butylbenzyl)(2-pyridylmethyl)]ethylenediamine)) (Figure 15). On studying their redox behavior concurrently with their luminescence, both compounds were observed to be reversibly oxidized to their phenoxyl radical species, accompanied by a quantitative intramolecular quenching of the luminescence of > 95%, depending on whether the monoradical or diradical species was accessed (Figure 15).Although it was not possible to identify the quenching mechanism, both complexes were nonetheless shown to be effective, robustly reversible, luminescence switches controlled via the redox-state of the ligand.

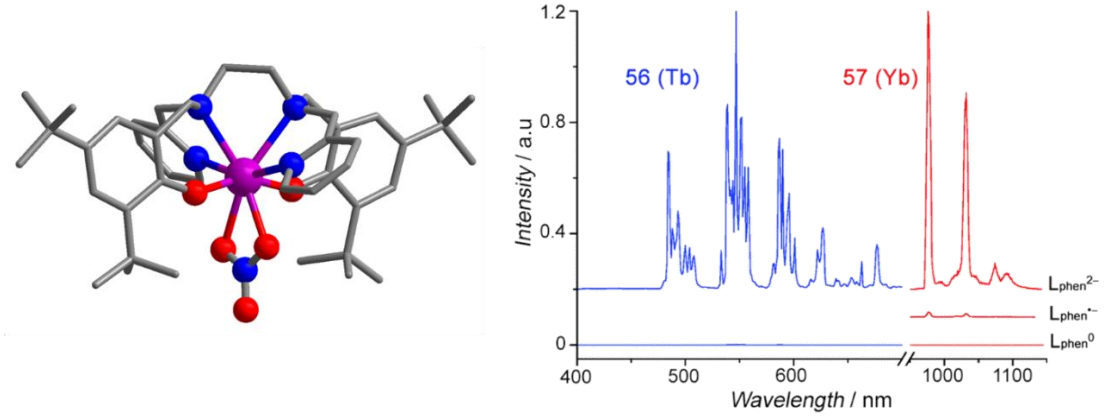

Figure 15. Left: Structure of **58** (color scheme as per Figure 8). Right: luminescence spectra for **58** (red) and **59** (blue) at 77 K where ligand is in different oxidation state as denoted. Adapted with permission.[109a] Copyright (2017) Royal Society of Chemistry.

Scheme 3. Redox-active ligands, other than Pc derivatives which are presented in

Scheme **4**, as discussed in the main text.

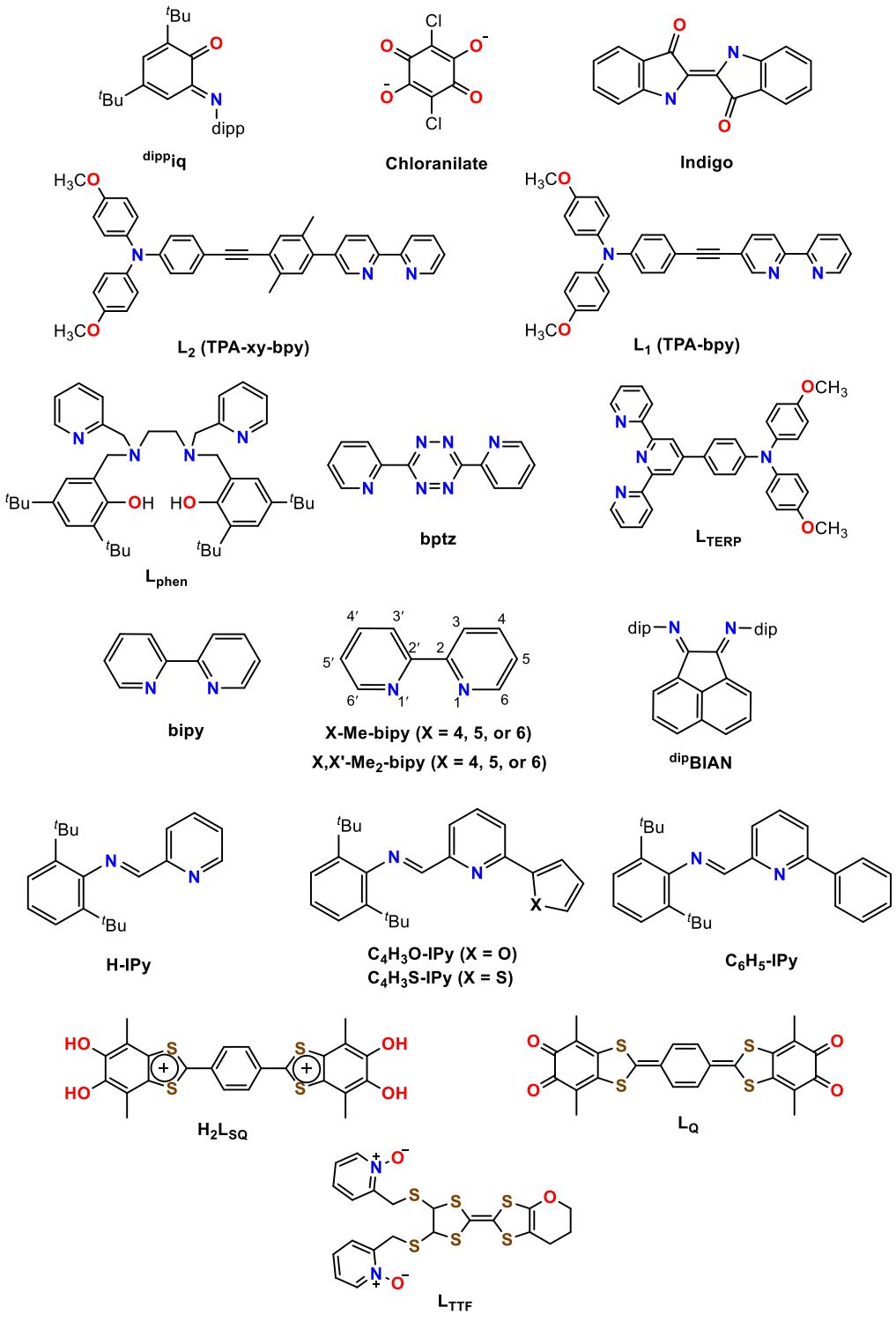

A very recent report thoroughly investigated the solvation effects that impact the redox-controlled luminescence switching in analogous Eu(III) and Sm(III) compounds.[30d] Similarly to Yano *et al.* (*vide supra*), Chen and co-workers were interested in using a triphenylamine system as the redox-active component modified with a 2,2'-bipyridine (bpy) coordinating moiety (Figure 16). The ancillary diketonate ligand (2-thenoyltrifluoroacetone (tta)) then acts as the sensitizer. Two triphenylamine (tpha) ligands were investigated, L_1 (tpha-bpy) and L_2 (tpha-xy-bpy), where a xylene (xy) moiety resides between the tpha and bpy of the ligand (

Scheme **3**), giving rise to [Ln(tta)$_3$(L$_1$)] (Ln = Eu (**60**), Sm (**61**)) and [Eu(tta)$_3$(L$_2$)] (**62**). The photophysical properties of these compounds show strong solvent dependence. Emission in less polar solvents results in 4*f* ↔ 4*f* transitions as well as ligand-centered luminescence, resulting in white-light emission in such solvents. In more polar solvents, the complexes mainly exhibit 4*f* ↔ 4*f* transitions. This is due to the differences in energy between Eu(III) and the T state of L$_1$: when the energy gap is large enough ISC to the ligand is prevented and so **60** exhibits pure red Eu(III) based emission. This was confirmed through significant photophysical investigations and DFT calculations. Single-component white-light emitters have great potential in the preparation of simplified optical devices, bypassing the need for mixing two (blue/yellow) or three (red/blue/green) separate components. Spectroelectrochemistry was used to investigate the reversibility of the luminescence on oxidation of L$_1$ and L$_2$ to the respective radical cations (L$_1^{\bullet+}$ and L$_2^{\bullet+}$) in **60**–**62**, with quenching of the luminescence observed for **60** and **61** originating from the intramolecular energy transfer from the Ln(III) ions to the non-emissive excited states of the radical cations. Complex **62** does not exhibit switching, as the introduction of the xylene spacer in L$_2$ increases the energy levels of the excited states of the ligand, hence efficient quenching cannot take place.

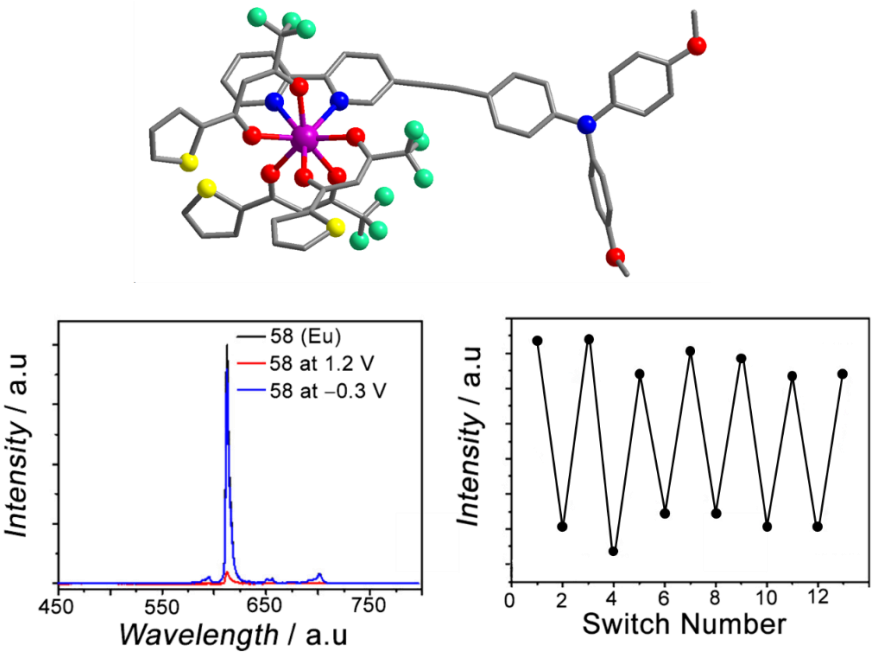

Figure 16. Above: Structure of **60-Eu** (color scheme as per Figure 8 and sulfur = yellow). Below: Luminescence switching study through emission at 612 nm for **60-Eu** with switching induced via alternating the applied electrochemical potential between 1.2 V (red) and −0.3 V (blue) vs Ag$^+$/Ag

(dry MeCN, 0.25 M (n-$C_4H_9)_4NPF_6$). Adapted with permission.[30d] Copyright (2020) American Chemical Society.

4.2. Magnetic Properties of Lanthanoid(III) Complexes with Redox-Active Ligands

Perhaps the best known example of redox-active ligands incorporated into Ln-SMMs is the archetypal phthalocyanine (Pc) ligand (

Scheme **4**). In 2003, the double-decker [Tb(Pc)$_2$] complex (**63**) was the first lanthanoid-based SMM to be reported.[110] Comprehensive investigations of the magnetic properties of the three interconvertible redox states ([Tb(Pc)$_2$]$^-$ ↔ [Tb(Pc)$_2$]^0 ↔ [Tb(Pc)$_2$]$^+$) using ac susceptibility measurements and magnetic circular dichroism (MCD) spectroscopy revealed that all three exhibit slow relaxation of magnetization at low temperatures.[111] Since 2003, molecules of this type have been exceptionally well studied through variation of the lanthanoid, modifications to the ligands, different structural architectures (*e*.*g*. triple decker complexes), which have sought to understand these factors in relation to their redox and magnetic properties.[112] As a result of their interesting magnetic behavior and amenable structure, Ln-Pc compounds have been extensively investigated for use in nanoscale devices, particularly for their application in spintronic devices, as they are robust and sublimable.[8a] However, due to their low redox potentials they are easily oxidized or reduced in the presence of mild reagents, which can present problems when deposited onto surfaces.[112h, 113] Despite this drawback, the 16 sites for substitutions offered by the phthalocyanine ligands provide significant scope for investigation. For example, in 2013 Veciana and collaborators functionalized the Pc ligand with electroactive cyclic imides which stabilized the anionic double-decker complexes [TBA][Tb(L$_n$)$_2$] (L = phthalocyaninatotetradicarboximide; n = 1 = tetrapentadecyl (**64**); n = 2 = tetrapropyl (**65**); n = 3 = tetra((S)-methyl(phenyl)methyl (**66**); TBA = tetrabutylammonium) (

Scheme **4**).[114] In comparison to the unsubstituted [$TbPc_2$] the first oxidation potentials for all three complexes were significantly shifted by approximately 0.7 V (+0.3 V for substituted *cf*. –0.4 V for unsubstituted vs Fc/Fc^+).[114] Investigation of the ac magnetic susceptibility found that the SMM behavior is comparable to that observed in the unsubstituted $[Tb(Pc)_2]^-$ complex, which is dominated by thermal Orbach relaxation, and relatively consistent across the series despite the different substituent on the imido nitrogen. Similarly to $[Tb(Pc)_2]^-$, butterfly-shaped hysteresis curves were observed stemming from a contribution from QTM to the magnetic relaxation at lower temperatures, which is more efficient with respect to complex **65** (L_2). By increasing the stability window (~1.2 V) of these complexes using more electron rich phthalocyanine rings, charge transfer is restricted between these SMMs and inorganic substrates onto which they have been deposited for devices.[8c, 112i]

Scheme 4. Phthalocyanine ligand derivatives discussed within this review in their neutral form

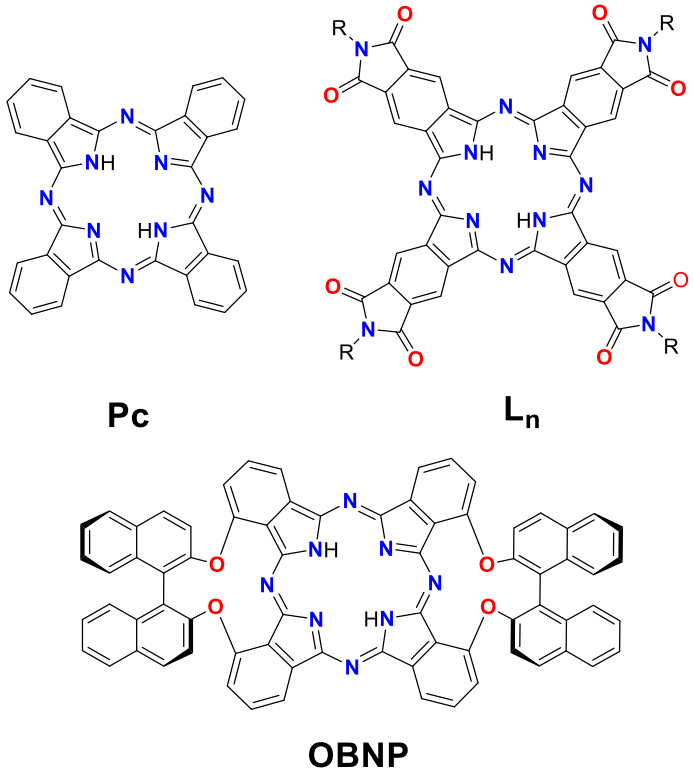

Due to their large ionic radii and high coordination numbers, lanthanoid ions can form both planar and sandwich type structures with Pc ligands and their derivatives. Both homoleptic and heteroleptic mixed-sandwich compounds have been investigated with a view to tuning the magnetic properties. New heteroleptic triple-decker lanthanoid porphyrin-bis-phthalocyanine complexes, decorated with bulky groups in the peripheral positions, have been prepared via microwave-assisted synthesis.[115] Constructing heteroleptic triple-decker complexes offers a larger number of oxidation states, with reversible electrochemistry and facile ligand oxidation. Although these types of structures had been reported previously,[112e, 116] this was the first case using spectroelectrochemistry to closely monitor the electron-transfer process. The triple-decker complexes were found to undergo four ligand-centered reversible one-electron oxidations and three reversible one-electron reductions. The sites at which these occur where then assigned based on the associated redox potentials and changes the UV-Vis spectra during the electron-transfer process. Furthermore, the Tb analogue exhibits field-induced SMM behavior (1000 Oe) with contributions from various relaxation processes, as opposed to the dominant Orbach

relaxation observed for the traditional $[Tb(Pc)_2]^-$ complex. In 2019, a reversible chemical transformation between a chiral heteroleptic double-decker phthalocyaninato-porphyrinato Dy(III) complex was reported.[117] Both enantiomers of chiral mixed complexes in the reduced protonated form (R)/(S)-{DyH[Pc(OBNP)$_2$](TClPP)} (**67**) (Pc(OBNP)$_2$ = binaphthyl-substituted phthalocyaninate, TClPP = 5,10,15,20-tetrakis(4-chlorophenyl)porphyrinate) and neutral unprotonated species (R)/(S)- {Dy[Pc(OBNP)$_2$](TClPP)} (**68**) were designed. In the case of **68,** where there is a Dy-radical interaction, SMM behavior was only evident on application of an applied field. This contrasts with **67,** with the ligand in the neutral redox state, which shows SMM behavior at zero-field. The two complexes are easily switched by chemical oxidation/reduction; hence these related compounds contribute to the small number of Ln-SMMs with redox-switchable magnetic properties. The similarities in the Dy(III) coordination geometries in **67** and **68** excludes geometric factors as the cause of the negative impact of the Dy-radical interaction, but suggests instead that this may arise as a result of the change in the CF experienced by the Dy(III) for the neutral versus radical ligand (with ~10% reduced electrostatic interaction for radical) which may alter the uniaxial magnetic anisotropy.[117-118]

Incorporation of redox-active ligands into SMMs also offers the possibility of promoting strong exchange interactions that can result in large thermal barriers to the relaxation of magnetization through subduing antagonistic QTM.[119] One of the most notable examples is the significant magnetic blocking temperature of 14 K for a N_2^{3-} radical-bridged diterbium complex $[K(18\text{-crown-6})(THF)_2][(TbN(SiMe_3)_2)_2(THF))_2(\mu\text{-}N_2^{\bullet-})]$ (**69**), reported in 2011 by Long and co-workers.[120] After this report, investigation into radical bridged lanthanoid systems for these applications expanded significantly, and is still an area of avid interest.[121] Layfield *et al.* investigated the properties of lanthanoid dinuclear complexes $[(Ln(Cp^*)_2)_2(\mu\text{-ind})]^{n-}$ Ln = Gd (**70**) and Dy (**71**) with Cp ancillary ligands and an indigo (ind) radical bridging ligand with the three accessible redox states of indigo (–2 to –4) probed (Figure 17).[122] The Gd analogue **70** was synthesized to straightforwardly determine coupling constants, based on modelling of the magnetic susceptibility data using a spin Hamiltonian, to assist in the comparison of coupling strengths in the open shell $(ind)^{3-}$ radical bridged complex versus the closed-shell $(ind)^{2-}$ and $(ind)^{4-}$ states. A much larger coupling constant was determined for the radically bridged complex ($J_{Gd\text{-}rad}$ = –11 cm^{-1}; –2J formalism), one of the largest coupling constants reported for a lanthanoid, indicating strong antiferromagnetic exchange. The relaxation dynamics of the Dy analogue **71** revealed modest barriers which did not change substantially with the nature of the radical ligand,

suggesting a full understanding the interaction between metal and radical ligands (*e.g.* donor atoms, formal charges) requires further consideration.

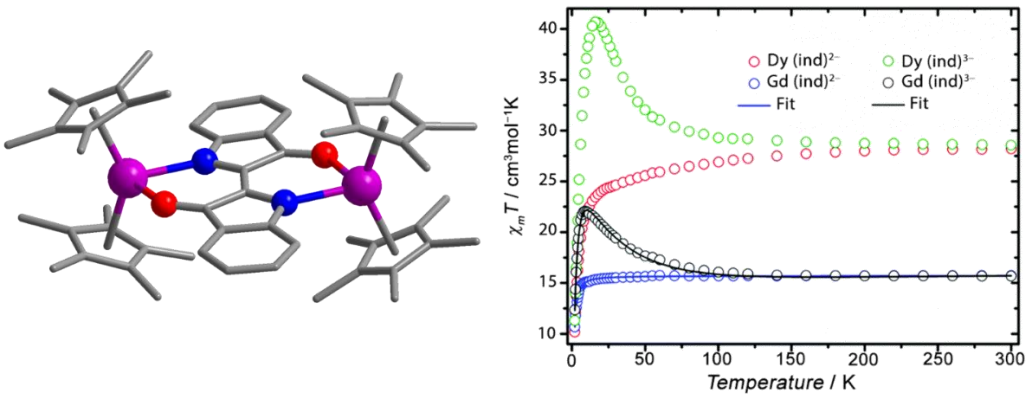

Figure 17. Left: Structure of **71** (color scheme as per Figure 8). Right: plots of $\chi_m T$ vs T for **70** and **71** in an applied field of 10 kOe with the ligand in the closed shell $(ind)^{2-}$ and open-shell radical $(ind)^{3-}$ redox state. The solid lines are fits of the data for **70** in each case. Adapted with permission.[122] Copyright (2017) Royal Society of Chemistry.

Despite the potential for redox-active ligands to impart switchable behavior on Ln-SMMs,[123] such considerations are little discussed in comparison to their ability to enhance the SMM energy barrier or modulate QTM. Although there are significant studies of radical reactivity in a variety of metal complexes for catalysis, this is still relatively unexplored for the lanthanoids and so this presents an area of interest for multiple research communities.[124] The first report of this behavior was in 2017 by the Dunbar group.[125] Two related Dy(III) compounds were isolated in their neutral and radical anion forms - $[Dy_2(tmhd)_6(bptz)]$ (**72**) and $[CoCp_2][Dy_2(tmhd)_6(bptz^{\bullet-})]$ (**73**) (where tmhd = 2,2,6,6-tetramethyl-3,5- heptane dionate; bptz = 3,6-bis(2-pyridyl)-1,2,4,5-tetrazine) as shown in Figure 18. Compound **73** was formed upon the ligand-centered (bptz) reduction of **72** with $CoCp_2$ in toluene, accompanied by a significant change in the orientation of the principal axes. Rather than the three aryl rings of the bptz ligand being coplanar, they are instead inclined towards the $[CoCp_2]^+$ counterion (Figure 18). The magnetic susceptibility data are consistent with two uncoupled Dy(III) ions in the case of **72** and suggest antiferromagnetic coupling between the radical and each Dy center with an additional $S = 1/2$ radical in **73**. Dynamic

susceptibility measurements revealed that neutral **72** exhibits temperature independent relaxation typical of QTM. This is in complete contrast to the radical-containing **73,** where a clear temperature dependence was observed. This suggests that the radical ligand suppresses QTM and allows **71** to display relaxation at zero field.

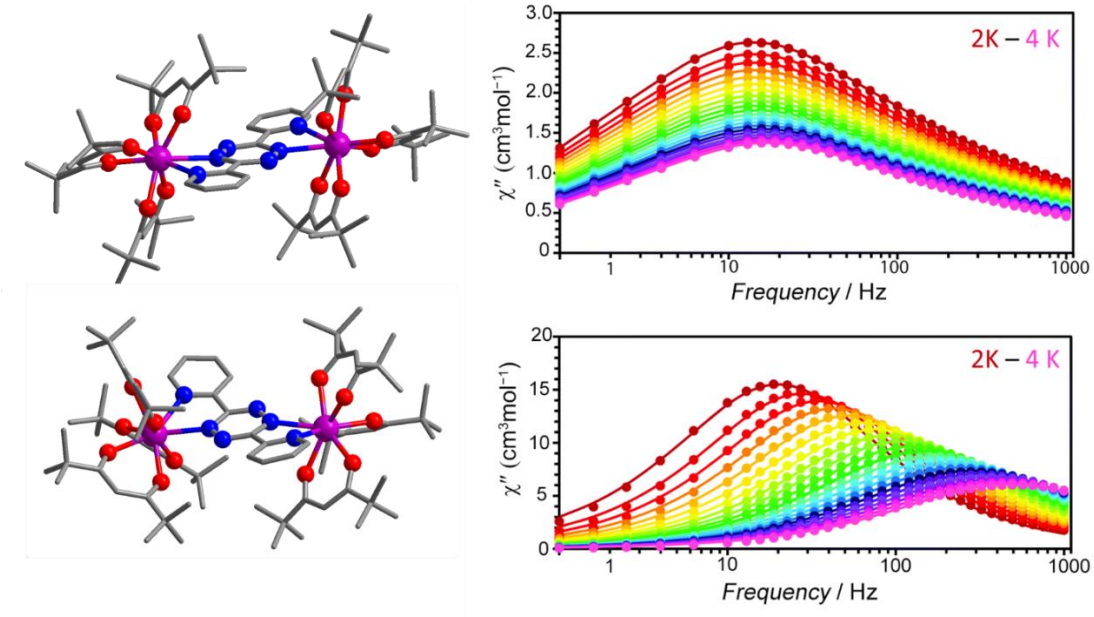

Figure 18. Structure (color scheme as per Figure 8) and out-of-phase (χ'') ac magnetic susceptibility data from 2 K to 4 K for **72** ($bptz^0$) above and **73** ($bptz^{\bullet-}$) below. Adapted with permission.[125] Copyright (2017) Royal Society of Chemistry

In 2017, Boskovic *et al*. reported the synthesis and characterization of a family of tetraoxolene-bridged lanthanoid dinuclear complexes of the form $[(Ln(HB(pz)_3)_2)_2(\mu$-tetraoxolene)] (**74**) (Ln = Eu, Gd, Tb, Dy, Ho, Er and Yb; $HBpz_3$ = hydrotris(pyrazol-1-yl)borate, tetraoxolene = chloroanilate (CA_2), 2,5-dihydroxy-1,4-benzoquinone (μ-dhbq), 3,6-dimethyl benzoquinone (μ-Me_2dhbq)) with the bridging tetraoxolenes isolated in the closed-shell dianonic form.[126] When combined with Dy, both the dichloro- and dimethyl-substituted tetraoxolene ligands showed SMM behavior under applied fields with effective energy barriers to magnetization reversal determined as 47 and 24 K. Solution electrochemical studies were used to confirm the ligand-centered redox activity of the tetraoxolene ligands, with reversible one-electron reductions

suggesting access to the trianionic radical-bridged complexes. This access to the radical form was soon after utilized by van Slageren and co-workers with the report of the open-shell chloroanilate analogs $[CoCp_2][(Ln(HB(pz)_3)_2)_2(\mu\text{-}CA^{\bullet-})]$ (Ln = Dy (**75**), Tb (**76**), Gd (**77**)), accessed from the corresponding $[(Ln(HB(pz)_3)_2)_2(\mu\text{-}CA)]$ analogues (Dy (**78**), Tb (**79**), Gd (**80**)) analogues as well as the rare-earth Y analogue, via reduction by cobaltocene (Figure 19).[127] The reduction could also be performed electrochemically, and tracked through spectroelectrochemistry, with peaks consistent with ligand reduction evident in the UV-Vis spectra (Figure 19). Isolation of the radical-containing complexes provided the opportunity for magnetic characterization which indicated modest antiferromagnetic magnetic coupling between the radical and Gd(III) ions (J = -2 cm^{-1}; -2J formalism) and in agreement with high-field EPR spectroscopy. Consequently, the radical-bridged Dy and Tb complexes display SMM behavior in zero applied field whereas for the neutral μ-CA, this is only observed under an applied field. Boskovic and co-workers expanded on this further with the fluoranilate (μ-FA) and bromanilate (μ-BA) analogues. The Dy-μ-BA complex $[(Dy(HB(pz)_3)_2)_2(\mu\text{-}BA)]$ (**81**) exhibits an out-of-phase response in the ac susceptibility under an applied field, whilst the exchange coupling between the Dy(III) and the $\mu\text{-}BA^{\bullet-}$ in the reduced compound $[CoCp_2][(Dy(HB(pz)_3)_2)_2(\mu\text{-}BA^{\bullet-})]$ (**82**) induces slow relaxation of magnetization in zero applied field.[128]

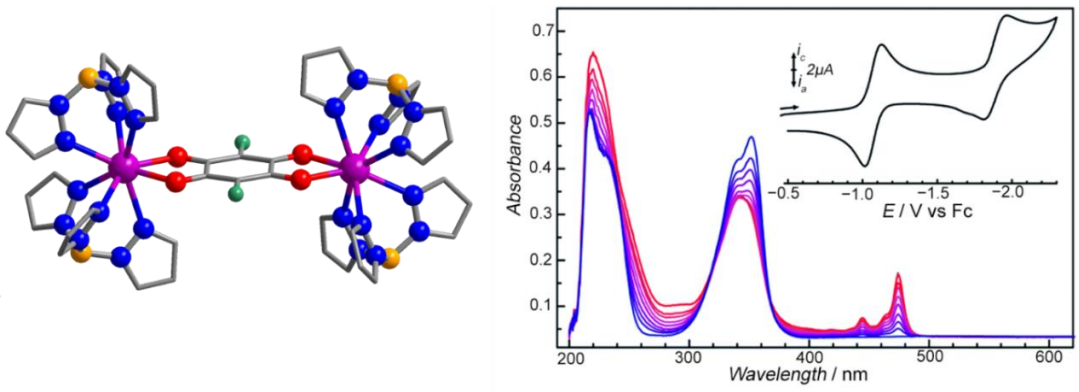

Figure 19. Left: structure of **75** (color scheme as per Figure 8. Right: corresponding changes in the UV-Vis spectrum of **75** (blue) during first reduction (CH_2Cl_2, 0.1 M Bu_4NPF_6) with progression to red showing formation of reduced species with the cyclic voltammogram shown inset as measured at 295 K. Adapted from reference 127 published by Royal Society of Chemistry.[127]

4.3. Combining Magnetic and Photophysical Properties in Lanthanoid(III) Complexes with Redox-Active Ligands

An increasing focus on multifunctional materials has afforded growing interest in combining luminescence and SMM behavior in the same molecule.[129] Of particular interest is using luminescence properties to facilitate investigating SMMs on surfaces, for instance for determining surface localization, concentrations and quantum properties.[21b]

The research group of Ouahab has been very active in this area, investigating the archetypal tetrathiafulvalene (TTF) ligand system. Such ligands are isolable in multiple redox states, can act as sensitizers for lanthanoid luminescence, and have been used previously to make SMMs, thus are good candidates to study the synergy between photophysical and magnetic behavior.[130] In 2015, based on previous studies using TTF ligands that allowed lanthanoid complexes to display either luminescence *or* SMM behavior, modifications to the ligand system (replacement of dithio with dioxo moieties)[30c] allowed for the combination of both luminescence and SMM behavior in a single complex.[131] The study involved the synthesis of dinuclear $[Dy(hfac)_3(L_{TTF})]_2$ (**83**) and mononuclear $[Ln(tta)_3(L_{TTF})]\cdot xCH_2Cl_2$ (Ln(III) = Dy and x = 1.41 (**84**); Yb and x = 2 (**85**)). Both **83** and **85** were found to behave as SMMs, while the lack of SMM behavior for **84** was attributed to a different orientation of the principal anisotropy axes compared to dinuclear **83**. This is due to the stabilization of the charge density around the Dy vs Yb (oblate *vs* prolate) with the equatorial ligand field of the ligand stabilizing the prolate Yb ion giving rise to SMM behavior. In addition, Yb monomer **85** was found to luminesce. Although no switching of the photophysical or magnetic properties was observed, solution state cyclic voltammetry indicated that all complexes exhibited ligand-centered redox-activity. Complex **85** can therefore be described as a redox-active luminescent field-induced SMM.

More recently, Pointillart and co-workers reported extended di-*tert*-butyl dioxolene TTF triads (H_2L_{SQ}) previously used to achieve SMM behavior in a Dy complex to form the dinuclear complex $[Yb_2(hfac)_6(H_2L_{SQ})]\cdot 0.5CH_2Cl_2$ (**86**).[132] The ligand could also be chemically oxidized to the quinone (Q) state to form the redox isomer $[Yb_2(hfac)_6(L_{\mathbf{Q}})]$ (**87**). Both Yb compounds behave as field-induced SMMs, with the rate of relaxation substantially increased (factor of 5) in the case of the quinone compound (Figure 20). In addition, the semiquinone moiety efficiently sensitizes the Yb(III) luminescence, while the quinone results in a quenching of the luminescence. This is an important pioneering example of modulation of both magnetic and luminescence properties through control of the ligand redox state.

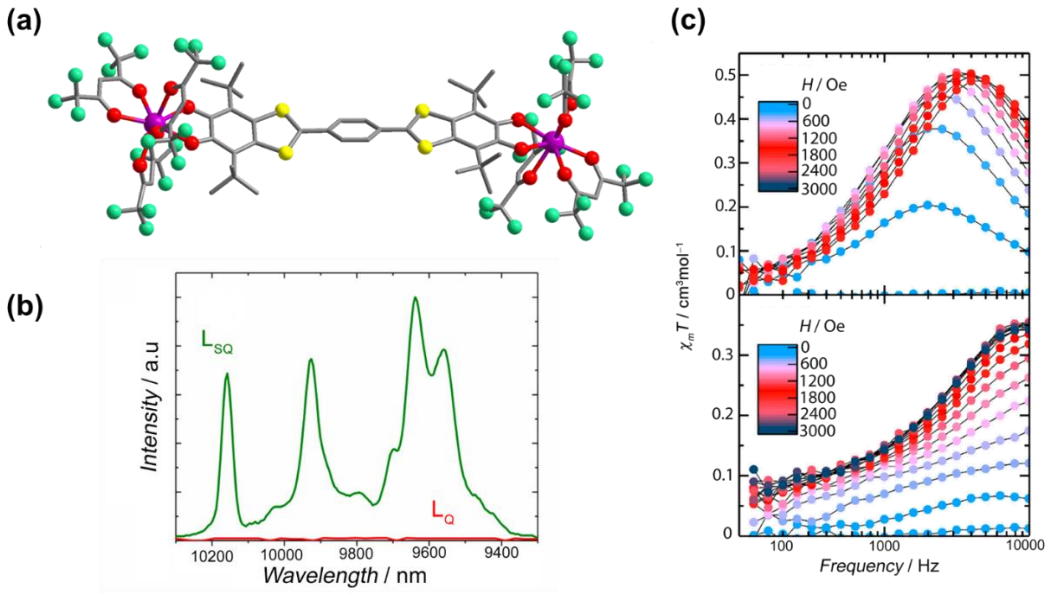

Figure 20. a) Structure of **86** (color scheme as per Figure 8). b) Solid-state emission spectra at 77 K of **86** (green) and **87** (red) with irradiation energy of 16,670 cm^{-1}. c) comparison of the out-of-phase magnetic susceptibility (χ'') for **86** (above) and **87** (below). Adapted (open-access) from reference 132a.[132a]

5. Redox-active Ligands Combined with Lanthanoid-Centered Redox-activity

Although examples are increasing of lanthanoid complexes with the metal in unusual oxidation states, or featuring redox-active ligands, the combination of both aspects in the same molecule remains little explored. Using redox-active ligands in conjunction with lanthanoid metals that are amenable to a change in oxidation state (*e.g.* Eu(II)/(III) or Ce(III)/(IV)) offers the potential to transfer and store electrons and modulate reactivity. It also offers access to unique electronic properties and the phenomenon of valence tautomerism.

The late Richard Andersen contributed significantly to the study of the electronic structure of lanthanoids with redox-active ligands along with co-worker Grégory Nocton.[53h, 133] Of particular note was the investigation of the YbCp system in conjunction with various bpy analogues, which sought to probe multiconfigurational ground states, where the valence of these systems was found to lie between two integer values for Yb(II)/Yb(III).[133a] This behavior was termed

'intermediate valence tautomerism'. Valence tautomerism involves a stimulated intramolecular electron transfer between a redox-active ligand and metal, yielding two different valence tautomers with different charge distributions.[3] The electron transfer is stimulated by some external perturbation such as temperature, with the transition impacted by several factors including ancillary ligand, electronic modifications to the redox-active ligand, cooperativity, counterion, and solvation. Intramolecular electron transfer between the ligand and lanthanoid requires that the relevant frontier orbitals are of comparable energy.[134] In 2001, Andersen reported unusual magnetic behavior for [$Yb^{III}(Me_5C_5)_2(bpy^{\bullet-})$] (**88**).[135] Although extensive characterization (^{1}H-NMR, electronic absorption spectra, IR and single crystal X-ray diffraction) indicated that the bipyridyl complex was paramagnetic due to the radical $bpy^{\bullet-}$, magnetic measurements afforded susceptibility values that were in between those expected for [$Yb^{III}(Me_5C_5)_2(bpy^{\bullet-})$] and [$Yb^{II}(Me_5C_5)_2(bpy^0)$]. A similar investigation for a range of complexes involving substituted X-bpy ligands (X = Me, ^{t}Bu, OMe, Ph, CO_2Me, and CO_2Et) showed similar indications of intermediate valence. In the case of methylated bpy, however, some unusual temperature dependence was observed in the magnetic susceptibility data.[136] This was investigated more thoroughly with a series of $(Me_5C_5)_2$Yb(Me_x-bpy) complexes (where x = 1, 2) varying the substitutions between the 4, 5 and 6 positions: [YbCp*$_2$(4-Me-bpy)] (**89**), [YbCp*$_2$(5-Me-bpy)] (**90**), [YbCp*$_2$(6-Me-bpy)] (**91**), [YbCp*$_2$(4,4′-Me_2-bpy)] (**92**), [YbCp*$_2$(5,5′-Me_2-bpy)] (**93**), [YbCp* (6,6′-Me_2-bpy)] (**94**) (Figure 21) [133c] Through this investigation it was established that the methyl substituent position dictates whether the ground state configuration is of predominantly Yb(II) or Yb(III) character.

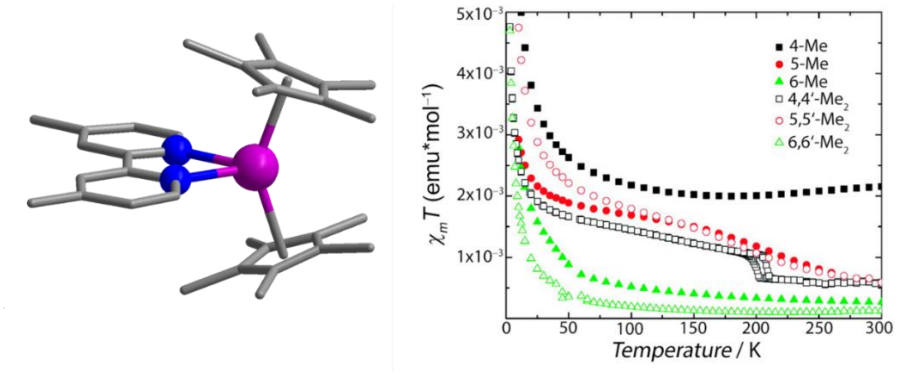

Figure 21. Left: Structure of **92** (4,4′-Me_2-bpy) (color scheme as per Figure 8). Right: variable temperature magnetic susceptibility, $\chi_m T$, for all Me-substituted analogues of **92** in a field of 5 kOe. Adapted with permission.[133c] Copyright (2010) American Chemical Society.

The XANES data suggest that all methylated analogues can be described as mixed-valence Yb(II/III), the 4-Me-bpy analogue (**87**) closer to Yb(II) and the 6,6′-Me_2-bpy analogue (**92**) closer to Yb(III) (Figure 22). The difference in the temperature independent behavior of the unsubstituted bpy versus the temperature dependent behavior of the methylated bpy is due to a difference in their multiconfigurational ground states. For $(Me_5C_5)_2Yb(bpy)$, the ground state wavefunction is made up of both the open shell singlet $(Me_5C_5)_2Yb^{III}(bpy^{\bullet-})$ and the closed shell singlet $(Me_5C_5)_2Yb^{II}(bpy^0)$. For $(Me_5C_5)_2Yb(Me_x\text{-bpy})$, the temperature dependence arises from an equilibrium between the ground and 1st excited open shell singlet states, which lie close in energy. Both the ground and 1st excited states are multiconfigurational, but the former is dominated by the Yb(III) f^{13} configuration and the latter by the Yb(II) f^{14} configuration. The ground state is dominated by Yb(III), and thus is favored by enthalpy due to the shorter Yb-N/C bond lengths, whereas the excited state which is dominated by Yb(II) is favored by entropy due to the longer bond lengths. The enthalpy changes are sufficiently small between the two states that the 1st excited state at low temperature can become the ground state at higher temperatures. It is important to note therefore that rather than a mixture of molecules in either the trivalent or divalent state, the multiconfigurational states are intrinsic to each molecule. As this behavior arises from multiconfigurational states, this behavior is dubbed *intermediate* valence tautomerism.[137]

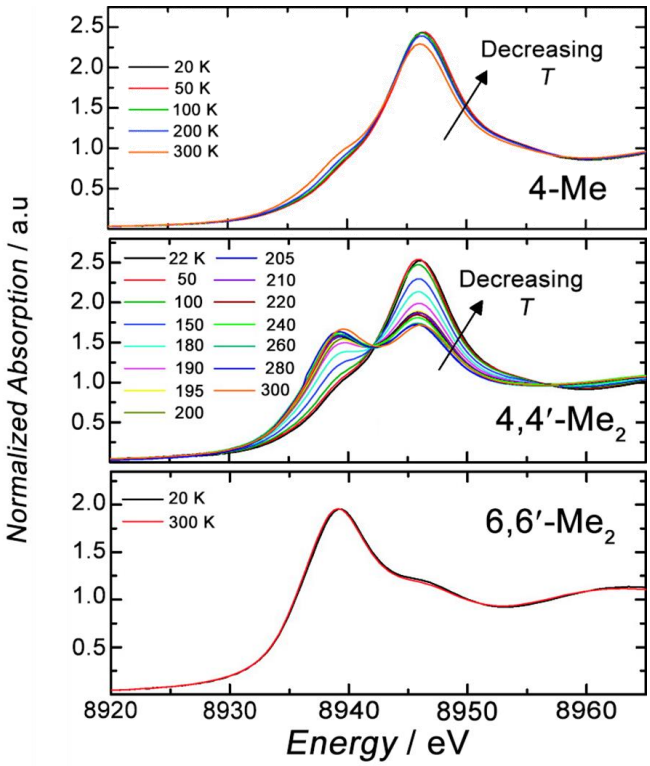

Figure 22. Variable temperature L_3-edge XANES for **89**, **92**, **94**. Adapted with permission.[133c] Copyright (2010) American Chemical Society.

In a more recent example, Lyssenko and co-workers revisited the archetypal ytterbocenes investigating the impact of steric bulk of a series of iminopyridine (IPy) redox-active co-ligands.[138] As a consequence of metal ion size decrease accompanying oxidation of Yb(II) to Yb(III), metal to ligand electron transfer is inhibited and a diamagnetic closed shell $[Yb^{II}(\eta^5\text{-}C_9H_7)_2(IPy^0)]$ (**95**) results.[139] Extension of the investigation to $YbCp^*_2$ with unsubstituted and 6-(hetero)aryl-substituted X-IPy (where X = H for A-IPy, C_4H_3O for B-IPy, C_4H_3S for C-IPy, C_6H_5 for D-IPy) ligands afforded a series of di- (for LB - LD) and trivalent Yb (for LA) complexes (Figure 23**Figure 23.** Above: structure of **96** (color scheme as per Figure 8) with ligand LA highlighted with yellow bonds, and depictions of the ligands B-IPy, C-IPy and D-IPy as taken from the single-crystal data for **97**-**99**. Below: magnetic moment (μ_{eff}) vs *T* for **97**-**99**. Adapted from reference 138 published by Royal Society of Chemistry.[138]).[138] Although these ligands have similar electron-accepting properties, they vary in both their denticity and steric demands. Use of the unsubstituted A-IPy gave rise to $[Yb^{III}Cp^*_2(A\text{-}IPy)^{\bullet-}]$ (**96**) whereas use of the substituted B-IPy – D-IPy yielded $[Yb^{II}Cp^*_2(X\text{-}IPy)^0]$ (X = B (**97**), C (**98**), D (**99**)). The radical-anionic ligand A-IPy and the neutral B-

IPy and C-IPy ligands coordinated in a bidentate fashion (N/N, N/O, N/S respectively), whereas the neutral ligand D-IPy adopts a monodentate mode (Figure 23). Although magnetic data suggest multiconfigurational ground states for **96**, with the most significant contribution from the $Yb^{III}(D\text{-}IPy)^{\bullet-}$ state, data for **97** and **98** are indicative of a $Yb^{II}(X\text{-}IPy)^{0}$ (where X = B and C) closed shell configuration. Complex **99** exhibits a very unusual magnetic moment profile (Figure 23). The data collected between 280 and 2.4 K lie between that of an antiferromagnetically coupled $Yb^{III}(D\text{-}IPy)^{\bullet-}$ and diamagnetic closed shell $Yb^{II}(D\text{-}IPy)^{0}$, but with no indication of multiconfigurational behavior.[133g] On increasing the temperature, the magnetic moment rose, consistent with a strong antiferromagnetically coupled Yb(III) radical system, but was found to be irreversible on another cool-heat cycle. However, the magnetic moment reached the same value above 270K. As the structure was determined below 270 K, there is no guarantee that the structure of **99** above 270 K is the same as that determined through single crystal X-ray diffraction studies performed at 100 K. Rather than attributing the $Yb^{III}(LD)^{\bullet-}$ to the high temperature behavior, and the structurally characterized **99** a diamagnetic character, they concede that this is only speculative and that more evidence is required. However, valence tautomerism was ruled out, as a closed shell configuration would be favorable at higher temperature on an entropic basis. It is possible however that some structural rearrangement could take place which favors the $Yb^{III}(D\text{-}IPy)^{\bullet-}$ charge distribution via a coupled structural-electronic transition, but there are no data to confirm this. The DFT calculations confirm the ambiguity of the ground state composition, with a very small energy difference between the open-shell singlet (anti-ferromagnetically coupled $Yb^{III}(D\text{-}IPy)^{\bullet-}$), the triplet state (ferromagnetically coupled $Yb^{III}(D\text{-}IPy)^{\bullet-}$), and the closed-shell singlet ($Yb^{II}(D\text{-}IPy)^{0}$).

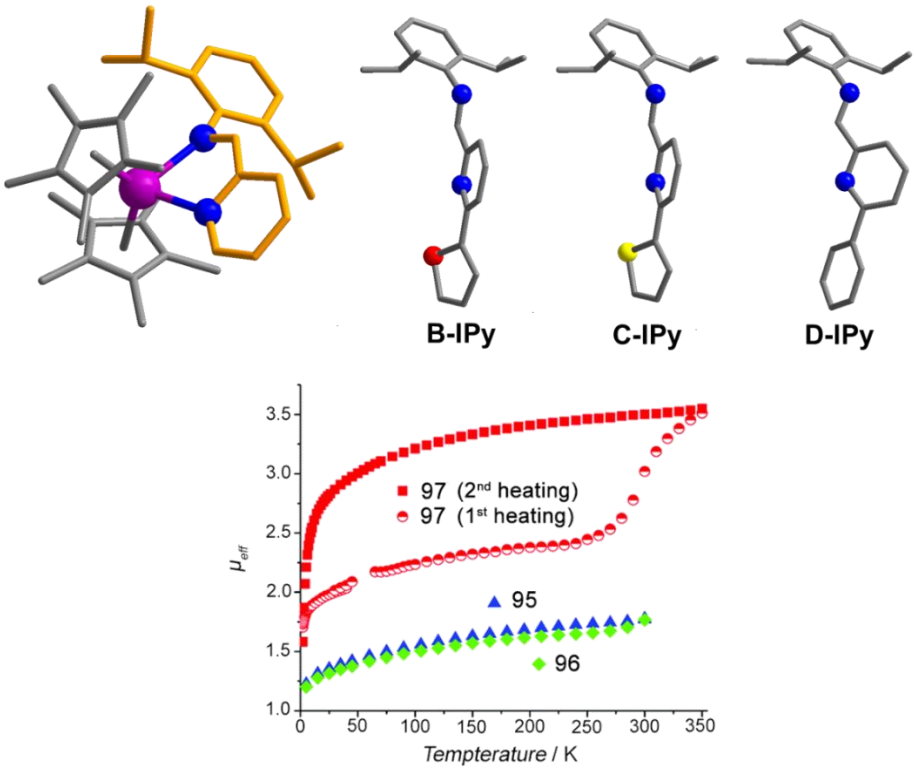

Figure 23. Above: structure of **96** (color scheme as per Figure 8) with ligand LA highlighted with yellow bonds, and depictions of the ligands B-IPy, C-IPy and D-IPy as taken from the single-crystal data for **97**-**99**. Below: magnetic moment (μ_{eff}) vs *T* for **97**-**99**. Adapted from reference 138 published by Royal Society of Chemistry.[138]

The only example of true lanthanoid valence tautomerism was reported by Fedushkin and co-workers, through investigative work with the ligand 1,2-bis[(2,6-diisopropylphenyl)imino]-acenaphthene (dpp-BIAN), which is capable of achieving multiple redox-active states.[23a, 140] In 2009, Fedushkin reported the dinuclear complex [Yb(dpp-BIAN)(μ-Br)(DME)]$_2$ (**100**).[23a] Variable temperature absorption spectroscopy and Evans method magnetic measurements indicate an interconversion between {Yb^{II}(dpp-BIAN)$^{\bullet-}$Br and {Yb^{III}(dpp-BIAN)$^{2-}$Br} in solution as the temperature was lowered (Figure 24). The distinction between the temperature dependent behavior observed for complex **88** and the $(Me_5C_5)_2Yb(Me_x\text{-bpy})$ series reported by Andersen should be noted, as in the latter case the temperature dependence arises through the small energy difference in multi-configurational ground and excited states, with the lanthanoid valence intermediate between the divalent and trivalent states. To date, the only example of VT for a lanthanoid complex in the solid-state is a single polymorph of the chloride analogue [Yb(dpp-BIAN)(μ-Cl)(DME)]$_2$ (**101**) (Figure 25).[23b] Although two different polymorphs and one

solvatomorph were identified by single crystal X-ray diffraction studies, only one polymorph exhibits VT upon heating and cooling, as confirmed through magnetometry and variable temperature single-crystal X-ray diffraction studies. The transition occurs at only one of the metal centers. At low temperature two Yb(III) ions are coordinated to closed shell dpp-BIAN^{2-} ligands, but upon heating one of the Yb centers is reduced to Yb(II) with an S = 1/2 radical dpp-BIAN$^{\bullet-}$ ligand (Figure 24). The success in observing VT in these related complexes results from the closeness of the reduction potentials of $Yb^{III} + e^- \rightarrow Yb^{II}$ and $(dpp\text{-}BIAN)^{\bullet-} + e^- \rightarrow (dpp\text{-}BIAN)^{2-}$, and so if redox-matching is suitably harnessed it should be possible to expand the observation of this behavior to other systems. However, given that this was only observed for a single polymorph in the solid-state, and the rarity of the observation of VT in lanthanoid systems, this emphasizes the importance of other aspects of the system which have to be fine-tuned (e.g. crystal packing, solvation) to achieve this behavior. It is worth noting that VT in cobalt-dioxolene complexes, the most widely studied VT systems, are driven by the entropy change associated with the change in bond-lengths and electronic degeneracy on moving between low spin Co(III) and high spin Co(II). Such spin-state transitions are not possible for lanthanoids due to their near degenerate 4*f* orbitals and so the entropic driver for lanthanoid VT is less obvious.

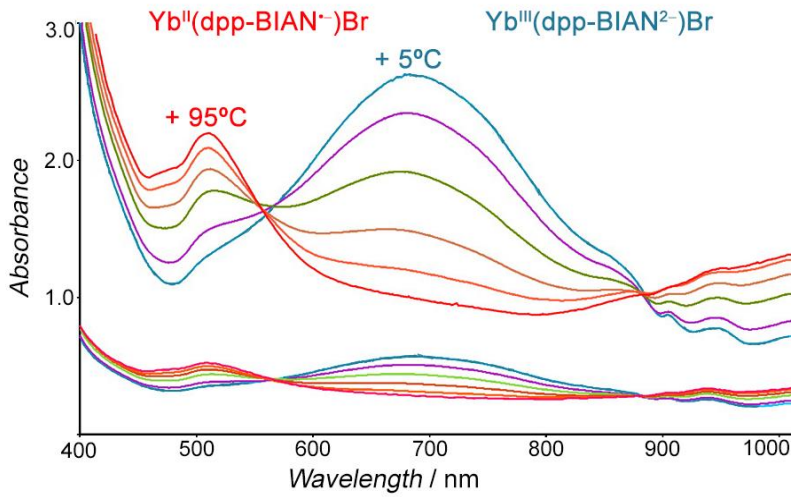

Figure 24. Temperature dependence of the absorption spectra of **100** in DME demonstrating interconversion between $Yb^{II}(dpp\text{-}BIAN)^-Br$ at 95°C to $Yb^{III}(dpp\text{-}BIAN)^{2-}Br$ at 5°C. Adapted with permission.[23a] Copyright (2009) American Chemical Society.

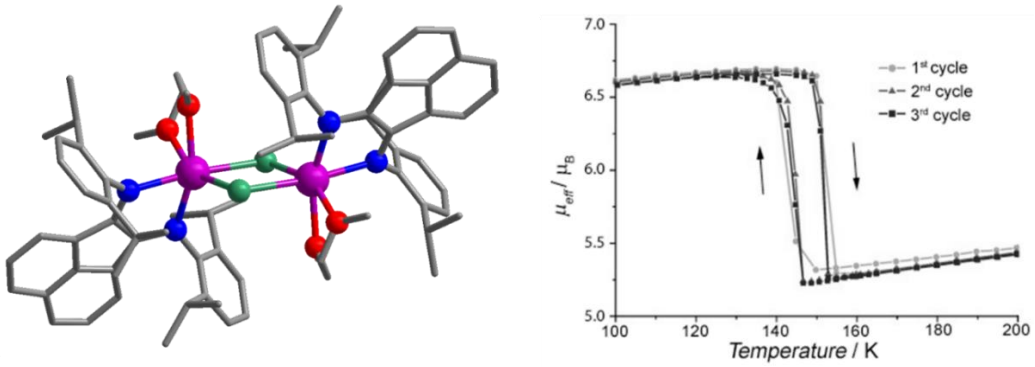

Figure 25. Left: Structure of **101** (colour code as per Figure 8). Right: magnetic hysteresis plotted as μ_{eff} vs *T*. Adapted with permission.[23b] Copyright (2012) Wiley-VCH Verlag GmbH & Co. KGaA, Weinheim.

Although Fedushkin and co-workers were later able to isolate the europium analogues [(dpp-BIAN$^{\bullet-}$)Eu^{II}(μ-Cl)(dme)]$_2$ (**102**) and [(dpp-BIAN$^{\bullet-}$)Eu^{II}(μ-Br)(dme)]$_2$ (**103**), the magnetic moments remain constant over a wide temperature range (295 to 25 K) and are typical of Eu(II) in the presence of dpp-bian radical ligands.[140a] Continuing the search for compounds that display genuine redox isomerism, the complexes [Eu^{II}(dpp-BIAN^{2-})(dme)$_2$] (**104**) and [Yb^{II}(dpp-BIAN^{2-})(dme)$_2$] (**105**) were reacted with bpy.[140b] This afforded several complexes which contained both bpy and dpp-BIAN derived redox-active ligands, but with the dianionic dpp-BIAN showing no change in oxidation state: [Eu^{II}(dpp-BIAN^{2-})(bpy)$_2$] (**106**) and [Yb^{III}(dpp-BIAN^{2-})(bpy$^{\bullet-}$)(bpy)] (**107**). On reaction of the Yb(II) precursor complex **105**, electron transfer from the metal to bpy resulted in oxidation at the metal center and reduction to the radical anionic state of the bpy ligand. Despite the closeness of the reduction potentials of Yb(III)/(II) and dipp-BIAN($^{\bullet-}$)/($^{2-}$) thermally-induced VT was not observed. This reinforces the rarity of such behavior, and careful design approached that must be pursued to achieve VT in future lanthanoid compounds.

6. Summary and Outlook

The library of molecular lanthanoid complexes with accessible redox features is growing. Although traditionally used in their trivalent oxidation state, exploration of the di- and tetra-valent states is increasing. Although the practical applications for lanthanoids in unusual oxidation states are limited due to the issue of stability, the relevant chemistry is of significant interest from a fundamental point of view. Advances in the chemistry of divalent lanthanoids has been driven by the isolation of complexes of new lanthanoid metals in this oxidation state, notably through the pioneering work of Bill Evans in lanthanoid cyclopentadienyl chemistry. The magnetic and luminescence properties of the more accessible divalent ions (Sm, Eu, Yb) are reasonably well understood in the context of solid-state materials, it has only been recently that researchers have started to investigate these in molecular systems. With electronic configurations the same as those of their right-hand neighbor in the periodic table in the trivalent state, but with a lower charge, divalent lanthanoid ions exhibit the necessary electronic characteristics for interesting magnetic and photophysical properties. However, their chemistry is still relatively unexplored and there is much scope for new research. A strategy for obtaining stable Ln(II) complexes lies in moving the redox potential towards more positive values by using ligands with softer donor atoms or bulky ligands to control the coordinative environment. An elegant survey of the stabilization of Ln(II) and Ln(III) states by Mazzanti *et al.* conveys this concept nicely, progressively moving from N donor to N,O donor ligands, observing that adding more oxophilic character stabilizes the Ln(III) state.[99] Although the redox potentials of the tetravalent lanthanoids are somewhat less accessible than the divalent, they have potential to benefit industrial process such as purification of lanthanoid ores and the separation of lanthanoids from actinoids during processing of spent nuclear fuel. With increasing demand for lanthanoid metals, improving such processes is crucial from the viewpoint of sustainability. By far the most well-studied is Ce(IV), with increasing investigation of the reactivity opening up the potential of these complexes to be used in new areas, such as photocatalysis. For stabilization of the tetravalent lanthanoids, more electron-rich ligands should be employed or those with significant orbital overlap to increase the degree of covalency. Isolation of Ln(IV) species (other than Ce(IV)) is much more recent with significant contributions from the groups of Mazzanti and La Pierre in the form of several Tb(IV), and the first Pr(IV), molecular complexes.[113–115] This work provides insights into how these oxidation states can be achieved and controlled, even while acknowledging stability issues with some of the compounds, presenting an exciting new direction for lanthanoid chemistry.

The magnetic and luminescence properties of lanthanoid ions in all oxidation states are of significant interest. Their use in SMMs relies on their intrinsic magnetic anisotropy in combination with judicious choice of ligand to impart the required symmetry and facilitate magnetic bistability. The design of luminescent molecular lanthanoid complexes relies on the position of the triplet state of a coordinated sensitizer, with molecular distortions often beneficial in allowing for the relaxation of the Laporte rule which normally forbids the 4*f*-4*f* transitions. For divalent lanthanoid ions, due to a comparative lowering of the 5*d* orbital energy, 5*d*-4*f* transitions (Laporte allowed) also arise, affording bands within the UV-Vis range that are particularly promising for optical applications. Both the magnetic and optical properties of the lanthanoid ions can be enhanced through use of redox-active ligands. For SMMs, use of radical ligands allows for strong coupling between lanthanoid centers and suppresses antagonistic QTM. For luminescence, using redox-active ligands enables more control over the properties, enhancing potential applications as biological redox probes. Integration of both luminescence and SMM behavior within one molecule could allow for new multifunctional materials and offer a specific (luminescent) probe for SMMs deposited onto surfaces or devices. This poses a synthetic challenge in finding a 'middle-ground' with a ligand scaffold that meets the requirements of controlled symmetry for SMM behavior whilst permitting some lower symmetry distortions that could enable luminescence within the same molecule. The highly anisotropic Ln(II) ions could be a good choice to study such synergistic properties due to the increased probability of transitions for luminescence from low-lying 5*d* orbitals, which may prevail even in higher symmetry environments. Most crucially, incorporation of redox-active ligands has allowed both luminescent compounds and SMMs to show switchable behavior. This is promising for electric control over these properties, which is potentially important for their implementation in next generation devices.

The use of lanthanoids to develop a new class of VT molecular switches has been considered as part of this review. Given the rarity of its observation one must be careful not to overstep in what can be taken from the single report of this behavior in terms of design in future VT lanthanoid compounds.[45] However, several factors need to be considered. Firstly, given that valence tautomerism was only observed for one polymorph of the compound (out of two different polymorphs and a solvatomorph), a comprehensive understanding of relatively subtle lattice and solvation effects is important. Therefore, complexes where multiple counterions, solvents or subtle changes to the ligand scaffold could be investigated could pose an advantage. Also important is the ability to functionalize the ligands with different groups to provide necessary steric protection, coordination and electronic effects. Secondly, the electrochemical potential of the

redox couples of the lanthanoid with the ancillary ligand in both oxidation states and those of the redox-active ligand will need to be sufficiently similar to facilitate electron transfer. Thirdly, lanthanoid metals with two accessible redox states (Yb(II)/(III), Eu(II)/(III) and Ce(III)/(IV)) must be the focus to enable a systematic study into the origins of this behavior. Success in this endeavor will inevitably require combining experimental investigations with computational studies to allow elucidation of electronic structure and ultimately computational prediction of candidate compounds for synthesis and measurement. Calculations of lanthanoid systems are non-trivial and computationally expensive, however significant advances in theoretical methods have occurred in recent years. Ultimately a considered and systematic approach may see the rise of lanthanoid-based molecular switches. If tied to luminescent, SMM or catalytic behavior, this could pave the way for a completely new class of functional molecular materials with substantial promise for applications.

Biographies

Moya A. Hay graduated with a BSc(Hons) in Chemistry from the University of Glasgow in 2015. She obtained her PhD (2019) under the supervision of Mark Murrie at the University of Glasgow investigating the magnetic anisotropy of transition metal complexes. Since August 2019, she has been a postdoctoral research fellow in the group of Colette Boskovic in the School of Chemistry at the University of Melbourne, harnessing redox-active ligands to target new functional metal complexes.

Colette Boskovic obtained her BSc(Hons) and PhD degrees from the University of Melbourne, undertaking research under the supervision of Tony Wedd. She returned to the University of Melbourne in 2004, where she is now Associate Professor, after postdoctoral positions with George Christou at Indiana University and Hans Güdel at the University of Bern. Her research interests lie in the fields of molecular magnetism, polyoxometalate chemistry, lanthanoid chemistry, redox-active ligands and switchable molecular materials.

The authors declare no conflicts of interest.

Acknowledgements C.B. and M.H. thank the Australian Research Council for financial support (DP190100854). We thank Maja Dunstan and Jett Janetzki for their invaluable feedback on the manuscript. Thank you to Douglas Venters for assistance in preparing Figure 1.

Keywords: Lanthanoid • Redox-active • Valence Tautomerism • Molecular magnetism • Luminescence

References

[1] a)M. D. Manrique-Juárez, S. Rat, L. Salmon, G. Molnár, C. M. Quintero, L. Nicu, H. J. Shepherd and A. Bousseksou, *Coord. Chem. Rev.* **2016**, *308*, 395-408; b)O. Sato, J. Tao and Y.-Z. Zhang, *Angew. Chem. Int. Ed.* **2007**, *46*, 2152-2187; c)S. Hayami, S. M. Holmes and M. A. Halcrow, *J. Mater. Chem* **2015**, *3*, 7775-7778.

[2] K. Senthil Kumar and M. Ruben, *Coord. Chem. Rev.* **2017**, *346*, 176-205.

[3] T. Tezgerevska, K. G. Alley and C. Boskovic, *Coord. Chem. Rev.* **2014**, *268*, 23-40.

[4] a)E. Evangelio and D. Ruiz-Molina, *C R Chim* **2008**, *11*, 1137-1154; b)A. Droghetti and S. Sanvito, *Phys. Rev. Lett.* **2011**, *107*, 47201-47201.

[5] a)J. Kobylarczyk, E. Kuzniak, M. Liberka, S. Chorazy, B. Sieklucka and R. Podgajny, *Coord. Chem. Rev.* **2020**, *419*, 213394-213394; b)G. N. Newton, M. Nihei and H. Oshio, *Eur. J. Inorg. Chem.* **2011**, *2011*, 3031-3042; c)K. R. Dunbar, C. Achim and M. Shatruk in *Charge Transfer-Induced Spin-Transitions in Cyanometallate Materials*, Ch6, **2013**, pp. 171-202.

[6] a)R. Sessoli, D. Gatteschi, A. Caneschi and M. A. Novak, *Nature* **1993**, *365*, 141-143; b)A. Lunghi, F. Totti, R. Sessoli and S. Sanvito, *Nat. Commun* **2017**, *8*, 14620-14620; c)D. Gatteschi and R. Sessoli, *Angew. Chem. Int. Ed.* **2003**, *42*, 268-297.

[7] a)O. Cador, B. Le Guennic and F. Pointillart, *Inorg. Chem. Front.* **2019**, *6*, 3398-3417; b)Y.-J. Ma, J.-X. Hu, S.-D. Han, J. Pan, J.-H. Li and G.-M. Wang, *J. Am. Chem. Soc.* **2020**, *142*, 2682-2689; c)D.-Q. Wu, D. Shao, X.-Q. Wei, F.-X. Shen, L. Shi, D. Kempe, Y.-Z. Zhang, K. R. Dunbar and X.-Y. Wang, *J. Am. Chem. Soc.* **2017**, *139*, 11714-11717; d)H. Tian, J.-B. Su, S.-S. Bao, M. Kurmoo, X.-D. Huang, Y.-Q. Zhang and L.-M. Zheng, *Chem. Sci.* **2018**, *9*, 6424-6433.

[8] a)E. Coronado, *Nature Reviews Materials* **2019**, *5*, 87-104; b)M. Cinchetti, V. A. Dediu and L. E. Hueso, *Nature Materials* **2017**, *16*, 507-515; c)S. G. McAdams, A.-M. Ariciu, A. K. Kostopoulos, J. P. S. Walsh and F. Tuna, *Coord. Chem. Rev.* **2017**, *346*, 216-239.

[9] a)H. Coufal, L. Dhar and C. D. Mee, *MRS Bull.* **2006**, *31*, 374-378; b)G. Hao, R. Cheng and P. A. Dowben, *J. Phys.: Condens. Matter* **2020**, *32*, 234002-234002.
[10] a)A. Gaita-Ariño, F. Luis, S. Hill and E. Coronado, *Nat. Chem.* **2019**, *11*, 301-309; b)A.-M. Ariciu, D. H. Woen, D. N. Huh, L. E. Nodaraki, A. K. Kostopoulos, C. A. P. Goodwin, N. F. Chilton, E. J. L. McInnes, R. E. P. Winpenny, W. J. Evans and F. Tuna, *Nat. Commun* **2019**, *10*, 3330-3330; c)J. Ferrando-Soria, E. Moreno Pineda, A. Chiesa, A. Fernandez, S. A. Magee, S. Carretta, P. Santini, I. J. Vitorica-Yrezabal, F. Tuna, G. A. Timco, E. J. L. McInnes and R. E. P. Winpenny, *Nat. Commun* **2016**, *7*, 11377-11377.
[11] a)J. Linares, E. Codjovi and Y. Garcia, *Sensors* **2012**, *12*, 4479-4492; b)B. Benaicha, K. Van Do, A. Yangui, N. Pittala, A. Lusson, M. Sy, G. Bouchez, H. Fourati, C. J. Gómez-García, S. Triki and K. Boukheddaden, *Chem. Sci.* **2019**, *10*, 6791-6798.
[12] G. Molnár, S. Rat, L. Salmon, W. Nicolazzi and A. Bousseksou, *Adv. Mater.* **2018**, *30*, 1703862-1703862.
[13] T. Cheisson and E. J. Schelter, *Science* **2019**, *363*, 489 LP-493.
[14] M. T. Kaczmarek, M. Zabiszak, M. Nowak and R. Jastrzab, *Coord. Chem. Rev.* **2018**, *370*, 42-54.
[15] a)G. Aromí and O. Roubeau in *Lanthanide molecules for spin-based quantum technologies*, *Vol. 56* Eds.: J.-C. G. Bünzli and V. K. Pecharsky, Elsevier, **2019**, pp. 1-54; b)M. Atzori and R. Sessoli, *J. Am. Chem. Soc.* **2019**, *141*, 11339-11352.
[16] a)P. L. Arnold, M. W. McMullon, J. Rieb and F. E. Kühn, *Angew. Chem. Int. Ed.* **2015**, *54*, 82-100; b)F. T. Edelmann, *Chem. Soc. Rev.* **2012**, *41*, 7657-7672; c)H. Pellissier, *Coord. Chem. Rev.* **2017**, *336*, 96-151.
[17] a)D. N. Woodruff, R. E. P. Winpenny and R. A. Layfield, *Chem. Rev.* **2013**, *113*, 5110-5148; b)J. Rinehart and J. Long, *Chem. Sci.* **2011**, *2*, 2078-2078.
[18] a)E. Pershagen and K. E. Borbas, *Coord. Chem. Rev.* **2014**, *273-274*, 30-46; b)A. J. Amoroso and S. J. A. Pope, *Chem. Soc. Rev.* **2015**, *44*, 4723-4742.
[19] a)G. L. Tripodi, T. C. Correra, C. F. F. Angolini, B. R. V. Ferreira, P. Maître, M. N. Eberlin and J. Roithová, *Eur. J. Org. Chem.* **2019**, *2019*, 3560-3566; b)C. Pagis, M. Ferbinteanu, G. Rothenberg and S. Tanase, *ACS Catal.* **2016**, *6*, 6063-6072.
[20] a)J. Andrez, J. Pécaut, P.-A. Bayle and M. Mazzanti, *Angew. Chem. Int. Ed.* **2014**, *53*, 10448-10452; b)M. Xémard, M. Cordier, E. Louyriac, L. Maron, C. Clavaguéra and G. Nocton, *Dalton Trans.* **2018**, *47*, 9226-9230; c)Y. Zheng, C.-S. Cao, W. Ma, T. Chen, B. Wu, C. Yu, Z. Huang, J. Yin, H.-S. Hu, J. Li, W.-X. Zhang and Z. Xi, *J. Am. Chem. Soc.* **2020**, *142*, 10705-10714; d)D. Werner, X. Zhao, S. P. Best, L. Maron, P. C. Junk and G. B. Deacon, *Chem. Eur. J* **2017**, *23*,

2084-2102; e)J. K. Molloy, C. Philouze, L. Fedele, D. Imbert, O. Jarjayes and F. Thomas, *Dalton Trans.* **2018**, *47*, 10742-10751; f)N. F. M. Mukthar, N. D. Schley and G. Ung, *Dalton Trans.* **2020**, *Advance Article*.

[21] a)X. Yi, K. Bernot, F. Pointillart, G. Poneti, G. Calvez, C. Daiguebonne, O. Guillou and R. Sessoli, *Chem. Eur. J* **2012**, *18*, 11379-11387; b)R. Marin, G. Brunet and M. Murugesu, *Angew. Chem. Int. Ed.* **2019**, 10.1002/anie.201910299.

[22] Y. Qiao and E. J. Schelter, *Acc. Chem. Res.* **2018**, *51*, 2926-2936.

[23] a)I. L. Fedushkin, O. V. Maslova, E. V. Baranov and A. S. Shavyrin, *Inorg. Chem.* **2009**, *48*, 2355-2357; b)I. L. Fedushkin, O. V. Maslova, A. G. Morozov, S. Dechert, S. Demeshko and F. Meyer, *Angew. Chem. Int. Ed.* **2012**, *51*, 10584-10587.

[24] M. W. Löble, J. M. Keith, A. B. Altman, S. C. E. Stieber, E. R. Batista, K. S. Boland, S. D. Conradson, D. L. Clark, J. Lezama Pacheco, S. A. Kozimor, R. L. Martin, S. G. Minasian, A. C. Olson, B. L. Scott, D. K. Shuh, T. Tyliszczak, M. P. Wilkerson and R. A. Zehnder, *J. Am. Chem. Soc.* **2015**, *137*, 2506-2523.

[25] R. A. Layfield and M. Murugesu, *Lanthanides and Actinides in Molecular Magnetism*, WILEY-VCH, **2015**.

[26] a)J. Pellico, C. M. Ellis and J. J. Davis, *Contrast Media & Molecular Imaging* **2019**, *2019*, 1-13; b)V. Zeleňák, M. Almáši, A. Zeleňáková, P. Hrubovčák, R. Tarasenko, S. Bourelly and P. Llewellyn, *Sci. Rep.* **2019**, *9*, 15572-15572.

[27] A. De Bettencourt-Dias, *Luminescence of Lanthanide Ions in Coordination Compounds and Nanomaterials*, John Wiley & Sons, Ltd, **2014**, p. 1-48.

[28] L. Armelao, S. Quici, F. Barigelletti, G. Accorsi, G. Bottaro, M. Cavazzini and E. Tondello, *Coord. Chem. Rev.* **2010**, *254*, 487-505.

[29] A. Vogler and H. Kunkely, *Inorg. Chim. Acta* **2006**, *359*, 4130-4138.

[30] a)B. A. Corbin, J. L. Hovey, B. Thapa, H. B. Schlegel and M. J. Allen, *J. Organomet. Chem.* **2018**, *857*, 88-93; b)M. Suta and C. Wickleder, *J. Lumin.* **2019**, *210*, 210-238; c)M. Feng, F. Pointillart, B. Le Guennic, B. Lefeuvre, S. Golhen, O. Cador, O. Maury and L. Ouahab, *Chem. Asian J.* **2014**, *9*, 2814-2825; d)J. Chen, Z. Xie, L. Meng, Z. Hu, X. Kuang, Y. Xie and C.-Z. Lu, *Inorg. Chem.* **2020**, *59*, 6963-6977.

[31] H. Yin, P. J. Carroll, B. C. Manor, J. M. Anna and E. J. Schelter, *J. Am. Chem. Soc.* **2016**, *138*, 5984-5993.

[32] S. Cotton, *Lanthanide and Actinide Chemistry*, John Wiley & Sons, Ltd, **2006**, p 9-19.

[33] a)J.-L. Liu, Y.-C. Chen and M.-L. Tong, *Chem. Soc. Rev.* **2018**, *47*, 2431-2453; b)Z. Zhu, M. Guo, X.-L. Li and J. Tang, *Coord. Chem. Rev.* **2019**, *378*, 350-364; c)F. Pointillart, O. Cador, B. Le Guennic and L. Ouahab, *Coord. Chem. Rev.* **2017**, *346*, 150-175.

[34] a)F.-S. Guo, B. M. Day, Y.-C. Chen, M.-L. Tong, A. Mansikkamäki and R. A. Layfield, *Science* **2018**, *362*, 1400-1403; b)G. Fu-Sheng, D. B. M, C. Yan-Cong, T. Ming-Liang, M. Akseli and L. R. A, *Angew. Chem. Int. Ed.* **2017**, *56*, 11445-11449; c)C. A. P. Goodwin, F. Ortu, D. Reta, N. F. Chilton and D. P. Mills, *Nature* **2017**, *548*, 439-442.

[35] a)K. R. Meihaus, M. E. Fieser, J. F. Corbey, W. J. Evans and J. R. Long, *J. Am. Chem. Soc.* **2015**, *137*, 9855-9860; b)C. A. Gould, K. R. McClain, J. M. Yu, T. J. Groshens, F. Furche, B. G. Harvey and J. R. Long, *J. Am. Chem. Soc.* **2019**, *141*, 12967-12973; c)M. Xémard, M. Cordier, F. Molton, C. Duboc, B. Le Guennic, O. Maury, O. Cador and G. Nocton, *Inorg. Chem.* **2019**, *58*, 2872-2880.

[36] W. Zhang, A. Muhtadi, N. Iwahara, L. Ungur and L. F. Chibotaru, *Angew. Chem. Int. Ed.* **2020**, *59*, 12720.

[37] a)A. Chiesa, F. Cugini, R. Hussain, E. Macaluso, G. Allodi, E. Garlatti, M. Giansiracusa, C. A. P. Goodwin, F. Ortu, D. Reta, J. M. Skelton, T. Guidi, P. Santini, M. Solzi, R. De Renzi, D. P. Mills, N. F. Chilton and S. Carretta, *Phys. Rev. B* **2020**, *101*, 174402-174402; b)D. Aravena and E. Ruiz, *Dalton Trans.* **2020**, *49*, 9916-9928; c)L. T. A. Ho and L. F. Chibotaru, *Phys. Rev. B* **2018**, *97*, 24427-24427; d)L. Escalera-Moreno, J. J. Baldoví, A. Gaita-Ariño and E. Coronado, *Chem. Sci.* **2018**, *9*, 3265-3275.

[38] a)L. R. Morss, *Chem. Rev.* **1976**, *76*, 827-841; b)D. A. Johnson, *J. Chem. Educ.* **1980**, *57*, 475-475.

[39] G. Meyer, *Angew. Chem. Int. Ed.* **2008**, *47*, 4962-4964.

[40] a)D. W. Smith, *J. Chem. Educ.* **1986**, *63*, 228-228; b)S. Bratsch and H. B. Silber, *Polyhedron* **1982**, *1*, 219-223; c)L. F. Druding and J. D. Corbett, *J. Am. Chem. Soc.* **1961**, *83*, 2462-2467.

[41] A. W. G. Platt in *Lanthanides: Variable Valency*, (Ed. R. A. Scott), John Wiley & Sons, **2012**.

[42] J. D. Corbett, L. F. Druding, W. J. Burkhard and C. B. Lindahl, *Discuss. Faraday Soc.* **1961**, *32*, 79-83.

[43] a)M. N. Bochkarev, *Coord. Chem. Rev.* **2004**, *248*, 835-851; b)M. N. Bochkarev, I. L. Fedushkin, A. A. Fagin, T. V. Petrovskaya, J. W. Ziller, R. N. R. Broomhall-Dillard and W. J. Evans, *Angew. Chem. Int. Ed.* **1997**, *36*, 133-135; c)M. N. Bochkarev and A. A. Fagin, *Chem. Eur. J* **1999**, *5*, 2990-2992.

[44] M. Pourbaix, *Atlas of electrochemical equilibria in aqueous solutions*, **1974**, 183 – 197.

[45] a)P. Di Bernardo, A. Melchior, M. Tolazzi and P. L. Zanonato, *Coord. Chem. Rev.* **2012**, *256*, 328-351; b)A. W. G. Platt in *Divalent Lanthanides in Solution*, (Ed. R. A. Scott), John Wiley & Sons, **2013**, pp. 1-6; c)N. A. Piro, J. R. Robinson, P. J. Walsh and E. J. Schelter, *Coord. Chem. Rev.* **2014**, *260*, 21-36.

[46] T. P. Gompa, A. Ramanathan, N. T. Rice and H. S. La Pierre, *Dalton Trans.* **2020**, 10.1039/D0DT01400A.

[47] T. Kimura, R. Nagaishi, Y. Kato and Z. Yoshida, *J. Alloys Compd.* **2001**, *323-324*, 164-168.

[48] M. L. Marsh, F. D. White, D. S. Meeker, C. D. McKinley, D. Dan, C. Van Alstine, T. N. Poe, D. L. Gray, D. E. Hobart and T. E. Albrecht-Schmitt, *Inorg. Chem.* **2019**, *58*, 9602-9612.

[49] T. C. Jenks, A. N. W. Kuda-Wedagedara, M. D. Bailey, C. L. Ward and M. J. Allen, *Inorg. Chem.* **2020**, *59*, 2613-2620.

[50] J. A. Bogart, A. J. Lewis, M. A. Boreen, H. B. Lee, S. A. Medling, P. J. Carroll, C. H. Booth and E. J. Schelter, *Inorg. Chem.* **2015**, *54*, 2830-2837.

[51] G. Meyer, *Angewandte Chemie - International Edition* **2014**, *53*, 3550-3551.

[52] a)M. Szostak, N. J. Fazakerley, D. Parmar and D. J. Procter, *Chem. Rev.* **2014**, *114*, 5959-6039; b)N. W. Davies, A. S. P. Frey, M. G. Gardiner and J. Wang, *Chem. Commun.* **2006**, *46*, 4853-4855; c)G. B. Deacon, P. C. Junk, J. Wang and D. Werner, *Inorg. Chem.* **2014**, *53*, 12553-12563; d)M. G. Gardiner and D. N. Stringer, *Materials* **2010**, *3*, 841-862; e)W. J. Evans, *J. Alloys Compd.* **2009**, *488*, 493-510.

[53] a)T. J. Marks in *Chemistry and Spectroscopy of f-Element Organometallics. Part 1: the Lanthanides*, *Vol. 24* (Ed. S. J. Lippard), John Wiley & Sons, **1978**, pp. 51-107; b)E. O. Fischer and H. Fischer, *J. Organomet. Chem.* **1965**, *3*, 181-187; c)V. E. Fleischauer, G. Ganguly, D. H. Woen, N. J. Wolford, W. J. Evans, J. Autschbach and M. L. Neidig, *Organometallics* **2019**, *38*, 3124-3131; d)R. G. Hayes and J. L. Thomas, *J. Am. Chem. Soc.* **1969**, *91*, 6876-6876; e)W. J. Evans, I. Bloom, W. E. Hunter and J. L. Atwood, *J. Am. Chem. Soc.* **1981**, *103*, 6507-6508; f)G. Nocton and L. Ricard, *Dalton Trans.* **2014**, *43*, 4380-4387; g)N. A. Pushkarevsky, M. A. Ogienko, A. I. Smolentsev, I. N. Novozhilov, A. Witt, M. M. Khusniyarov, V. K. Cherkasov and S. N. Konchenko, *Dalton Trans.* **2016**, *45*, 1269-1278; h)R. L. Halbach, G. Nocton, C. H. Booth, L. Maron and R. A. Andersen, *Inorg. Chem.* **2018**, *57*, 7290-7298; i)C. T. Palumbo, L. E. Darago, M. T. Dumas, J. W. Ziller, J. R. Long and W. J. Evans, *Organometallics* **2018**, *37*, 3322-3331.

[54] a)T. D. Tilley, R. A. Andersen and A. Zalkin, *J. Am. Chem. Soc.* **1982**, *104*, 3725-3727; b)G. W. Rabe, G. P. A. Yap and A. L. Rheingold, *Inorg. Chem.* **1997**, *36*, 3212-3215.

[55] D. R. Cary and J. Arnold, *Inorg. Chem.* **1994**, *33*, 1791-1796.

[56] a)T. D. Tilley, A. Zalkin, R. A. Andersen and D. H. Templeton, *Inorg. Chem.* **1981**, *20*, 551-554; b)C. A. P. Goodwin, N. F. Chilton, L. S. Natrajan, M.-E. Boulon, J. W. Ziller, W. J. Evans and D. P. Mills, *Inorg. Chem.* **2017**, *56*, 5959-5970; c)T. P. Gompa, N. Jiang, J. Bacsa and H. S. La Pierre, *Dalton Trans.* **2019**, *48*, 16869-16872.

[57] a)T. Cheisson, L. Ricard, F. W. Heinemann, K. Meyer, A. Auffrant and G. Nocton, *Inorg. Chem.* **2018**, *57*, 9230-9240; b)T. Cheisson, A. Auffrant and G. Nocton, *Organometallics* **2015**, *34*, 5470-5478.

[58] a)O. A. Gansow, A. R. Kausar, K. M. Triplett, M. J. Weaver and E. L. Yee, *J. Am. Chem. Soc.* **1977**, *99*, 7087-7089; b)T. C. Jenks, M. D. Bailey, B. A. Corbin, A. N. W. Kuda-Wedagedara, P. D. Martin, H. B. Schlegel, F. A. Rabuffetti and M. J. Allen, *Chem. Commun.* **2018**, *54*, 4545-4548; c)N.-D. H. Gamage, Y. Mei, J. Garcia and M. J. Allen, *Angew. Chem. Int. Ed.* **2010**, *49*, 8923-8925; d)C. U. Lenora, R. J. Staples and M. J. Allen, *Inorg. Chem.* **2020**, *59*, 86-93.

[59] a)A. N. W. Kuda-Wedagedara, C. Wang, P. D. Martin and M. J. Allen, *J. Am. Chem. Soc.* **2015**, *137*, 4960-4963; b)C. U. Lenora, F. Carniato, Y. Shen, Z. Latif, E. M. Haacke, P. D. Martin, M. Botta and M. J. Allen, *Chem. Eur. J* **2017**, *23*, 15404-15414.

[60] a)A. K. J. Dick, A. S. P. Frey, M. G. Gardiner, M. Hilder, A. N. James, P. C. Junk, S. Powanosorn, B. W. Skelton, J. Wang and A. H. White, *J. Organomet. Chem.* **2010**, *695*, 2761-2767; b)S. Shinoda, M. Nishioka and H. Tsukube, *J. Alloys Compd.* **2009**, *488*, 603-605; c)P. Starynowicz, *J. Alloys Compd.* **2001**, *323-324*, 159-163; d)M. E. Burnett, B. Adebesin, A. M. Funk, Z. Kovacs, A. D. Sherry, L. A. Ekanger, M. J. Allen, K. N. Green and S. J. Ratnakar, *Eur. J. Inorg. Chem.* **2017**, *2017*, 5001-5005; e)F. D. White, C. Celis-Barros, J. Rankin, E. Solís-Céspedes, D. Dan, A. N. Gaiser, Y. Zhou, J. Colangelo, D. Páez-Hernández, R. Arratia-Pérez and T. E. Albrecht-Schmitt, *Inorg. Chem.* **2019**, *58*, 3457-3465; f)G.-Y. Adachi, K. Tomokiyo, K. Sorita and J. Shiokawa, *J. Chem. Soc., Chem. Commun.* **1980**, 10.1039/C39800000914, 914-915; g)P. Starynowicz, K. Bukietyńska, S. Gołąb, W. Ryba-Romanowski and J. Sokolnicki, *Eur. J. Inorg. Chem.* **2002**, *2002*, 2344-2347; h)J. Christoffers and P. Starynowicz, *Polyhedron* **2008**, *27*, 2688-2692; i)L. A. Ekanger, D. R. Mills, M. M. Ali, L. A. Polin, Y. Shen, E. M. Haacke and M. J. Allen, *Inorg. Chem.* **2016**, *55*, 9981-9988.

[61] J. Andrez, G. Bozoklu, G. Nocton, J. Pécaut, R. Scopelliti, L. Dubois and M. Mazzanti, *Chem. Eur. J* **2015**, *21*, 15188-15200.

[62] Y.-Z. Ma, N. A. Pushkarevsky, T. S. Sukhikh, A. E. Galashov, A. G. Makarov, P. W. Roesky and S. N. Konchenko, *Eur. J. Inorg. Chem.* **2018**, *2018*, 3388-3396.

[63] a)R. P. Kelly, D. Toniolo, F. F. Tirani, L. Maron and M. Mazzanti, *Chem. Commun.* **2018**, *54*, 10268-10271; b)R. P. Kelly, L. Maron, R. Scopelliti and M. Mazzanti, *Angew. Chem. Int. Ed.* **2017**, *56*, 15663-15666.

[64] a)G. B. Deacon, A. Gitlits, P. W. Roesky, M. R. Bürgstein, K. C. Lim, B. W. Skelton and A. H. White, *Chem. Eur. J* **2001**, *7*, 127-138; b)J. Hitzbleck, A. Y. O'Brien, G. B. Deacon and K. Ruhlandt-Senge, *Inorg. Chem.* **2006**, *45*, 10329-10337; c)G. B. Deacon, A. Gitlits, B. W. Skelton and A. H. White, *Chem. Commun.* **1999**, *13*, 1213-1214; d)J. Hitzbleck, G. B. Deacon and K. Ruhlandt-Senge, *Eur. J. Inorg. Chem.* **2007**, *2007*, 592-601; e)S. Beaini, G. B. Deacon, M. Hilder, P. C. Junk and D. R. Turner, *Eur. J. Inorg. Chem.* **2006**, *2006*, 3434-3441.

[65] a)S. Hamidi, G. B. Deacon, P. C. Junk and P. Neumann, *Dalton Trans.* **2012**, *41*, 3541-3552; b)B. Liu, Y. Yao, M. Deng, Y. Zhang and Q. Shen, *J Rare Earth* **2006**, *24*, 264-267; c)H. Guo, H. Zhou, Y. Yao, Y. Zhang and Q. Shen, *Dalton Trans.* **2007**, *2007*, 3555-3561; d)Z. Du, H. Zhou, H. Yao, Y. Zhang, Y. Yao and Q. Shen, *Chem. Commun.* **2011**, *47*, 3595-3597; e)S. Kumar and S. K. Gupta, *Inorganic and Nano-Metal Chemistry* **2019**, *49*, 113-119; f)L. Maria, V. R. Sousa, I. C. Santos, E. Mora and J. Marçalo, *Polyhedron* **2016**, *119*, 277-285; g)L. Maria, M. Soares, I. C. Santos, V. R. Sousa, E. Mora, J. Marçalo and K. V. Luzyanin, *Dalton Trans.* **2016**, *45*, 3778-3790.

[66] a)S. Zhou, S. Wang, E. Sheng, L. Zhang, Z. Yu, X. Xi, G. Chen, W. Luo and Y. Li, *Eur. J. Inorg. Chem.* **2007**, *2007*, 1519-1528; b)B. M. Wolf, C. Stuhl and R. Anwander, *Chem. Commun.* **2018**, *54*, 8826-8829; c)J. Garcia and M. J. Allen, *Eur. J. Inorg. Chem.* **2012**, *2012*, 4550-4563; d)S.-O. Hauber and M. Niemeyer, *Inorg. Chem.* **2005**, *44*, 8644-8646; e)H. S. Lee and M. Niemeyer, *Inorg. Chem.* **2010**, *49*, 730-735; f)S. Yao, H.-S. Chan, C.-K. Lam and H. K. Lee, *Inorg. Chem.* **2009**, *48*, 9936-9946; g)H. M. Nicholas and D. P. Mills in *Lanthanides: Divalent Organometallic Chemistry*, (Ed. R. A. Scott), John Wiley & Sons, **2017**, pp. 1-10; h)D. Heitmann, C. Jones, D. P. Mills and A. Stasch, *Dalton Trans.* **2010**, *39*, 1877-1882; i)M. L. Cole, G. B. Deacon, C. M. Forsyth, P. C. Junk, K. Konstas, J. Wang, H. Bittig and D. Werner, *Chem. Eur. J* **2013**, *19*, 1410-1420.

[67] M. N. Bochkarev, I. L. Fedushkin, S. Dechert, A. A. Fagin and H. Schumann, *Angew. Chem. Int. Ed.* **2001**, *40*, 3176-3178.

[68] a)M. Xémard, A. Jaoul, M. Cordier, F. Molton, O. Cador, B. Le Guennic, C. Duboc, O. Maury, C. Clavaguéra and G. Nocton, *Angew. Chem. Int. Ed.* **2017**, *56*, 4266-4271; b)S. R. Ciccone, D. N. Huh, W. J. Evans, S. Roy, S. Bekoe and F. Furche, *Angew. Chem. Int. Ed.* **2020**, *59,* 16141. c)A. Momin, F. Bonnet, M. Visseaux, L. Maron, J. Takats, M. J. Ferguson, X.-F. Le Goff and F. Nief, *Chem. Commun.* **2011**, *47*, 12203-12205; d)J. Cheng, J. Takats, M. J. Ferguson and R.

McDonald, *J. Am. Chem. Soc.* **2008**, *130*, 1544-1545; e)F. Nief, D. Turcitu and L. Ricard, *Chem. Commun.* **2002**, *15*, 1646-1647.

[69] C. Felser, K. Ahn, R. K. Kremer, R. Seshadri and A. Simon, *J. Solid State Chem.* **1999**, *147*, 19-25.

[70] a)G. Meyer, *J. Solid State Chem.* **2019**, *270*, 324-334; b)P. B. Hitchcock, M. F. Lappert, L. Maron and A. V. Protchenko, *Angew. Chem. Int. Ed.* **2008**, *47*, 1488-1491.

[71] a)M. R. MacDonald, J. E. Bates, J. W. Ziller, F. Furche and W. J. Evans, *J. Am. Chem. Soc.* **2013**, *135*, 9857-9868; b)G. Meyer, *Angew. Chem. Int. Ed.* **2014**, *53*, 3550-3551.

[72] N. B. Mikheev, L. N. Auerman, I. A. Rumer, A. N. Kamenskaya and M. Z. Kazakevich, *Russ. Chem. Rev.* **1992**, *61*, 990-998.

[73] a)M. Cristina Cassani, M. F. Lappert and F. Laschi, *Chem. Commun.* **1997**, *16*, 1563-1564; b)M. C. Cassani, D. J. Duncalf and M. F. Lappert, *J. Am. Chem. Soc.* **1998**, *120*, 12958-12959; c)M. Cristina Cassani, Y. K. Gun'ko, P. B. Hitchcock, A. G. Hulkes, A. V. Khvostov, M. F. Lappert and A. V. Protchenko, *J. Organomet. Chem.* **2002**, *647*, 71-83.

[74] a)M. R. MacDonald, J. W. Ziller and W. J. Evans, *J. Am. Chem. Soc.* **2011**, *133*, 15914-15917; b)W. J. Evans, D. S. Lee, C. Lie and J. W. Ziller, *Angew. Chem. Int. Ed.* **2004**, *43*, 5517-5519.

[75] M. R. MacDonald, J. E. Bates, M. E. Fieser, J. W. Ziller, F. Furche and W. J. Evans, *J. Am. Chem. Soc.* **2012**, *134*, 8420-8423.

[76] a)J. W. Lauher and R. Hoffmann, *J. Am. Chem. Soc.* **1976**, *98*, 1729-1742; b)R. G. Denning, J. Harmer, J. C. Green and M. Irwin, *J. Am. Chem. Soc.* **2011**, *133*, 20644-20660.

[77] M. E. Fieser, M. R. MacDonald, B. T. Krull, J. E. Bates, J. W. Ziller, F. Furche and W. J. Evans, *J. Am. Chem. Soc.* **2015**, *137*, 369-382.

[78] W. J. Evans, *Organometallics* **2016**, *35*, 3088-3100.

[79] T. C. Jenks, M. D. Bailey, Jessica L. Hovey, S. Fernando, G. Basnayake, M. E. Cross, W. Li and M. J. Allen, *Chem. Sci.* **2018**, *9*, 1273-1278.

[80] R. A. Flowers II, *Synlett* **2008**, *10*, 1427-1439.

[81] a)J. J. M. Nelson and E. J. Schelter, *Inorg. Chem.* **2019**, *58*, 979-990; b)K. Binnemans, P. T. Jones, B. Blanpain, T. Van Gerven, Y. Yang, A. Walton and M. Buchert, *J. Clean. Prod.* **2013**, *51*, 1-22.

[82] a)A. R. Willauer, C. T. Palumbo, F. Fadaei-Tirani, I. Zivkovic, I. Douair, L. Maron and M. Mazzanti, *J. Am. Chem. Soc.* **2020**, *142*, 5538-5542; b)C. T. Palumbo, I. Zivkovic, R. Scopelliti and M. Mazzanti, *J. Am. Chem. Soc.* **2019**, *141*, 9827-9831.

[83] a)Y. M. So and W. H. Leung, *Coord. Chem. Rev.* **2017**, *340*, 172-197; b)K. Binnemans in *Applications of tetravalent cerium compounds*, *Vol. 36* Elsevier, **2006**, pp. 281-392; c)V. Nair and A. Deepthi, *Chem. Rev.* **2007**, *107*, 1862-1891.

[84] a)L. A. Solola, A. V. Zabula, W. L. Dorfner, B. C. Manor, P. J. Carroll and E. J. Schelter, *J. Am. Chem. Soc.* **2016**, *138*, 6928-6931; b)L. A. Solola, P. J. Carroll and E. J. Schelter, *J. Organomet. Chem.* **2018**, *857*, 5-9.

[85] a)A. B. Canaj, M. Siczek, T. Lis, M. Murrie, E. K. Brechin and C. J. Milios, *Dalton Trans.* **2017**, *46*, 7677-7680; b)T. Behrsing, A. M. Bond, G. B. Deacon, C. M. Forsyth, M. Forsyth, K. J. Kamble, B. W. Skelton and A. H. White, *Inorg. Chim. Acta* **2003**, *352*, 229-237; c)A. C. Behrle, J. R. Levin, J. E. Kim, J. M. Drewett, C. L. Barnes, E. J. Schelter and J. R. Walensky, *Dalton Trans.* **2015**, *44*, 2693-2702; d)Y.-L. Sang, X.-S. Lin, X.-C. Li, Y.-H. Liu and X.-H. Zhang, *Inorg. Chem. Commun.* **2015**, *62*, 115-118; e)P. S. Gradeff, K. Yunlu, A. Gleizes and J. Galy, *Polyhedron* **1989**, *8*, 1001-1005; f)P. Jewula, J.-C. Berthet, J.-C. Chambron, Y. Rousselin, P. Thuéry and M. Meyer, *Eur. J. Inorg. Chem.* **2015**, *2015*, 1529-1541; g)A. Mishra, A. J. Tasiopoulos, W. Wernsdorfer, E. E. Moushi, B. Moulton, M. J. Zaworotko, K. A. Abboud and G. Christou, *Inorg. Chem.* **2008**, *47*, 4832-4843; h)V. Mereacre, A. M. Ako, M. N. Akhtar, A. Lindemann, C. E. Anson and A. K. Powell, *Helv. Chim. Acta* **2009**, *92*, 2507-2524; i)G. Maayan and G. Christou, *Inorg. Chem.* **2011**, *50*, 7015-7021; j)D. G. Karmalkar, M. Sankaralingam, M. S. Seo, R. Ezhov, Y.-M. Lee, Y. N. Pushkar, W.-S. Kim, S. Fukuzumi and W. Nam, *Angew. Chem. Int. Ed.* **2019**, *58*, 16124-16129; k)B. E. Klamm, C. J. Windorff, M. L. Marsh, D. S. Meeker and T. E. Albrecht-Schmitt, *Chem. Commun.* **2018**, *54*, 8634-8636.

[86] D. W. Wester, G. J. Palenik and R. C. Palenik, *Inorg. Chem.* **1985**, *24*, 4435-4437.

[87] a)J. Gottfriedsen, *Z. Anorg. Allg. Chem.* **2005**, *631*, 2928-2930; b)J. Schläfer, S. Stucky, W. Tyrra and S. Mathur, *Inorg. Chem.* **2013**, *52*, 4002-4010; c)U. J. Williams, D. Schneider, W. L. Dorfner, C. Maichle-Mössmer, P. J. Carroll, R. Anwander and E. J. Schelter, *Dalton Trans.* **2014**, *43*, 16197-16206; d)E. M. Broderick, P. S. Thuy-Boun, N. Guo, C. S. Vogel, J. Sutter, J. T. Miller, K. Meyer and P. L. Diaconescu, *Inorg. Chem.* **2011**, *50*, 2870-2877.

[88] J. Schläfer, W. Tyrra and S. Mathur, *Inorg. Chem.* **2014**, *53*, 2751-2753.

[89] B. D. Mahoney, N. A. Piro, P. J. Carroll and E. J. Schelter, *Inorg. Chem.* **2013**, *52*, 5970-5977.

[90] P. L. Arnold, K. Wang, S. J. Gray, L. M. Moreau, C. H. Booth, M. Curcio, J. A. L. Wells and A. M. Z. Slawin, *Dalton Trans.* **2020**, *49*, 877-884.

[91] a)S. Giessmann, S. Blaurock, V. Lorenz and F. T. Edelmann, *Inorg. Chem.* **2007**, *46*, 8100-8101; b)Y. K. Gun'ko, R. Reilly, F. T. Edelmann and H.-G. Schmidt, *Angew. Chem. Int. Ed.* **2001**, *40*, 1279-1281.

[92] J. Friedrich, Y. Qiao, C. Maichle-Mössmer, E. J. Schelter and R. Anwander, *Dalton Trans.* **2018**, *47*, 10113-10123.

[93] a)E. Rousset, R. W. Gable, A. Starikova and C. Boskovic, *Crystal Growth & Design* **2020**, *20*, 3396-3405; b)E. Rousset, M. Piccardo, M.-E. Boulon, R. W. Gable, A. Soncini, L. Sorace and C. Boskovic, *Chem. Eur. J* **2018**, *24*, 14768-14785; c)S. F. Haddad and K. N. Raymond, *Inorg. Chim. Acta* **1986**, *122*, 111-118; d)T. A. Pham, A. B. Altman, S. C. E. Stieber, C. H. Booth, S. A. Kozimor, W. W. Lukens, D. T. Olive, T. Tyliszczak, J. Wang, S. G. Minasian and K. N. Raymond, *Inorg. Chem.* **2016**, *55*, 9989-10002.

[94] a)H. B. Lee, J. A. Bogart, P. J. Carroll and E. J. Schelter, *Chem. Commun.* **2014**, *50*, 5361-5363; b)W. L. Dorfner, P. J. Carroll and E. J. Schelter, *Dalton Trans.* **2014**, *43*, 6300-6303; c)J. E. Kim, P. J. Carroll and E. J. Schelter, *Chem. Commun.* **2015**, *51*, 15047-15050; d)J. A. Bogart, C. A. Lippincott, P. J. Carroll, C. H. Booth and E. J. Schelter, *Chem. Eur. J* **2015**, *21*, 17850-17859; e)T. Cheisson, K. D. Kersey, N. Mahieu, A. McSkimming, M. R. Gau, P. J. Carroll and E. J. Schelter, *J. Am. Chem. Soc.* **2019**, *141*, 9185-9190.

[95] a)P. B. Hitchcock, M. F. Lappert and A. V. Protchenko, *Chem. Commun.* **2006**, *33*, 3546-3548; b)U. J. Williams, B. D. Mahoney, A. J. Lewis, P. T. DeGregorio, P. J. Carroll and E. J. Schelter, *Inorg. Chem.* **2013**, *52*, 4142-4144; c)G. Balazs, F. G. N. Cloke, J. C. Green, R. M. Harker, A. Harrison, P. B. Hitchcock, C. N. Jardine and R. Walton, *Organometallics* **2007**, *26*, 3111-3119; d)M. Dolg and O. Mooßen, *J. Organomet. Chem.* **2015**, *794*, 17-22; e)I. J. Casely, S. T. Liddle, A. J. Blake, C. Wilson and P. L. Arnold, *Chem. Commun.* **2007**, *47*, 5037-5039; f)M. Gregson, E. Lu, J. McMaster, W. Lewis, A. J. Blake and S. T. Liddle, *Angew. Chem. Int. Ed.* **2013**, *52*, 13016-13019; g)Y. Bian, J. Jiang, Y. Tao, M. T. M. Choi, R. Li, A. C. H. Ng, P. Zhu, N. Pan, X. Sun, D. P. Arnold, Z.-Y. Zhou, H.-W. Li, T. C. W. Mak and D. K. P. Ng, *J. Am. Chem. Soc.* **2003**, *125*, 12257-12267; h)P. Dröse, A. R. Crozier, S. Lashkari, J. Gottfriedsen, S. Blaurock, C. G. Hrib, C. Maichle-Mössmer, C. Schädle, R. Anwander and F. T. Edelmann, *J. Am. Chem. Soc.* **2010**, *132*, 14046-14047; i)D. Werner, G. B. Deacon, P. C. Junk and R. Anwander, *Chem. Eur. J* **2014**, *20*, 4426-4438; j)A. R. Crozier, A. M. Bienfait, C. Maichle-Mössmer, K. W. Törnroos and R. Anwander, *Chem. Commun.* **2013**, *49*, 87-89; k)P. L. Damon, G. Wu, N. Kaltsoyannis and T. W. Hayton, *J. Am. Chem. Soc.* **2016**, *138*, 12743-12746; l)M. K. Assefa, D.-C. Sergentu, L. A. Seaman, G. Wu, J. Autschbach and T. W. Hayton, *Inorg. Chem.* **2019**, *58*, 12654-12661.

[96] a)J. R. Robinson, P. J. Carroll, P. J. Walsh and E. J. Schelter, *Angew. Chem. Int. Ed.* **2012**, *51*, 10159-10163; b)J. R. Robinson, Y. Qiao, J. Gu, P. J. Carroll, P. J. Walsh and E. J. Schelter, *Chem. Sci.* **2016**, *7*, 4537-4547; c)D. Werner, G. B. Deacon, P. C. Junk and R. Anwander, *Dalton Trans.* **2017**, *46*, 6265-6277.

[97] a)N. T. Rice, I. A. Popov, D. R. Russo, J. Bacsa, E. R. Batista, P. Yang, J. Telser and H. S. La Pierre, *J. Am. Chem. Soc.* **2019**, *141*, 13222-13233; b)J. R. Levin, W. L. Dorfner, P. J. Carroll and E. J. Schelter, *Chem. Sci.* **2015**, *6*, 6925-6934.

[98] a)M. Gregson, E. Lu, F. Tuna, E. J. L. McInnes, C. Hennig, A. C. Scheinost, J. McMaster, W. Lewis, A. J. Blake, A. Kerridge and S. T. Liddle, *Chem. Sci.* **2016**, *7*, 3286-3297; b)D. Schädle, M. Meermann-Zimmermann, C. Schädle, C. Maichle-Mössmer and R. Anwander, *Eur. J. Inorg. Chem.* **2015**, *2015*, 1334-1339; c)J. Jung, M. Atanasov and F. Neese, *Inorg. Chem.* **2017**, *56*, 8802-8816; d)M. Gregson, E. Lu, D. P. Mills, F. Tuna, E. J. L. McInnes, C. Hennig, A. C. Scheinost, J. McMaster, W. Lewis, A. J. Blake, A. Kerridge and S. T. Liddle, *Nat. Commun* **2017**, *8*, 14137-14137; e)N. T. Rice, I. A. Popov, D. R. Russo, T. P. Gompa, A. Ramanathan, J. Bacsa, E. R. Batista, P. Yang and H. S. La Pierre, *Chem. Sci.* **2020**, *11*, 6149-6159.

[99] N. T. Rice, J. Su, T. P. Gompa, D. R. Russo, J. Telser, L. Palatinus, J. Bacsa, P. Yang, E. R. Batista and H. S. La Pierre, *Inorg. Chem.* **2019**, *58*, 5289-5304.

[100] A. R. Willauer, C. T. Palumbo, R. Scopelliti, I. Zivkovic, I. Douair, L. Maron and M. Mazzanti, *Angew. Chem. Int. Ed.* **2020**, *59*, 3549-3553.

[101] a)W. Kaim and B. Schwederski, *Coord. Chem. Rev.* **2010**, *254*, 1580-1588; b)O. R. Luca and R. H. Crabtree, *Chem. Soc. Rev.* **2013**, *42*, 1440-1459.

[102] a)P. J. Chirik and K. Wieghardt, *Science* **2010**, *327*, 794 LP-795; b)W. Kaim and G. K. Lahiri, *Coord. Chem. Rev.* **2019**, *393*, 1-8; c)D. Zhu, I. Thapa, I. Korobkov, S. Gambarotta and P. H. M. Budzelaar, *Inorg. Chem.* **2011**, *50*, 9879-9887; d)V. K. K. Praneeth, M. R. Ringenberg and T. R. Ward, *Angew. Chem. Int. Ed.* **2012**, *51*, 10228-10234; e)D. L. J. Broere, R. Plessius and J. I. van der Vlugt, *Chem. Soc. Rev.* **2015**, *44*, 6886-6915.

[103] a)A. Rajput, A. K. Sharma, S. K. Barman, A. Saha and R. Mukherjee, *Coord. Chem. Rev.* **2020**, *414*, 213240-213240; b)K. P. Butin, E. K. Beloglazkina and N. V. Zyk, *Russ. Chem. Rev.* **2005**, *74*, 531-553; c)A. A. Starikova and V. I. Minkin, *Russ. Chem. Rev.* **2018**, *87*, 1049-1079; d)C. Römelt, T. Weyhermüller and K. Wieghardt, *Coord. Chem. Rev.* **2019**, *380*, 287-317.

[104] a)J. R. Hickson, S. J. Horsewill, C. Bamforth, J. McGuire, C. Wilson, S. Sproules and J. H. Farnaby, *Dalton Trans.* **2018**, *47*, 10692-10701; b)C. Camp, V. Guidal, B. Biswas, J. Pécaut, L. Dubois and M. Mazzanti, *Chem. Sci.* **2012**, *3*, 2433-2448; c)S. V. Klementyeva, N. P. Gritsan, M. M. Khusniyarov, A. Witt, A. A. Dmitriev, E. A. Suturina, N. D. D. Hill, T. L. Roemmele, M. T. Gamer,

R. T. Boeré, P. W. Roesky, A. V. Zibarev and S. N. Konchenko, *Chem. Eur. J* **2017**, *23*, 1278-1290; d)M. Hiller, T. Sittel, H. Wadepohl and M. Enders, *Chem. Eur. J* **2019**, *25*, 10668-10677; e)S. Demir, M. Nippe, M. I. Gonzalez and J. R. Long, *Chem. Sci.* **2014**, *5*, 4701-4711; f)F. Liu, G. Velkos, D. S. Krylov, L. Spree, M. Zalibera, R. Ray, N. A. Samoylova, C.-H. Chen, M. Rosenkranz, S. Schiemenz, F. Ziegs, K. Nenkov, A. Kostanyan, T. Greber, A. U. B. Wolter, M. Richter, B. Büchner, S. M. Avdoshenko and A. A. Popov, *Nat. Commun* **2019**, *10*, 571-571; g)D. Mouchel Dit Leguerrier, R. Barré, M. Bryden, D. Imbert, C. Philouze, O. Jarjayes, D. Luneau, J. K. Molloy and F. Thomas, *Dalton Trans.* **2020**, *49*, 8238-8246; h)H. Al Sabea, L. Norel, O. Galangau, H. Hijazi, R. Métivier, T. Roisnel, O. Maury, C. Bucher, F. Riobé and S. Rigaut, *J. Am. Chem. Soc.* **2019**, *141*, 20026-20030; i)G. Fernandez Garcia, V. Montigaud, L. Norel, O. Cador, B. Le Guennic, F. Totti and F. Pointillart, *Magnetochemistry* **2019**, *5*, 46-46.

[105] a)E. J. Coughlin, M. Zeller and S. C. Bart, *Angew. Chem. Int. Ed.* **2017**, *56*, 12142-12145; b)E. M. Matson, S. R. Opperwall, P. E. Fanwick and S. C. Bart, *Inorg. Chem.* **2013**, *52*, 7295-7304.

[106] M. Tropiano, N. L. Kilah, M. Morten, H. Rahman, J. J. Davis, P. D. Beer and S. Faulkner, *J. Am. Chem. Soc.* **2011**, *133*, 11847-11849.

[107] M. Yano, K. Matsuhira, M. Tatsumi, Y. Kashiwagi, M. Nakamoto, M. Oyama, K. Ohkubo, S. Fukuzumi, H. Misaki and H. Tsukube, *Chem. Commun.* **2012**, *48*, 4082-4084.

[108] a)E. T. Seo, R. F. Nelson, J. M. Fritsch, L. S. Marcoux, D. W. Leedy and R. N. Adams, *J. Am. Chem. Soc.* **1966**, *88*, 3498-3503; b)R. R. Nelson and R. N. Adams, *J. Am. Chem. Soc.* **1968**, *90*, 3925-3930; c)F. A. Neugebauer, S. Bamberger and W. R. Groh, *Chem. Ber.* **1975**, *108*, 2406-2415; d)J. P. Collin, S. Guillerez, J. P. Sauvage, F. Barigelletti, L. De Cola, L. Flamigni and V. Balzani, *Inorg. Chem.* **1991**, *30*, 4230-4238.

[109] a)J. K. Molloy, O. Jarjayes, C. Philouze, L. Fedele, D. Imbert and F. Thomas, *Chem. Commun.* **2017**, *53*, 605-608; b)A. Kaur, J. L. Kolanowski and E. J. New, *Angew. Chem. Int. Ed.* **2016**, *55*, 1602-1613.

[110] N. Ishikawa, M. Sugita, T. Ishikawa, S. Y. Koshihara and Y. Kaizu, *J. Am. Chem. Soc.* **2003**, *125*, 8694-8695.

[111] a)S. Takamatsu, T. Ishikawa, S.-y. Koshihara and N. Ishikawa, *Inorg. Chem.* **2007**, *46*, 7250-7252; b)M. Gonidec, E. S. Davies, J. McMaster, D. B. Amabilino and J. Veciana, *J. Am. Chem. Soc.* **2010**, *132*, 1756-1757.

[112] a)H. Konami, M. Hatano, N. Kobayashi and T. Osa, *Chem. Phys. Lett.* **1990**, *165*, 397-400; b)H. Shang, S. Zeng, H. Wang, J. Dou and J. Jiang, *Sci. Rep.* **2015**, *5*, 8838-8838; c)G. Lu, C. He, K. Wang, J. Sun, D. Qi, L. Gong, C. Wang, Z. Ou, S. Yan, S. Zeng and W. Zhu, *Inorg. Chem.*

2017, *56*, 11503-11512; d)Y. Horii, M. Damjanović, M. R. Ajayakumar, K. Katoh, Y. Kitagawa, L. Chibotaru, L. Ungur, M. Mas-Torrent, W. Wernsdorfer, B. K. Breedlove, M. Enders, J. Veciana and M. Yamashita, *Chem. Eur. J.* **2020**, *26*, 8621–8630; e)K.-H. Schweikart, V. L. Malinovskii, J. R. Diers, A. A. Yasseri, D. F. Bocian, W. G. Kuhr and J. S. Lindsey, *J. Mater. Chem.* **2002**, *12*, 808-828; f)G. Serrano, E. Velez-Fort, I. Cimatti, B. Cortigiani, L. Malavolti, D. Betto, A. Ouerghi, N. B. Brookes, M. Mannini and R. Sessoli, *Nanoscale* **2018**, *10*, 2715-2720; g)E. Moreno Pineda, T. Komeda, K. Katoh, M. Yamashita and M. Ruben, *Dalton Trans.* **2016**, *45*, 18417-18433; h)P. Zhu, F. Lu, N. Pan, Dennis P. Arnold, S. Zhang and J. Jiang, *Eur. J. Inorg. Chem.* **2004**, *2004*, 510-517; i)E. A. Kuzmina, T. V. Dubinina and L. G. Tomilova, *New J. Chem.* **2019**, *43*, 9314-9327; j)E. B. Orman, A. Koca, A. R. Özkaya, İ. Gürol, M. Durmuş and V. Ahsen, *J. Electrochem. Soc.* **2014**, *161*, H422-H429; k)H. Wang, T. Liu, K. Wang, C. Duan and J. Jiang, *Chemistry - A European Journal* **2012**, *18*, 7691-7694; l)Y. Chen, F. Ma, X. Chen, B. Dong, K. Wang, S. Jiang, C. Wang, X. Chen, D. Qi, H. Sun, B. Wang, S. Gao and J. Jiang, *Inorg. Chem. Front.* **2017**, *4*, 1465-1471.

[113] K. M. Kadish, T. Nakanishi, A. Gürek, V. Ahsen and I. Yilmaz, *J. Phys. Chem. B* **2001**, *105*, 9817-9821.

[114] M. Gonidec, D. B. Amabilino and J. Veciana, *Dalton Trans.* **2012**, *41*, 13632-13639.

[115] H.-G. Jin, X. Jiang, I. A. Kühne, S. Clair, V. Monnier, C. Chendo, G. Novitchi, A. K. Powell, K. M. Kadish and T. S. Balaban, *Inorg. Chem.* **2017**, *56*, 4864-4873.

[116] J. Lu, Y. Deng, X. Zhang, N. Kobayashi and J. Jiang, *Inorg. Chem.* **2011**, *50*, 2562-2567.

[117] N. Sun, H. Wang, T. Liu, D. Qi and J. Jiang, *Dalton Trans.* **2019**, *48*, 1586-1590.

[118] H. Wang, K. Wang, J. Tao and J. Jiang, *Chem. Commun.* **2012**, *48*, 2973-2975.

[119] S. Demir, I.-R. Jeon, J. R. Long and T. D. Harris, *Coord. Chem. Rev.* **2015**, *289-290*, 149-176.

[120] J. D. Rinehart, M. Fang, W. J. Evans and J. R. Long, *J. Am. Chem. Soc.* **2011**, *133*, 14236-14239.

[121] a)V. Vieru, N. Iwahara, L. Ungur and L. F. Chibotaru, *Sci. Rep.* **2016**, *6*, 24046-24046; b)C. Das, A. Upadhyay and M. Shanmugam, *Inorg. Chem.* **2018**, *57*, 9002-9011; c)C. A. Gould, L. E. Darago, M. I. Gonzalez, S. Demir and J. R. Long, *Angew. Chem. Int. Ed.* **2017**, *56*, 10103-10107; d)G. Brunet, M. Hamwi, M. A. Lemes, B. Gabidullin and M. Murugesu, *Commun. Chem.* **2018**, *1*, 88-88; e)S. Demir, M. I. Gonzalez, L. E. Darago, W. J. Evans and J. R. Long, *Nat. Commun* **2017**, *8*, 2144-2144; f)C. Chen, Z. Hu, J. Li, H. Ruan, Y. Zhao, G. Tan, Y. Song and X. Wang, *Inorg. Chem.* **2020**, *59*, 2111-2115.

[122] F.-S. Guo and R. A. Layfield, *Chem. Commun.* **2017**, *53*, 3130-3133.

[123] F. Pointillart, J. Flores Gonzalez, V. Montigaud, L. Tesi, V. Cherkasov, B. Le Guennic, O. Cador, L. Ouahab, R. Sessoli and V. Kuropatov, *Inorg. Chem. Front.* **2020**, *7*, 2322-2334.
[124] J. I. van der Vlugt, *Chem. Eur. J* **2019**, *25*, 2651-2662.
[125] B. S. Dolinar, S. Gómez-Coca, D. I. Alexandropoulos and K. R. Dunbar, *Chem. Commun.* **2017**, *53*, 2283-2286.
[126] M. A. Dunstan, E. Rousset, M.-E. Boulon, R. W. Gable, L. Sorace and C. Boskovic, *Dalton Trans.* **2017**, *46*, 13756-13767.
[127] P. Zhang, M. Perfetti, M. Kern, P. P. Hallmen, L. Ungur, S. Lenz, M. R. Ringenberg, W. Frey, H. Stoll, G. Rauhut and J. van Slageren, *Chem. Sci.* **2018**, *9*, 1221-1230.
[128] W. R. Reed, M. A. Dunstan, R. W. Gable, W. Phonsri, K. S. Murray, R. A. Mole and C. Boskovic, *Dalton Trans.* **2019**, *48*, 15635-15645.
[129] a)D. A. Gálico, R. Marin, G. Brunet, D. Errulat, E. Hemmer, S. A. Fernando, J. Moilanen and M. Murugesu, *Chem. Eur. J* **2019**, *25*, 14625-14637; b)J.-H. Jia, Q.-W. Li, Y.-C. Chen, J.-L. Liu and M.-L. Tong, *Coord. Chem. Rev.* **2019**, *378*, 365-381.
[130] F. Pointillart, B. le Guennic, O. Cador, O. Maury and L. Ouahab, *Acc. Chem. Res.* **2015**, *48*, 2834-2842.
[131] K. Soussi, J. Jung, F. Pointillart, B. Le Guennic, B. Lefeuvre, S. Golhen, O. Cador, Y. Guyot, O. Maury and L. Ouahab, *Inorg. Chem. Front.* **2015**, *2*, 1105-1117.
[132] a)B. Lefeuvre, J. Flores Gonzalez, F. Gendron, V. Dorcet, F. Riobé, V. Cherkasov, O. Maury, B. Le Guennic, O. Cador, V. Kuropatov and F. Pointillart, *Molecules* **2020**, *25*, 492-492; b)J. Flores Gonzalez, O. Cador, L. Ouahab, S. Norkov, V. Kuropatov and F. Pointillart, *Inorganics* **2018**, *6*, 45-45.
[133] a)M. D. Walter, C. H. Booth, W. W. Lukens and R. A. Andersen, *Organometallics* **2009**, *28*, 698-707; b)C. H. Booth, M. D. Walter, D. Kazhdan, Y.-J. Hu, W. W. Lukens, E. D. Bauer, L. Maron, O. Eisenstein and R. A. Andersen, *J. Am. Chem. Soc.* **2009**, *131*, 6480-6491; c)C. H. Booth, D. Kazhdan, E. L. Werkema, M. D. Walter, W. W. Lukens, E. D. Bauer, Y.-J. Hu, L. Maron, O. Eisenstein, M. Head-Gordon and R. A. Andersen, *J. Am. Chem. Soc.* **2010**, *132*, 17537-17549; d)G. Nocton, W. W. Lukens, C. H. Booth, S. S. Rozenel, S. A. Medling, L. Maron and R. A. Andersen, *J. Am. Chem. Soc.* **2014**, *136*, 8626-8641; e)G. Nocton, C. H. Booth, L. Maron, L. Ricard and R. A. Andersen, *Organometallics* **2014**, *33*, 6819-6829; f)G. Nocton, C. H. Booth, L. Maron and R. A. Andersen, *Organometallics* **2013**, *32*, 5305-5312; g)R. L. Halbach, G. Nocton, J. I. Amaro-Estrada, L. Maron, C. H. Booth and R. A. Andersen, *Inorg. Chem.* **2019**, *58*, 12083-12098; h)A. Jaoul, C. Clavaguéra and G. Nocton, *New J. Chem.* **2016**, *40*, 6643-6649.

[134] a)J. E. Kim, J. A. Bogart, P. J. Carroll and E. J. Schelter, *Inorg. Chem.* **2016**, *55*, 775-784; b)L. Duan, Y.-B. Jia, X.-G. Li, Y.-M. Li, H. Hu, J. Li and C. Cui, *Eur. J. Inorg. Chem.* **2017**, *2017*, 2231-2235; c)S. S. Galley, S. A. Pattenaude, C. A. Gaggioli, Y. Qiao, J. M. Sperling, M. Zeller, S. Pakhira, J. L. Mendoza-Cortes, E. J. Schelter, T. E. Albrecht-Schmitt, L. Gagliardi and S. C. Bart, *J. Am. Chem. Soc.* **2019**, *141*, 2356-2366; d)A. A. Skatova, D. S. Yambulatov, I. L. Fedyushkin and E. V. Baranov, *Russ. J. Coord. Chem.* **2018**, *44*, 400-409; e)A. A. Trifonov, B. G. Shestakov, D. M. Lyubov and K. A. Lyssenko, *Russ. Chem. Bull.* **2018**, *67*, 50-55; f)S. V. Klementyeva, A. N. Lukoyanov, M. Y. Afonin, M. Mörtel, A. I. Smolentsev, P. A. Abramov, A. A. Starikova, M. M. Khusniyarov and S. N. Konchenko, *Dalton Trans.* **2019**, *48*, 3338-3348.

[135] M. Schultz, J. M. Boncella, D. J. Berg, T. D. Tilley and R. A. Andersen, *Organometallics* **2002**, *21*, 460-472.

[136] M. D. Walter, D. J. Berg and R. A. Andersen, *Organometallics* **2006**, *25*, 3228-3237.

[137] G. Nocton, C. H. Booth, L. Maron and R. A. Andersen, *Organometallics* **2013**, *32*, 1150-1158.

[138] A. A. Trifonov, T. V. Mahrova, L. Luconi, G. Giambastiani, D. M. Lyubov, A. V. Cherkasov, L. Sorace, E. Louyriac, L. Maron and K. A. Lyssenko, *Dalton Trans.* **2018**, *47*, 1566-1576.

[139] A. A. Trifonov, B. G. Shestakov, I. D. Gudilenkov, G. K. Fukin, G. Giambastiani, C. Bianchini, A. Rossin, L. Luconi, J. Filippi and L. Sorace, *Dalton Trans.* **2011**, *40*, 10568-10575.

[140] a)I. L. Fedushkin, A. A. Skatova, D. S. Yambulatov, A. V. Cherkasov and S. V. Demeshko, *Russ. Chem. Bull.* **2015**, *64*, 38-43; b)I. L. Fedushkin, D. S. Yambulatov, A. A. Skatova, E. V. Baranov, S. Demeshko, A. S. Bogomyakov, V. I. Ovcharenko and E. M. Zueva, *Inorg. Chem.* **2017**, *56*, 9825-9833; c)I. L. Fedushkin, A. N. Lukoyanov and E. V. Baranov, *Inorg. Chem.* **2018**, *57*, 4301-4309.

Entry for the Table of Contents

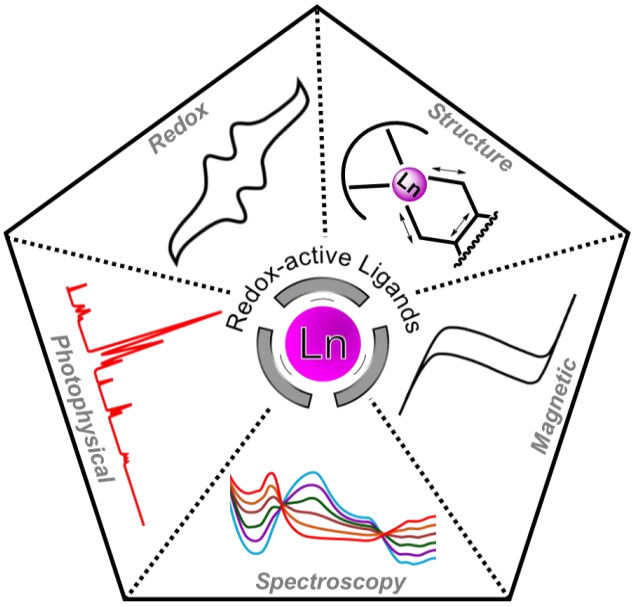

The redox-activity of lanthanoid complexes can arise from metal, ligand or rarely, both components. Harnessing the synergy between metal and ligand redox-activity will ultimately facilitate the development of new molecular materials with novel and enhanced functionality.